POLITECNICO DI TORINO

Master of Science in Environmental and Land Engineering

Master of Science Thesis

Climate Change and River Temperature in the Mediterranean: Data Modelling Workflow for the Vjosa River (Albania)



Supervisors

Paolo Vezza Guido Zolezzi (Università di Trento) Marta Crivellaro (Università di Trento)

Candidate

Denisa Shquti

Abstract:

River thermal regimes are essential for the ecological processes and for the growth and evolution of the river habitats. Sensitive river catchments like the Mediterranean ones are being very exposed to the alteration of the temperatures and the heatwaves and droughts and it looks like the impacts of these events on freshwater communities cannot be ignored anymore. In this thesis is represented a data driven framework to understand climatic variability, the analyse the performance of these datasets and a reconstruction of present and future river temperature and their impact on freshwater target species to support possible climate change managements in the upper Vjosa river, in Abania.

The first part is developed using QGIS for a morphometric overview of the upper Vjosa river catchment. Then, a historical climate analysis using ERA5 air temperature data from 1979 to 2024 is proposed for the region [1]. Furthermore, 30-year climate baseline was used from 1991 to 2020, to compute monthly, yearly temperature anomalies, and evaluate long term trends and a recent year like 2024 as benchmark against the climatic baseline.

Through an integrated reanalysis using data from ERA5, in situ loggers and local bulletins the work proposes a statistical downscaling of ERA5 air temperature data. Different correction techniques are used to improve agreement with the observations. The results show that reanalysis products typically capture seasonal variability but under represent warm extremes. The bias correction methods help to improve significantly the agreement with local measurements. The whole integrated workflow highlights how basin morphology, flow regime, and microclimate modulate thermal responses across Mediterranean settings.

The thesis outlines potential climate impacts and takes into consideration mitigation and adaptation strategies aligned with European policy frameworks. The possible scenarios quantify how heatwaves increase exceedances of physiological thresholds for target freshwater taxa, amplifying the disruption of the habitat, and elevating mortality risk in the absence of cold-water refuges.

This study offers a generalized workflow that integrates remotely and in situ-collected data with process-based modelling. The approach can be applied across Mediterranean rivers, including free flowing and more regulated systems, to understand better the climate impacts and to guide planning under a warming climate.

Table of Contents

Abstrac	zt:	2
Chapter	r 1 – Introduction	5
1.1	1	
1.2	1	
1.3	2	
1.4	3	
1.5	Error! Bookmark not defined.	
1.6 Aim	n of the study	8
Chapter	r 2 - Climate: Analysis and Data Methodology	9
2.1. I	In-Situ Instrumentation	10
2.1	1.1 Air Temperature	10
2.1	1.2 Water Temperature	11
2.1	1.3. Data Management	11
2.2 Q	QGIS overview: basin morphology and river network	12
2.2	2.1. Project set-up	12
2.2	2.2 Extraction of the Përmet catchment	12
2.2	2.3. Spatial clipping	13
2.2	2.4. Terrain derivatives	13
2.2	2.5. River-network metrics	15
2.2	2.6. Flat-terrain proportion	16
2.2	2.7. Bridge cross-section	16
2.3 C	Climate baseline and analysis from 1979-2024 with historical ERA5 data	17
2.3	3.1 Monthly climatology from 1991 to 2020	18
2.4 A	Anomalies	19
2.4	4.1. Monthly mean anomalies vs the baseline	19
2.4	4.2. Monthly mean Heatmap	21
2.4	4.3. Monthly anomalies of 2024 vs 1991-2020	23
2.5 N	Monthly evolution	24
2.5	5.1 Monthly analysis from 1979 to 2024	24
2.6 S	easonal anomalies	30
2.7 1	.2- Month moving average	32
2.8 N	Лаnn- Kendall Test	33
2.9 D	Oata approach and evaluation: ERA5, in-situ loggers, local bulletins	37
2.9	9.1 Correction methods: linear bias correction and quantile mapping	48

2.9.2 Water Temperature Analysis
Chapter 3 – Thermal Impact Assessment on fish biodiversity
3.1 Introduction
3.2 Target Species
3.3 Analysis
3.3.1 Thermal stress indicators
3.3.2 Frequency of Threshold Exceedance (Heatmap)
3.3.3 Exceedance Degree Days
3.3.4 Sub-Lethal Thermal Stress Thresholds
Chapter 4 – Possible future scenarios & strategies
4.1 Possible climate scenarios in Vjosa Basin
4.1.1 Possible impacts on the ecosystem
4.1.2 Adaptation and mitigation strategies through EU policy frameworks
Chapter 5 – Discussion and Conclusions
Bibliography:

Chapter 1 – Introduction

1.1 General Introduction

Rivers have always been recognized as essential not only our planet but also to human survival and identity. The expression "El río es vida" ("the river is life") which comes from the American latin countries is used a lot to emphasize the dependence of communities on river systems for food, water, and cultural continuity [2]. They are one of the most dynamic ecosystems on our planet and play a crucial role in the hydrological processes by sustaining biodiversity and providing services essential for both humans and nature.

In the last decades, the river thermal regimes had received a lot of attention, as water temperatures are one of the most important parameters that control the freshwater ecosystems. The water temperature and its variations influence the oxygen concentration, the nutrient's cycle and the survival of the aquatic life. [3].

Although in the last they have been constantly under pressure from multiple stress factors like climate change, modification of the use of land, the increasing of pollution, the hydropower development etc. All the factors mentioned above threaten and alter the natural hydrological and thermal dynamics of a river and that is why understanding and studying the river thermal regimes is essential for the development of conservation strategies, water management and climate mitigation and adaptation.

The Vjosa River which is also the case study of this thesis, is one of the almost entirely free-flowing rivers in Europe. Its natural hydro-morphological processes and the biodiversity are still untacked [4].

1.2 River Thermal Regime

The river thermal regime is a spatial temporal variation of the water temperature within the fluvial system. It is a reflection of multiple factors, which operate at different scales, like solar radiation, groundwater inputs, air temperature, channel morphology etc. The long-term cycles of heating and cooling are related to the catchment characteristics like altitude and climate, instead the short-term patterns, daily ones, are related to radiation cycles and storms.

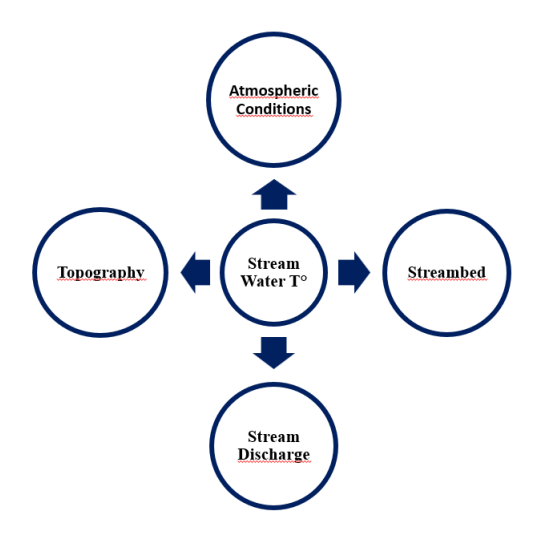


Figure 2.1: A scheme of the correlation between water to and outer patterns "adapted (Poole & Berman, 2001)"

According to [5] even though the air temperature is the most dominant driver at seasonal scales, the local factors like the groundwater flows and the vegetation can also modify the thermal responses at spatial scales. It is crucial to understand these processes because the smallest changes in water temperature can bring ecological impacts, especially during spawning or summer low flows.

Poole and Berman (2001) analysed the principles for understanding river thermal change by relating spatial and temporal drivers to the physical and chemical imprint of the landscape, the climate, and mounting anthropogenic demands. In the Mediterranean, for example, the net effect is a seasonal shift, with thermal pulses arriving during the wet months and steep thermal cliffs forming when dry, warm months decrease river flows and intensify solar absorption.

Rivers have a high spatial heterogeneity in their thermal regimes for example, the headwater streams are cooler instead the lowland rivers tend to be warmer and more exposed. The tributary junctions and the channels help create localized thermal shelters for sensitive species during heatwaves. All this spatial and temporal variability makes river temperature modelling a challenge but it is necessary in the management of the freshwater.

1.3 The Vjosa River: A European Case

The Vjosa River, originating in the Pindus Mountains in Greece (where it is known as the Aoos). It flows for about 270 km before reaching the Adriatic Sea in Albania. The river is one of the last large rivers in Europe that flows freely and its catchment area is more than 6,700 km². Its hydro-morphological processes are still untacked, with a complicated system of braided channels, floodplains, wetlands, and side arms. These dynamics help make a patchwork of habitats that support a very high level of biodiversity [7].



Figure 2.2: Vjosa River (M. Crivellaro, May 2025)

According to Schinegger et al. (2013) Vjosa is a "hotspot of freshwater biodiversity," highlighting its ecological importance at both regional and continental scales. The presence of numerous endemic and endangered species of fish, macroinvertebrates, and riparian flora and its near-natural status makes it an invaluable reference system for understanding river functioning under minimal human disturbance.

1.4 Rivers in the Mediterranean and Balkan Region

A lot of studies have confirmed and proved the vulnerability of Mediterranean rivers to climate change. In southern Spain simulated high emission scenarios (RCP8.5) have shown a significative reduction of streamflow's by 40% and rise of the water temperatures. (Marcos-Garcia et al., 2017)

In Turkey, [10] Yavuz et al. (2025) on his study found strong relations between temperature, flow variability, and oxygen concentrations affecting directly the ecosystem health.

In the Balkans, hydrological studies highlight increasing frequency of floods in winter and droughts in summer, both of which reshape thermal regimes and ecological stability (Papadaki et al., 2022).

The Drin and Aoos/Vjosa systems have been cited as emblematic examples of Mediterranean rivers undergoing rapid climate stress.

The Balkan Peninsula is recognized as one with important biodiversity in Europe, with rivers that play an important role on maintaining this richness. The hydrological studies highlight an increase in the frequency of floods during cold seasons and droughts in the warm seasons both affecting and reshaping the thermal regimes and stability of rivers (Papadaki et al., 2022). [11]

According to a study about Croatian rivers, it was documented a high conservation value of freshwater ecosystems in the region, highlighting the presence of numerous endemic species in respect to the Western Europe. However, in the study was also pointed an increase of pollution, invasive species, and especially hydropower development. Žganec (2012). In Albania a dominant threat of river integrity has become the push for hydropower. A high number of projects have been planned or constructed in recent years, often with limited or without environmental assessment.

According to (Zajkov et al. 2023) study about the hydropower expansion in the Balkans, even small-scale dams can fragment river habitats, alter the sediment dynamic and disrupt the thermal regimes. Also, for Vjosa there have been a lot of large-scale dam projects which have raised internationals concern since they threat the wildernesses of this last, but since now none of this project has move forward since Vjosa took the status of a National Park on March 15, 2023, by the Albanian government, establishing it as Europe's first wild river national park.

1.5 Climate Change and Freshwater Ecosystems

Climate change represents a major driver of change in the freshwater systems. The effects of climate change as the rise of air temperatures, altered precipitation and frequent extreme events affect directly the flow and the water temperature. Some generated models anticipate that by the end of the century the mean thermal norms of Mediterranean rivers could shift by 2–3 °C (Estrela-Segrelles et al., 2023). Also, the Mediterranean river's hydrological regimes are exhibiting reduced annual discharges and reconfigured patterns of seasonal discharge (Carlson et al., 2024).

A study on the impacts of climate change on fish communities in the southern US shows how warming temperatures shift the community composition toward warm water species and a reduction in the cold-water habitats. Pease et al. (2011). The same mechanisms are relevant for Balkan's rivers, since many species have a narrow thermal tolerance. Milošević et al. (2016) studied the impacts of climate change on macroinvertebrate species present in the Balkan rivers, finding distributional shifts of mayflies and stoneflies connected with warming waters. Such studies provide big evidence that the ecological impacts of climate change are already present in the region. Especially mountain rivers as in our case Vjosa may be particularly vulnerable to these impacts. Since these types of rivers have an important role as "water towers of the world" supplying water to billions of people it is important to protect and work toward their maintenance Viviroli et al. (2020).

The Vjosa, despite its near-pristine condition, is not immune to these impacts as represented in hydrological and morphological studies. These studies reveal that the river has undergone changes in the channel morphology linked to climate change (Crivellaro et al., 2024). Therefore, also Albania as other south regions faces the challenge of preserving unique

ecosystems like the Vjosa while working toward adaptation and mitigations water management strategies.

1.6 Aim of the study

This thesis aims to develop a **data-driven framework** to evaluate river thermal regimes in the upper Vjosa catchment and assess their impacts on freshwater biodiversity under current climate and discuss projected conditions. In detail, the work aims to:

- 1. Quantify historical and recent trends in air and water temperature in the upper Vjosa River using a combination of ERA5 reanalysis, in situ loggers, and local climate data.
- 2. Evaluate the performance of reanalysis datasets and apply statistical downscaling and bias-correction methods to improve agreement with local observations.
- 3. Reconstruct present-day river temperature scenarios, highlighting exceedances of critical thermal thresholds for target freshwater species, such as *Salmo farioides* for the Vjosa river and one of its small tributaries, the Lengarica river.
- 4. Assess and discuss the ecological implications of heatwaves and altered thermal regimes for species survival, habitat quality, and ecosystem resilience. Integrate such discussion for climate-adaptive management and conservation strategies aligned with European policy frameworks, including the EU Water Framework Directive.

Chapter 2 - Climate: Analysis and Data Methodology

In this chapter through the characterisation of the morphology of Vjosa basin and its network in QGIS and a climate analysis from 1979 to 2020 it is studied and analysed a climate workflow which it is crucial for the chapters that will follow. Also, different databases are evaluated between them and corrected with correction methods to understand and reflect better on their accuracy.

This study adopts an integrated measurement strategy to characterize the thermal regime of the upper Vjosa basin by combining high-frequency in-situ logger data with gridded reanalysis datasets (ERA5). This hybrid approach leverages the complementary strengths of both data types while mitigating their individual limitations Isaak & Horan, 2011; Hersbach et al., 2020).

Local logger observations provide accurate, site-specific records of air and water temperature, essential for detecting diurnal dynamics and fine-scale thermal heterogeneity. However, they are spatially sparse and typically cover short time spans. Conversely, ERA5 provides spatially consistent, multi-decadal climate information (1979–present), which is valuable for establishing climatologist, anomalies, and trends (Hersbach et al., 2020). Yet, its coarse spatial resolution (~30 km) cannot resolve the complex topography of alpine valleys such as the Vjosa.

For this study climate and reanalysis data were used since they are essential sources of input,

being in situ metereological data difficult to be retrieved and higly fragmented over time. A big part of the data was downloaded from ERA5. It is a database produced by the European Centre for Medium-Range Weather Forecasts (ECMWF) and it represents the current state-of-the-art in global reanalysis.

Wanders et al. (2019) highlighted the improved temporal, spatial resolution, the consistency and reliability of ERA5 data compared to earlier datasets. The database provides hourly data for a wide range of atmospheric variables essential for hydrological models. In this thesis, ERA5 data are used to run the air2stream model and to analyse the thermal dynamic of Vjosa.

However, as noted by Wanders et al. (2019), ERA5 still exhibits biases at local scales as will be seen in the next chapters where a detailed analyse is done to explain the bias of ERA5 data in respect to local and installed logger data.

2.1. In-Situ Instrumentation

2.1.1 Air Temperature

The air temperature of the valley is recorded using electronic loggers with on-board memory. The air logger was mounted 1.5–2 m above ground in one of the walls of CESVI an NGO located in Permet that takes care about the environmental and local causes.

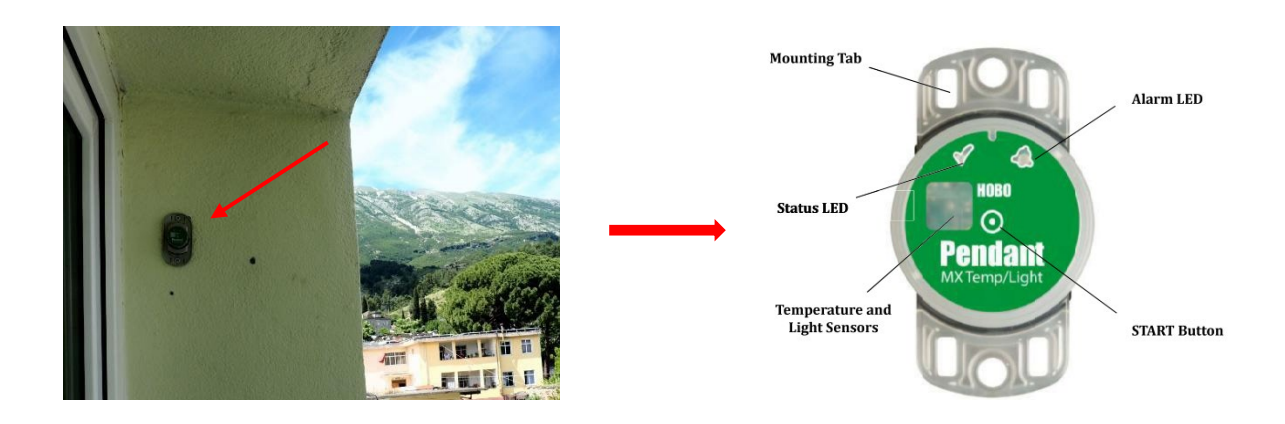


Figure 2.1, a, b: Air logger installed at CESVI office, Permet May 2025 and the logger model

The air logger position is almost 200m away from the Permeti Bridge where another water sensor is installed.

2.1.2 Water Temperature

Also, the water temperature I measured with the loggers which were installed one in Permeti Bridge in Vjosa and the other one in Vjosa's tributary, Lengarica. Both loggers were attached to metal bars and then these metal bars were submersed in the water and fixed on the rocks along the river channel. Besides the installation of the air logger, two more loggers were installed. One logeer was installed in Vjosa and the other one in Langarica. The decision to install the logger also in Lengarica was made because this last is an important tributary of Vjosa and one of the most important side rives of the basin. It plays an important role as an ecological corridor between Vjosa corridor and the other protected areas.





Figure 2.4, a,b: The installation of the water logger in Vjosa and in Langarica (Crivellaro, May 2025)

2.1.3. Data Management

The logger configuration was made following specific manual streps in our case to emasure the temperature every 10 minutes even though in th following steps we will see that the data is transformed into hourly. The maintenance will be followed by the NGO who also delivered the logger's data every week. The data is retrieved in csv files also back up in the cloud.

Instead, the ERA5 data is extracted from the website (ECMWF) which is global reanalysis providing hourly data from 1940, as nc. format, always hourly and 2m near surface. They usually are extracted in K but for this work always converted into °C. Era5 is quite valuable event high the baseline might be imperfect due to its coarse resolution. (Hersbach et al., 2020). ERA5 data is corrected through linear bias correction and quintile mapping methods.

2.2 QGIS overview: basin morphology and river network

Topography strongly modulates near-surface temperature. Valley cold-air pools form overnight under stable, clear conditions; these create sharp inversions with lower T min in valley bottoms than surrounding slopes. Breakup typically occurs within a few hours after sunrise, but persists longer in deep or snow-covered valleys. Such processes explain why reanalyses (with km-scale grids) can miss local minima, producing warm T min biases. Mapping station/logger sites against DEM-derived terrain in QGIS, and reporting station–grid elevation differences, allows us to diagnose these effects and interpret reanalysis–observation gaps.

2.2.1. Project set-up

The 10 m digital elevation model (DEM), the Vjosa river-network shapefiles, and the subcatchment polygons were loaded into a single QGIS project and organised into thematic groups (Raster, Hydrography, Catchments, Basemap). The project CRS was set to EPSG 32634.

Project /Properties /CRS /EPSG 32634 /drag layers into thematic groups.



Figure 2.6: DEM Albania, 10m



Figure 2.7: DEM Permet Catchement

2.2.2 Extraction of the Përmet catchment

The polygon that drains towards the town of Përmet was identified within the re-projected sub-catchment layer and exported as a GeoPackage (subcatch_permet). This feature defines the spatial extent for all subsequent analyses.

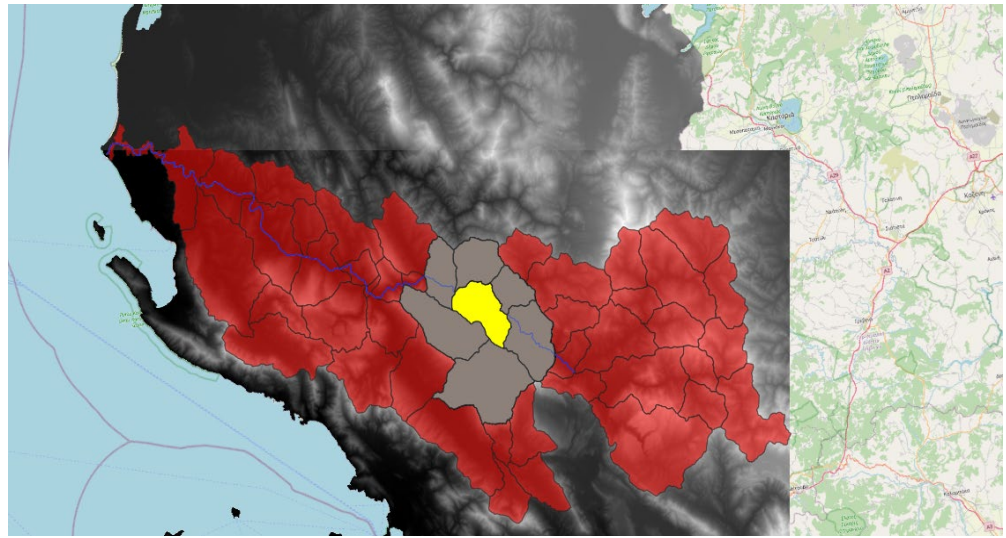


Figure 2.8: Permet Catchement

Select Features tool /click polygon draining to Përmet /Right-click layer / Export /Save Selected Features As / GeoPackage subcatch permet.

2.2.3. Spatial clipping

Using subcatch_permet as a mask, the national DEM was trimmed (*Clip Raster by Mask Layer*) to produce dtm_permet.tif. The river network was clipped in an analogous way (*Vector Clip*), yielding riverseg_permet, which contains only channels located inside the study catchment. Vector /Geoprocessing Tools

/Clip/Input = RiverSegments_32634/Overlay = subcatch_permet → riverseg_permet.

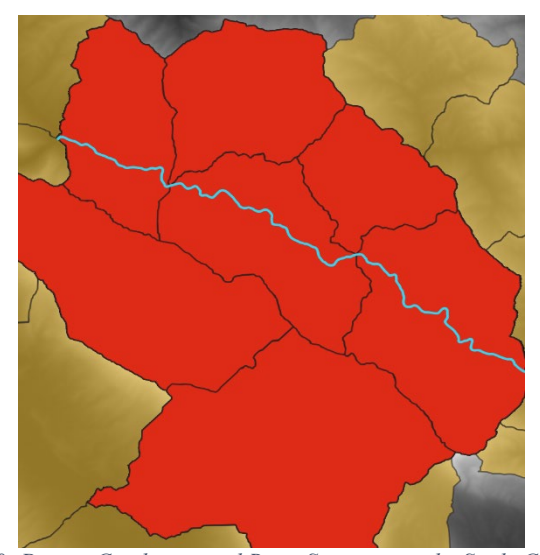


Figure 2.9: Permet Catchment and River Segments in the Study Catchment

2.2.4. Terrain derivatives

A slope raster (slopepermet.tif, units in percent) was generated from the clipped DEM via

Terrain / Slope. A binary raster highlighting areas with gradients below five percent (lt5.tif) was then produced with the raster calculator. Raster /Terrain Analysis /Slope → slopepermet.tif (unit = %).

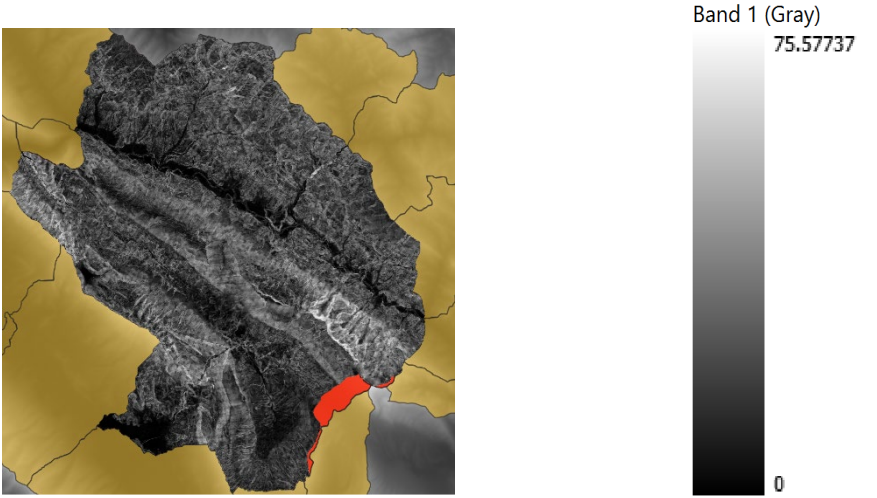


Figure 2.10.a, b: Slope map of the Permet catchment (left) with legend (right).

After re-projecting the DEM so every grid cell is measured in metres, I ran a slope calculation. The result is a greyscale picture where black means flat ground (0 °) and bright white means almost vertical ground (up to 76 °). Three things jump out:

- 1. Rugged ridges up top. Most of the northern and central catchment glows light grey to white, showing hillsides steeper than 40°. Rain hitting these slopes rushes off fast, carrying loose soil and rock with it.
- 2. A gentler middle valley. Cutting through the centre is a dark band with slopes under 10 °. This is the main valley floor—the natural highway that funnels water and fine sediment toward the outlet.
- **3.** A tight, steep exit. Right before the river leaves the basin, the valley walls pinch in and shoot up to 60–75°. This narrow gorge forces all that fast-moving water through one rocky choke point, making it a hotspot for erosion and debris flow.

Put simply, the Permet basin is built like a steep-roofed funnel—lots of slick, high ground pouring into one narrow spout. That shape explains why storms here can turn into sudden, powerful floods and why the river carries so much sediment downstream.





Figure 2.11.a, b: Slope < 5% map of the Permet catchment (left) with legend (right). Greyscale stretches from 0 (black) to 1 (white); the river reach selected is shown in red

On natural landscapes, anything steeper than about a 5 % gradient tends to drain quickly; water keeps moving downslope rather than ponding. Slopes gentler than 5 %—roughly 3 °— are flat enough that even a modest rise in stage can push water sideways and allow it to linger. Mapping those surfaces gives an instant first-guess at the modern or relict floodplain before you run any hydraulic model.

This map displays the binary raster produced with the expression ("slopepermet@1" ≤ 2.86) * 1, where 2.86 ° is the angular equivalent of a 5 % rise.

White pixels (value = 1) mark ground flatter than 5 %, while black pixels (value = 0) mark all steeper terrain. The white band that runs northwest–southeast through the basin is the modern flood-plain of the Vjosa/Aoös River. Smaller white islands along the southern and western margins are fluvial terraces or other low-slope benches. The near-absence of white cells at the outlet gorge (highlighted by the red study reach) underlines how abruptly the valley narrows and steepens at the basin exit. No white pixels appear in the northern headwaters, confirming that the upper catchment is uniformly steep.

2.2.5. River-network metrics

Segment lengths were computed for riverseg_permet (len_m = length). A location-based summary join aggregated these lengths within the catchment, returning both the total channel length and the number of segments. Drainage density was calculated as total-length-to-area ratio (km km⁻²).

	fid	value	area	length_count	length_sum	dens_km_km2	area_km2	drain_dens
1	21	34	104066873	1	52.558	0.50504063075	104.066874622	0.00050504063
2	22	32	92012503	2	69.504	0.75537562109	92.0125008786	0.00075537562
3	29	38	68226875	1	52.558	0.77034159781	68.2268751280	0.00077034159
4	32	36	117825625	1	52.558	0.44606595630	117.825624790	0.00044606595
5	33	78	176064370	1	16.946	0.09624888663	176.064374267	9.62488866390
6	37	44	149219377	1	52.558	0.35221967442	149.219375908	0.00035221967

Figure 2.12: Attribute table of river-network metrics

The table covers three pieces of information for each mapping unit (polygon) inside the Permet basin — its size, the length of stream channel it contains, and the resulting drainage density.

The drainage-density statistics reveal seven distinct hydrological zones within the Permet basin, each characterised by a different balance between catchment area and channel length. Polygon 34 occupies about 104 km² and contains roughly 52.6 km of mapped streams, giving a drainage density of approximately 0.51 km km². This value indicates a moderately dissected landscape where overland flow routes to the channel network relatively quickly.

Polygon 32, though smaller at 92 km², hosts nearly 69.5 km of channels. Its drainage density—about 0.76 km km⁻²—is the highest in the dataset and is typical of steep, closely incised terrain underlain by less-permeable material. Runoff generated here is expected to reach the main river rapidly.

Polygon 38 presents a similar hydrological signature: 68 km² of land supports 52.6 km of streams, yielding a density of roughly 0.77 km km⁻². Such values again point to steep slopes with limited capacity for surface-water storage.

Polygon 36, at 118 km², contains the same 52.6 km of channels, resulting in a drainage density of about 0.45 km km⁻². This intermediate value suggests a balance between rapid runoff generation and modest infiltration or temporary storage in soils.

Polygon 78 has a very low density. Although it encompasses almost 176 km², only 16.9 km of streams are mapped, producing a drainage density close to 0.10 km km². Hydrologically, this area will attenuate storm runoff, releasing water more gradually to the main stem. Polygon 44 covers roughly 149 km² and contains 52.6 km of channels, giving a drainage density of approximately 0.35 km km². The figure points to moderately low dissection.

In summary, polygons with densities above $\sim 0.7 \text{ km km}^{-2}$ (32 and 38) represent steep, rapidly responding source areas; densities between ~ 0.3 and 0.5 km km^{-2} (34, 36, 44) correspond to intermediate conditions; and polygon 78, with only 0.10 km km^{-2} , marks a low-gradient, storage-dominated environment.

2.2.6. Flat-terrain proportion

Counting the "true" pixels in lt5.tif by means of *Zonal Statistics* produced the absolute extent of terrain with < 5 % slope. Dividing by the total pixel count yielded the percentage of flat ground (*p flat*) inside the catchment.

	fid	value	area	flat_count	flat_sum	flat_mean	p_flatt
1	21	34	104066873	1022227	10953	0.01071484122	1.07148412241
2	22	32	92012503	903547	68113	0.07538401433	7.53840143346
3	29	38	68226875	669688	9197	0.01373326086	1.37332608617
4	32	36	117825625	1160028	75052	0.06469843831	6.46984383135
5	33	78	176064370	1729680	26326	0.01522015632	1.52201563294
6	37	44	149219377	1458762	28522	0.01955219562	1.95521956288
7	41	86	261702599	2452715	149934	0.06112980921	6.11298092114

Figure 2.13: Attribute table Flat-terrain proportion

The p_flat field is simply the percentage of each sub-area that is almost level (slope < 5 %). High values mean plenty of flood-plain or terrace surface; low values mean the land is mostly

steep.

Across the Permet basin most polygons register only 1–2 % flat ground. Those sectors are dominated by rugged hillslopes with very narrow valley floors.

Two polygons stand out with 6–8 % flat terrain. These contain the basin's broadest valley reaches or stepped river terraces—places where water can over-top the banks, spread out, and drop its sediment.

In short, the p_flat analysis confirms that the Permet catchment is a steep-walled funnel with only scattered, narrow flood-plain strips. Those strips play an outsized role in flood dynamics.

2.2.7. Bridge cross-section

A line perpendicular to the river at the CESVI bridge was designed (bridge_section). Points spaced at two-metre intervals were created along this line; raster sampling of the DEM attributed an elevation to each point. The point layer was exported as CSV and plotted (distance vs. elevation), providing a detailed transverse profile of the channel and its banks.

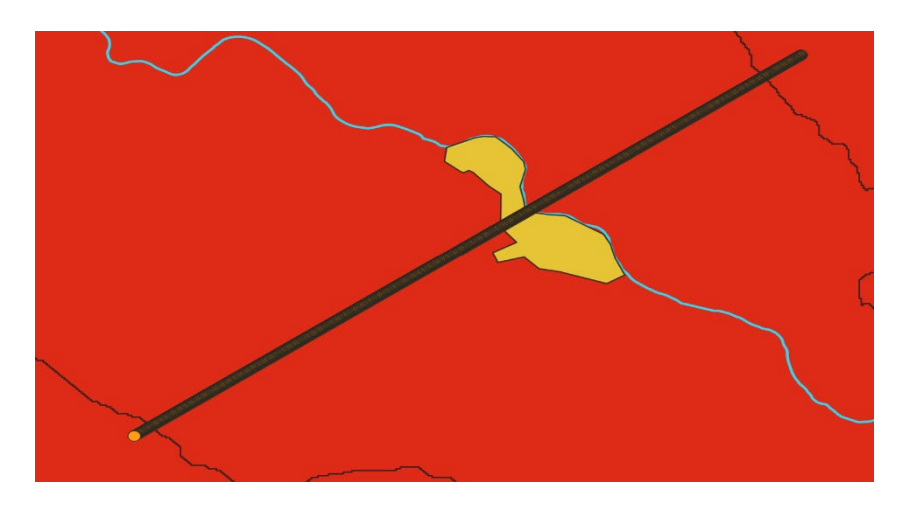


Figure 2.14: Permet Bridge Cross-section

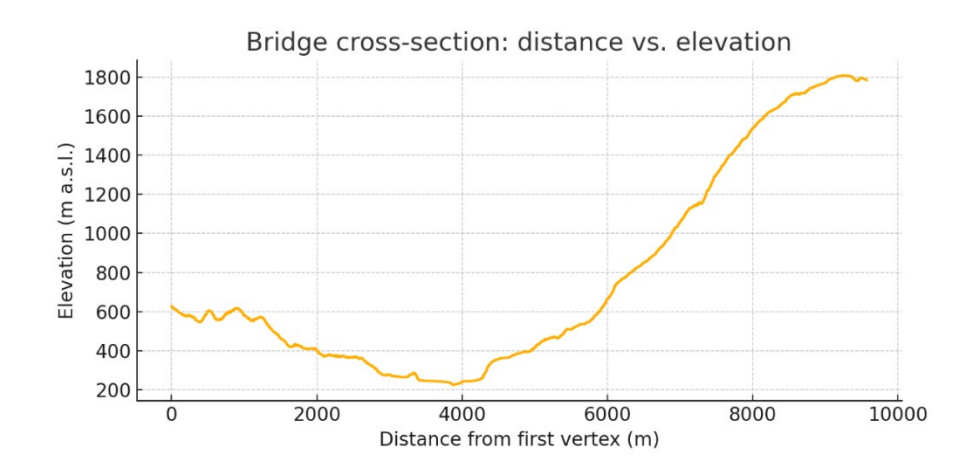


Figure 2.15: Permet Bridge Cross-section distance vs elevation

The orange curve is a straight-line transect that cut entirely across the Vjosa sub-catchment I

extracted.

The data below rapresents the geomorphic character of the Vjosa sub-catchment:

• Transect length (horizontal): 10 km

• Minimum elevation (river bed): 220 m a.s.l.

• Maximum elevation (ridge): 1 800 m a.s.l.

• Total relief: 1580 m

• Average valley-side slope (6–10 km segment): > 30 %

2.3 Climate baseline and analysis from 1979-2024 with historical ERA5 data

According to WMO guidance, climatological baselines are 30-year timelines and the current standard is 1991–2020 [22] (WMO, 2017). Monthly and annual normal were computed from ERA5data for this timeline. The plots that follow show the monthly climatology for the baseline, the monthly anomaly, the seasonal anomalies, a heatmap and monthly minimum, mean average and maximuim. All these steps are important to understand better the progression of clime and also the possible impacts on the river basin.

2.3.1 Monthly climatology from 1991 to 2020

Plotting the monthly climatology is a simple way to summarize the behaviour of temperatures in the long term as in our case.

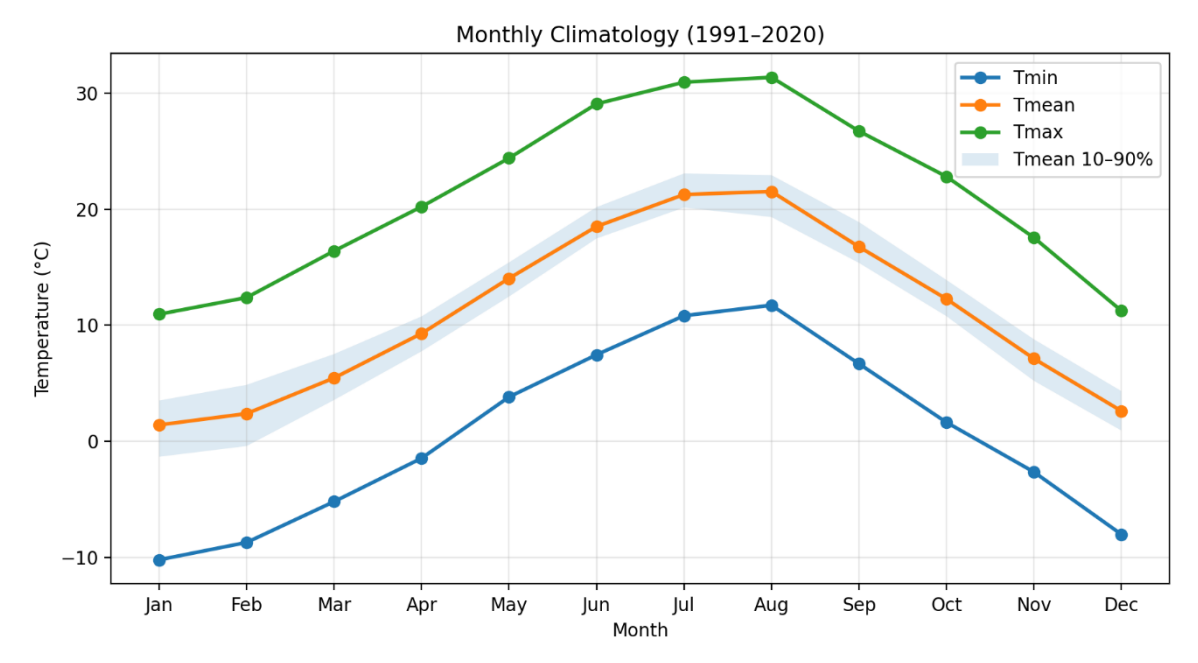


Figure 2.16: Monthly climatology 1991-2020

The plot represents the monthly climate using ERA5 data from 1991 to 2020. The blue curve shows the minima, the orange shows the mean and the green curve shows the maxima. The grey shadow curve represents the 10-90% range of the mean temperature for each month and it shows how much did the temperature varied from year to year during the baseline timeline.

Since not the same month has the same temperatures during the years, it was logical to calculate the 10^{th} and 90^{th} percentiles for every month which are tew boundaries describing the temperature range during the month. The 10^{th} percentile shows the temperature below which only 10% of the years fall usually representing the cold years, instead the 90^{th} percentile is the temperature above which only 10% of the years fall by representing the warm years.

This kind of percentile is important because it shows what is the normal for each month making it easier to understand when a year in the future falls out the normal range. For example, in the plot during winter the temperature varies between 0-10°C, during spring it raises and it reaches the maximum in summer near 30 °C followed by a decrease in autumn. It is a typical Mediterranean climate patter with dry summers and cool winters.

The plot was computed following the steps described below:

Hourly data was collected from ERA5 from 1991 to 2020 and for each month was compiled the monthly average temperature using the formula:

$$T_{m,y} = \frac{1}{N_{m,y}} \sum_{i=1}^{N_{m,y}} T_i$$

Where $N_{m,y}$ is the number of measurements for month m and year y.

After for each month through the timeline was calculated the average for T min, T max and T mean using:

$$C_m = \frac{1}{N_b} \sum_{y=1991}^{2020} T_{m,y}$$

In the end the 10th and 90th were calculated for the T mean for each month during the timeline.

2.4 Anomalies

2.4.1. Monthly mean anomalies vs the baseline

To understand better the variability monthly mean anomalies were computed relative to the baseline.

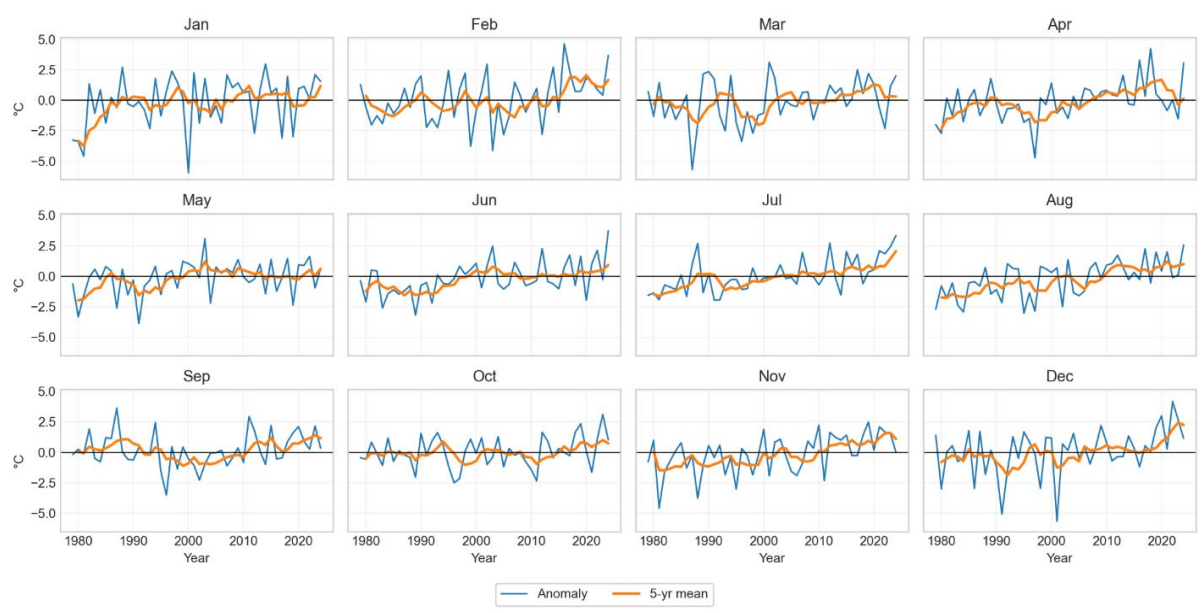


Figure 2.17: Monthly mean temperature anomalies (°C) relative to the 1991–2020 baseline, shown separately

The figure shows the monthly mean temperatures anomalies. Each panel represents a month across the years 1979-2024. The blue line is the monthly anomaly in respect of the baseline which is the black normal line. The orange curve is a 5-year running mean that shows the underlying trend.

In all the panels the orange curve rises from below zero in the decade of 1980-1990 to gain positive values after the 2000s underlining a shift toward warmer seasons.

During summer are noticed the strongest warming since the anomalies drift from negative to positive +2 °C in the last years. Also, the autumn months become warmer with passing year especially after 2005 where the summer starts to extend deeper into autumn and this last one is delayed. In general, every month shows a positive trend with main seasons summer and autumn which affect the warming increase.

These plots were accomplished starting from the hourly air temperature from ERA5, where these values were converted from K to °C and the average was calculated using the area weights. The monthly mean was computed and derived the baseline month climatology. The anomalies were plotted where the black line represents the baseline and the orange represents the 5-year running mean which is very helpful because it smooths the noise year after year by calculating the average of each value with its two previous.

The steps are described briefly below:

• Unit conversion: $T^{\circ c}(t) = T^{\kappa}(t) - 273.15$

• Area-weighted mean: $\underline{T}_t = \frac{\sum wi * Ti}{\sum_i wi}$, $w_i = \cos(\varphi_i)$

 $(\varphi_i = \text{latitude of grid cell i; replace with polygon area weights if available.})$

• Monthly mean:
$$\bar{T}_{m,y} = \frac{1}{N_{m,y}} \sum_{i=1}^{N_{m,y}} T_i$$

• Baseline (1991–2020):

$$C_m = \frac{1}{N_b} \sum_{y=1991}^{2020} T_{m,y}$$
 with $N_b = 30$

• Monthly anomaly:

$$A_{m,y} = T_{m,y} - C_m$$

• 5-year running mean:

$$\widetilde{A_{m,y}} = \frac{1}{W} \sum_{k=-2}^{2} A_{m,y+k} \quad W = 5$$

2.4.2. Monthly mean Heatmap

The previous monthly anomalies show the evolution of each month instead a heat map shows the same information but concentrated into a single matrix as in the picture below:

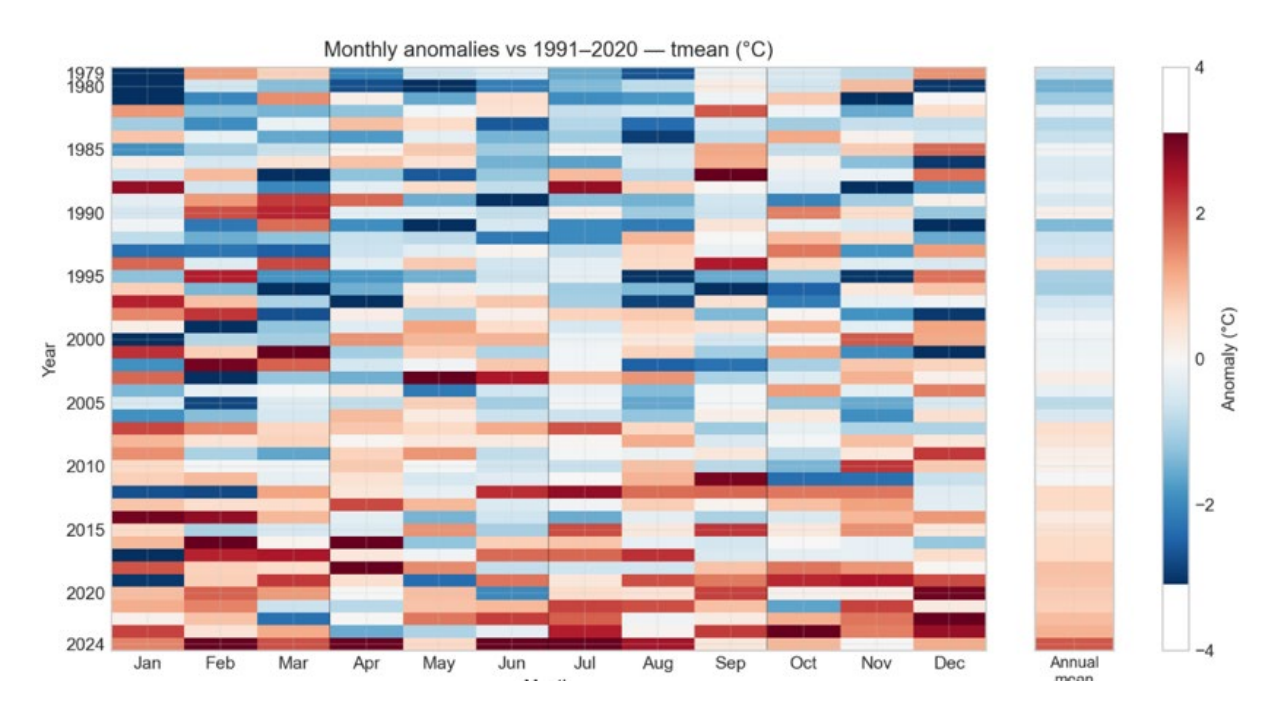


Figure 2.18: Monthly anomalies relative to the 1991–2020 baseline (°C)

The figure represents an anomaly heatmap. The heatmaps are plots in a grid form and are used to spot anomalies or hotspots using color intensity. For the timeline 1979 to 2024, a heatmap was made to spot the possible anomalies but also to understand how temperatures have changed in years. This kind of map is also an image of how climate is evolving and can also give us a glimpse of how the future might be.

As a baseline of 30 years was chosen the last timeline from 1991 to 2024 according to WMO since it defines "normals" as 30 years periods updated in each decade. [22][World Meteorological Organization. (2017)]. Baselines are important because they let us know how unusual the current conditions are and keeps studies comparable across different datasets.

Our heatmap reveals a shift in the regime of temperatures according to the change of colours. From 1980 until 1990 there was a predominance of the blue and white tiles. After the 1990s there was an increase of the red tiles which became more and more dominant after 2005 and "stable" like the new normal after 2015. Since 2000 and after 2010 most months are warmer than the baseline with anomalies +(1-3) °C. Long vertical red columns indicate warmer and repeated hot seasons. The winter months with passing years have shifted from blue to white to warm tones and also the blue tiles are much less frequent in the heatmap. There is some random cold outbreak but these outbreaks are more and more isolated with passing years. Also springs tiles after 2005 are redder and indicate earlier and milder ones as we can say for autumns which are more and more delayed with passing years.

The annual column indicates that anomalies are negative or zero in the 1980s,1990s but they start to become positive after 2000s, showing that the warming situation is yearly and not in single months.

In the summer seasons there is a coherence of red blocks which means that the like hood of

heat waves and the rise of water temperatures is more possible and frequent. The earlier and warmer springs accelerate the thermal build up which is intensified during summer but on the other side the autumns are delayed, warmer and shorter so also the period available for thermal recovery is shorter and not sufficient for the habitats. There is also winter but still the cold snaps are shorter so the capacity to offset the warming is shorter.

The anomalies are computed every month versus the baseline 1990-2020, in case another baseline was chosen the colour uniformity would be different.

The method used to create the heatmap is as it follows:

Data & domain:

Hourly ERA5 temperature was extracted for the timeline 1979–2024. Four daily hours were chosen:

A single catchment-mean series was formed using area weights wi (cell area* fraction inside the basin):

$$T(t) = \sum_{i} w_i T_i(t) / \sum_{i} w_i$$

• Temporal to monthly means:

The hourly values were averaged for each year and month:

$$T_{y,m} = \frac{1}{N} \sum_{h \in E(y,m)} T(h)$$

with N_{y,m} the number of valid hourly samples.

• Baseline (1991–2020):

The 12-month climatology over the WMO reference period was computed:

$$T_m^{\text{base}} = \frac{1}{30} \sum_{y=1991}^{2020} T_{y,m}$$

By using a 30-year window suppresses the noise of every year and the normal is more stable.

• Monthly anomalies:

Anomalies are calculated from the month of year normal: $A_{y,m} = T_{y,m} - T_m^{base}$

A positive $A_{v,m}$ indicates a warmer-than-normal month; a negative one indicates cooler.

Annual column:

Each year was summarized with a monthly weighted mean of the 12 monthly anomalies:

$$A_y^{\text{annual}} = \frac{\sum_m d_{y,m} A_{y,m}}{\sum_m d_{y,m}}$$

where $d_{y,m}$ is the number of days in a month.

The tiles of red and blue reveal the warm and colds months relative to the baseline while the annual bar is concentrated each year into a singular anomaly.

2.4.3. Monthly anomalies of 2024 vs 1991-2020

The year 2024 was taken into account to analyse the anomalies relative to the baseline for every single month. For each month was computed the mean temperature and after was compared with the mean temperature of the baseline: $Anomaly_{m,2024}=T_{m,2024}-C_m$ Where C_m is the baseline and $T_{m,2024}$ is the monthly mean temperature for 2024

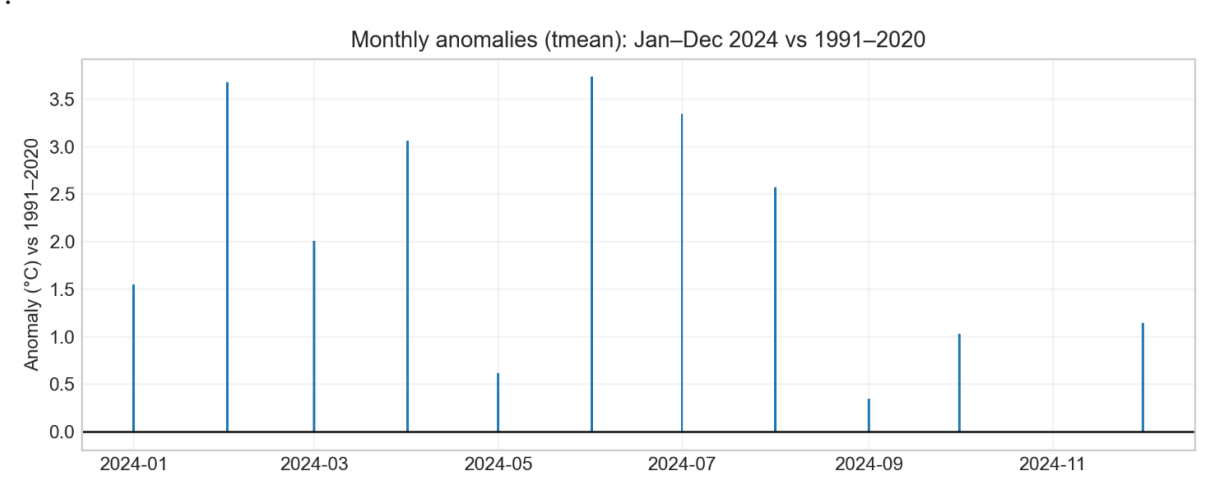


Figure 2.19: Monthly anomalies of 2024

According to the plot the year 2024 was warmer than the baseline with some anomalies during winter where there was a +3°C deviation. The peaks show warm conditions relative to the normal of the baseline. All the seasons are positioned above the baseline showing that 2024 was warmer than the baseline and indicating a possible continuous trend in the future positive anomalies, while autumn (September–November) exhibits smaller but still positive deviations, remaining above the baseline throughout the year.

2.5 Monthly evolution

2.5.1 Monthly analysis from 1979 to 2024

The monthly analysis examines the evolution of monthly temperature over the basin from January 1979 to December 2024.

January: min / mean / max (1979-2024) 15 Monthly minimum Monthly mean Monthly maximum 10 5 emperature (°C) 0 -10 -15 -20 -25 1980 2010 2020 1990 2000

January — Monthly minimum / mean / maximum (1979–2024)

Figure 2.20: January temperature summary

The figure represents the January air temperature conditions in the Vjosa basin from 1970 to 2024 using ERA5 2m data. For each January of these 45 years the blue line represents the coldest daily temperature recorded, the orange line represents the monthly mean and the green line represents the warmest daily temperature.

The mean values during January remain more or less stable around $0\text{-}3^{\circ}\text{C}$ and indicate cool winters. The monthly maxima stay around 9-14 °C and shows mild conditions for the daytime. The monthly minima show a lot of variability with cold temperature below -10°C and some occasional cases below -20°C . The volatility of the temperatures occurs because the min and max series captures one extreme day per month and the areas with a higher elevation can be colder than the valley floors.

February — Monthly minimum / mean / maximum (1979–2024)

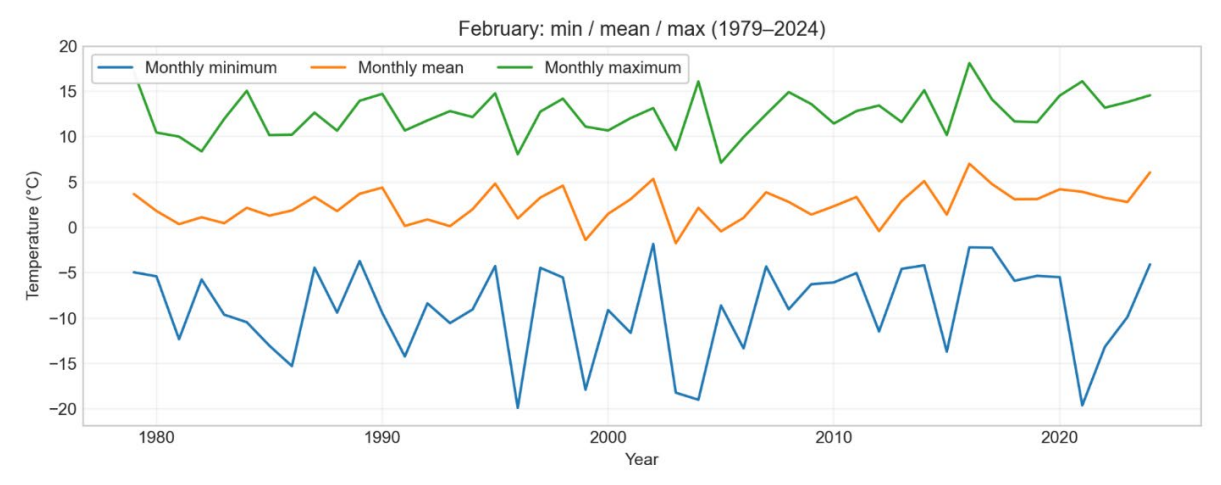


Figure 2.21: February temperature summary

The figure represents the February air temperature conditions in the Vjosa basin from 1970 to 2024 using ERA5 2m data. The blue line represents the coldest daily temperature for each February in 45 years and the minima it seems quite variable with surges below $-10\,^{\circ}$ C and also some extreme events near -18 to $-20\,^{\circ}$ C. Instead, the maxima and mean show a slight upward drift after 1995 also being consistent with late winter warming.

March — Monthly minimum / mean / maximum (1979–2024)

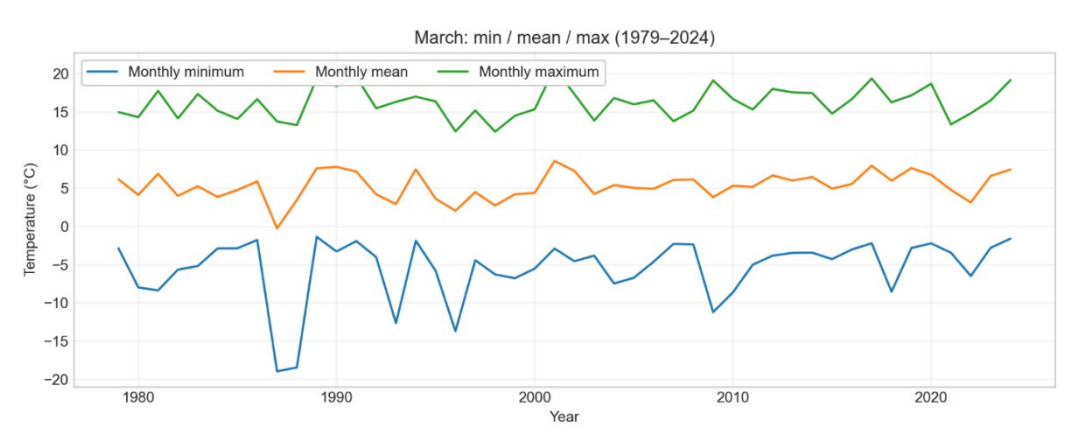


Figure 2.22: March temperature summary

The plot summarizes March air temperatures for 1979–2024. For every March the series report the coldest day of the month for the last 45 years with the blue line. Most years lie between -6 to 0 °C. Instead, the monthly mean which is the orange curve shows temperature that vary between 5-8 °C showing a transition during the spring. The maxima are typically 15-19 °C where some years reach the 20 °C. The minima and maxima curves show a little upward movement after 1995 but in the last two decades extreme minima are less frequent.

April — Monthly minimum / mean / maximum (1979–2024)

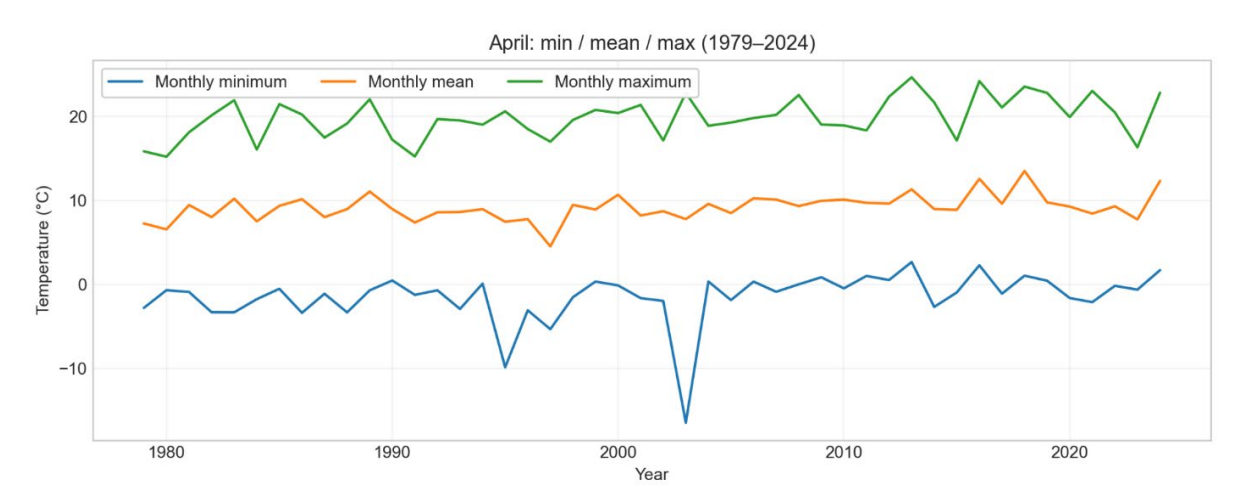


Figure 2.23: April temperature summary

The plot represents all the months of April fro1979 to 2024 in the Vjosa basin. The series report the minima in the blue curve, the mean monthly in the orange curve and the maxima in the green curve. The minima temperatures vary from years to years, for example near the year

2000 there is an extreme event with temperatures near -17 °C but in general the variation has been between -2 to 4°C. The monthly means fall between 8-11 °C and the maxima are 17-23 °C with some rare cases where the temperatures reach 25°C. The mean and maxima show a slight increase with passing of years which is consistent with the warming springs.

May — Monthly minimum / mean / maximum (1979–2024)

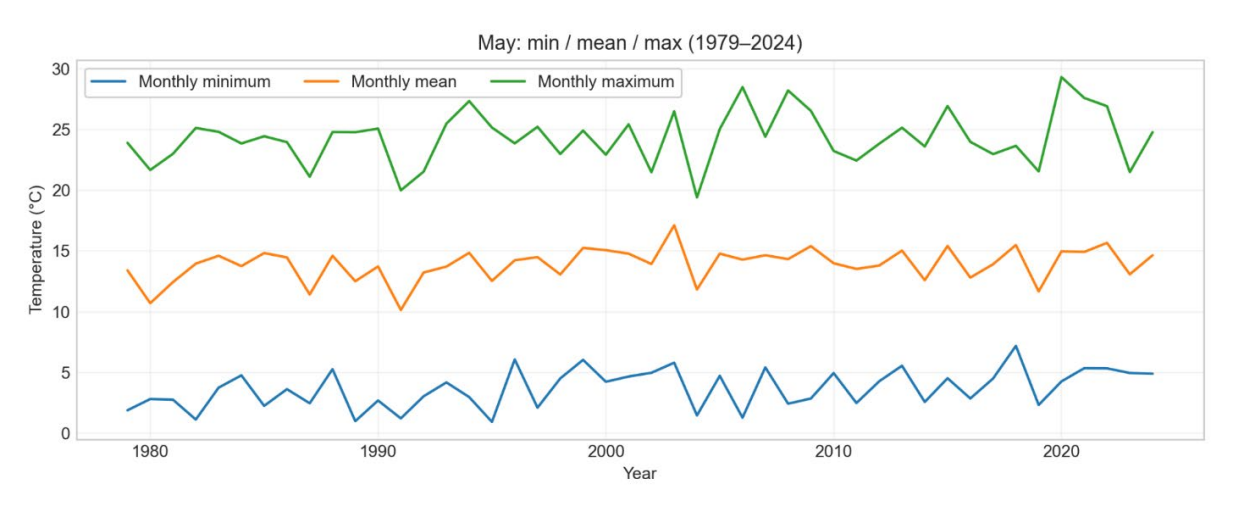


Figure 2.24: May temperature summary

The plot represents the May temperatures over the basin from 1979 to 2024 and for each May there is a minima, maxima and monthly average series. The monthly mean varies between 13-16°C and versus late 1990 there is a light increase. Minima range between 2-6°C in the 1980-1990 decade and the last 20 years it ranges toward 4-7°C suggesting that there has been a slight warming. The maxima are typically 22-28°C with some extreme events reaching 29°C showing frequent mild heat events.

June — Monthly minimum / mean / maximum (1979–2024)

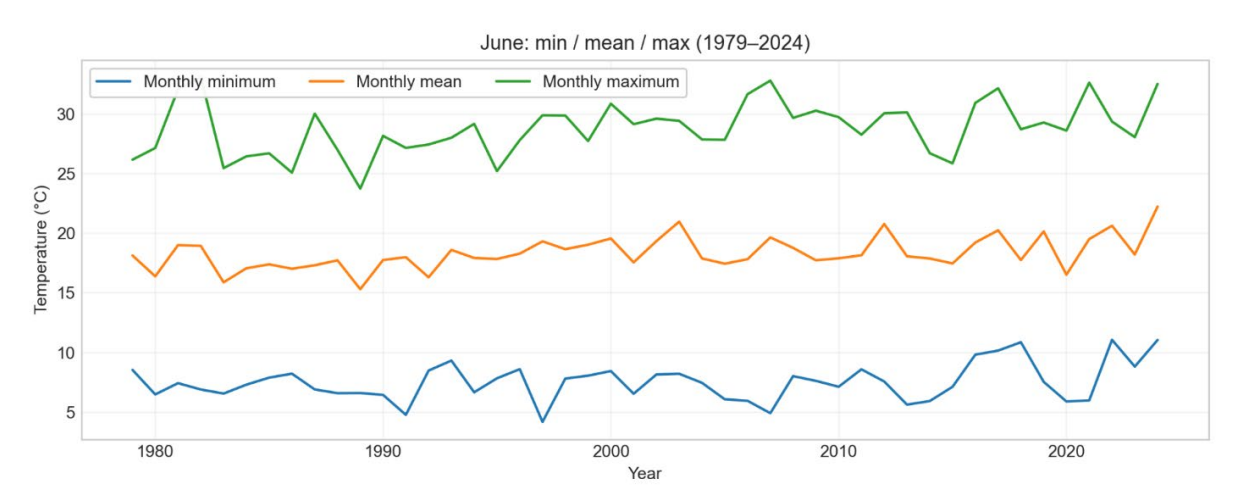


Figure 2.25 June temperature summary

The plot represents the June temperatures from 1979 to 2024 over the basin. Each curve represents the maxima, minima and the monthly average. The minima range between 5-11°Cand there is a small raise after 2010 suggesting some cold nights. The monthly maxima

range between 27-33°C and showing more frequent heat episodes after the 2010s. The monthly means lie between 16-21 °C slightly increasing after 1990 showing also the beginning of a decades with warmer summers.

July — Monthly minimum / mean / maximum (1979–2024)

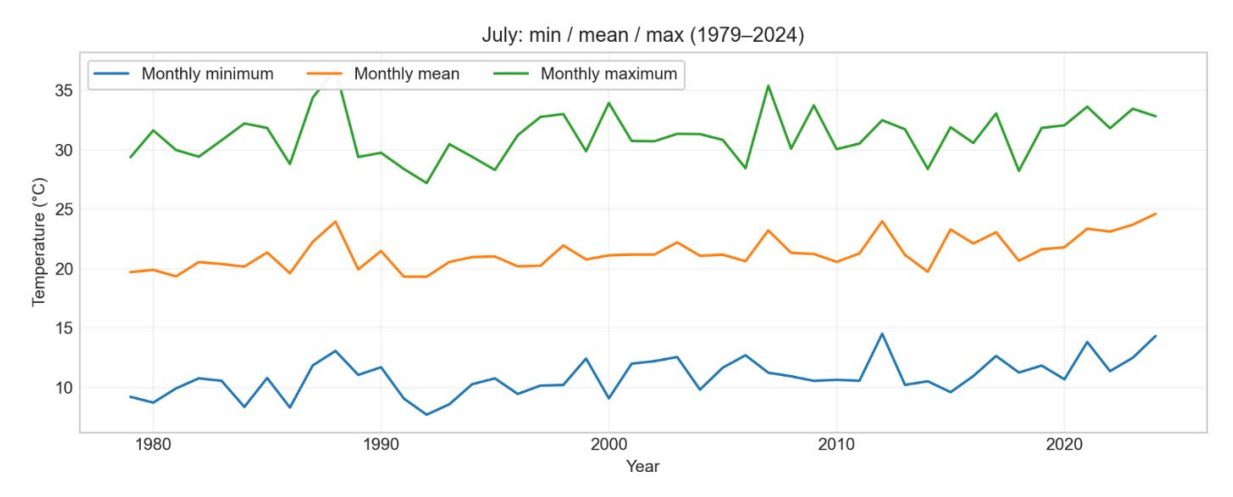


Figure 2.26 July temperature summary

The plot represents the July temperatures over the basin from 1979 to 2024. For every July there is a representation of the monthly minima, maxima and mean. The blue curve represents the minima and the temperatures vary between 8-12°C in the first decade 1980-1990. After in the recent decades there is a rise from 11 to 15°C which again tells about the warming summers. The mean monthly temperatures vary from 20-24°C with an increase after mid-1990s. The maxima lie between 29-34 °C with some peaks near 35°C in the last two decades. With passing years, July has become warmer with some more frequent warm extremes events and warmer nights.

August — Monthly minimum / mean / maximum (1979–2024)

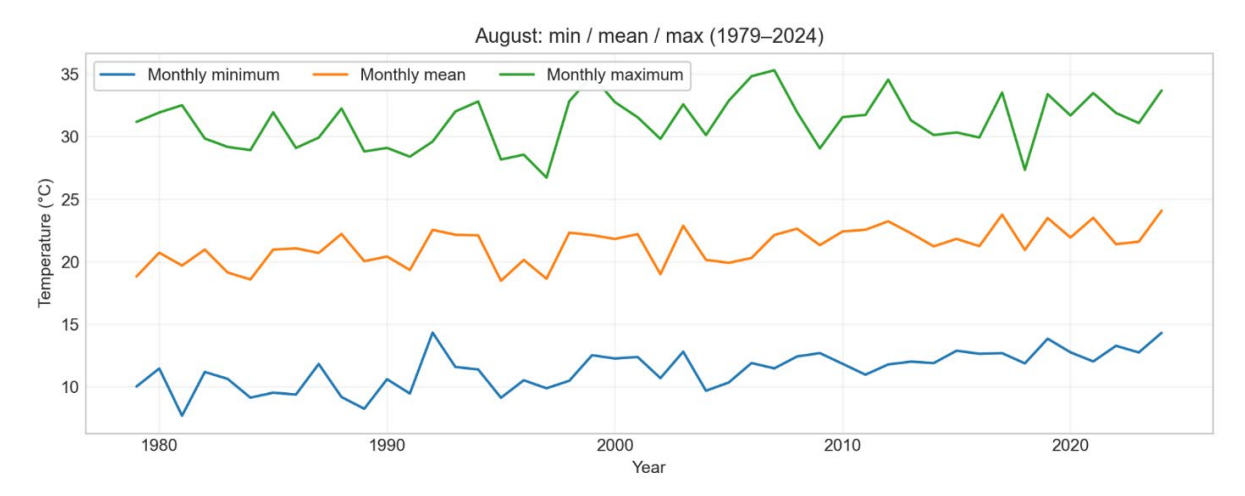


Figure 2.27: August temperature summary

The plot represents the August months from 1979 to 2024 over the basin. The three curves

represent the orange one the monthly mean, the blue one the minima and the green one the maxima. The monthly mean lies between 19 to 23 °C where there is an increase in the late 1990s. The minima vary between 9 to 11°C in the first years but after it reaches 12 to 14 °C showing that with passing years the summers used to get warmer. The maxima range typically between 29 to 35 °C with some hot spells after the 2000s. August shows during the years a persistent high maximum.

September — Monthly minimum / mean / maximum (1979–2024)

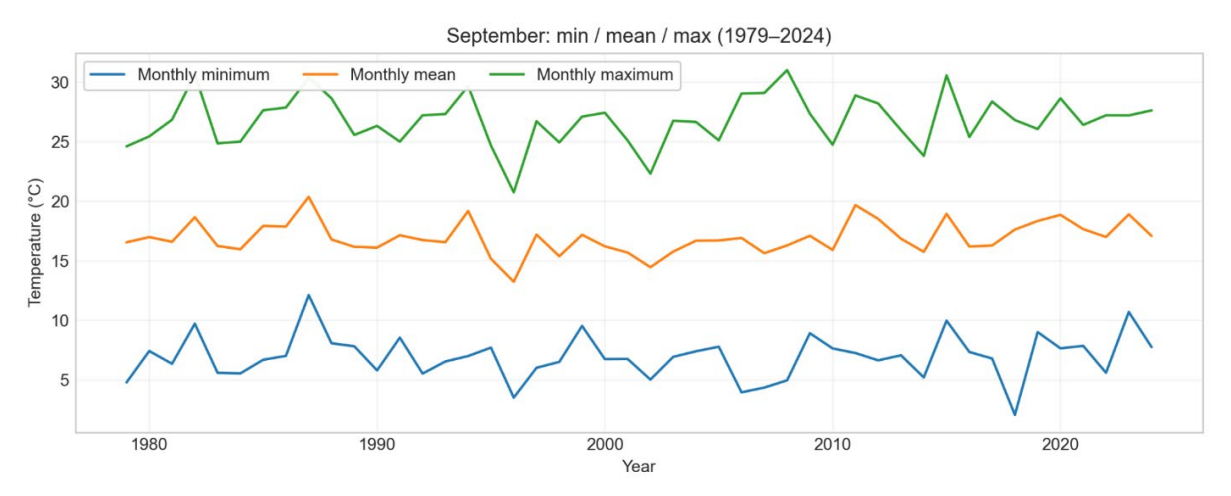


Figure 2.28: September temperature summary

The plot represents all the September temperatures from 1979 to 2024 for Vjosa basin. Every line represents the minima, maxima and mean monthly for each September. The series report the coldest days for each September with a minimum that varies from 4 to 10°C in the first decade and from 6 to 11°C in the recent decades. It shows that with passing years there is an increase in temperature and this is a sign of warming seasons. The mean monthly varies from 16 to 19 °C with a light increase from 2005 and after showing warming autumns. The maxima vary from 25 to 31 °C with some hot spells after 2010 showing that these hot spells extend into September too. The increase of minima and the slight increase of maxima suggest a slightly delayed transition to autumn.

October — Monthly minimum / mean / maximum (1979–2024)

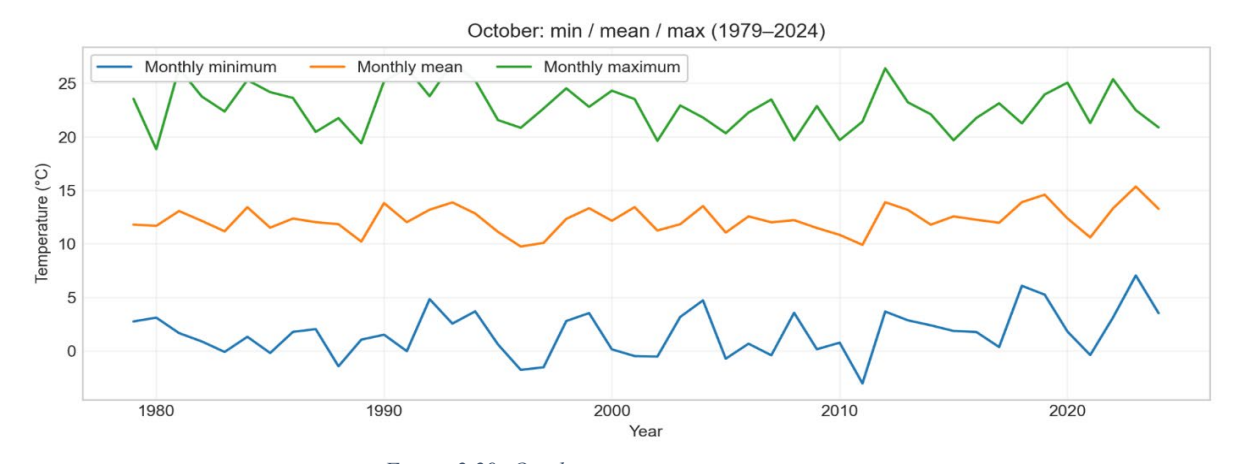


Figure 2.29: October temperature summary

The plot represents the October air temperature of the basin from 1979 to 2024. Each curve represents the minima, maxima and the mean monthly. Minima temperatures are variable because from the curve we can notice that on some years they vary between 0 and 6 °C but in the last years there have been some events with sub-zero temperatures. The monthly means vary from 11 to 14 °C and in the late 2000 after 2020 there has been a slight increase showing signs of milder autumns. The maxima temperatures typicality varies from 20 to 26 °C. October exhibits a warming of the mean values while the maxima are constant suggesting that the transition from summer to autumn is delayed.

November — Monthly minimum / mean / maximum (1979–2024)

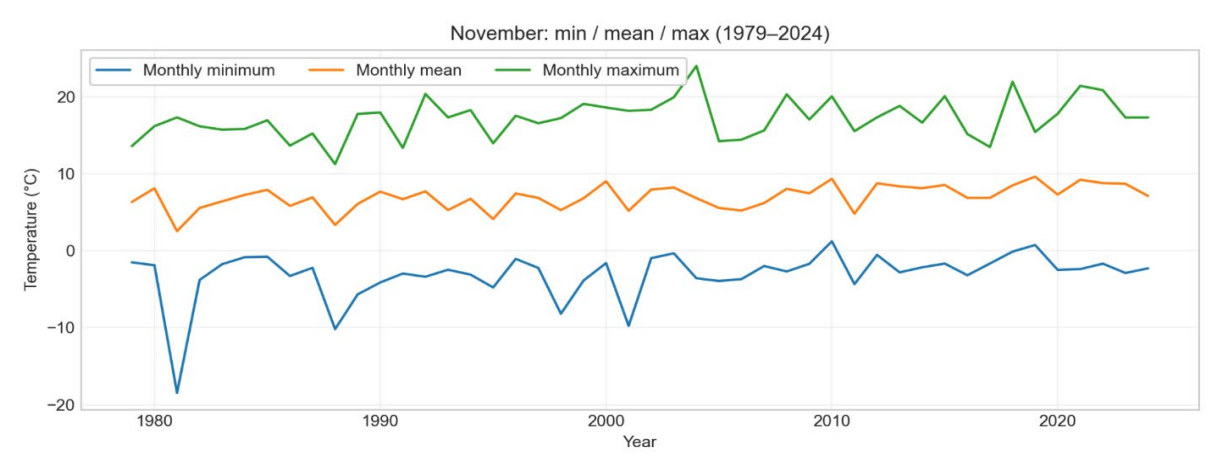


Figure 2.30: November temperature summary

The plot represents the series of November air temperatures over the basin from 199 to 2024. The three curves each of them represents the minima, maxima and the monthly mean. The minima temperature varies from 0 to 6 °C with an extreme drop of -18°C at the beginning of the 1980. The monthly mean lies between 5-9 °C with a little shift after the 2000s showing the milder late autumn. The maxima vary between 14 to 22 °C. November shows a gradual warming of the minima and mean.

December — Monthly minimum / mean / maximum (1979–2024)

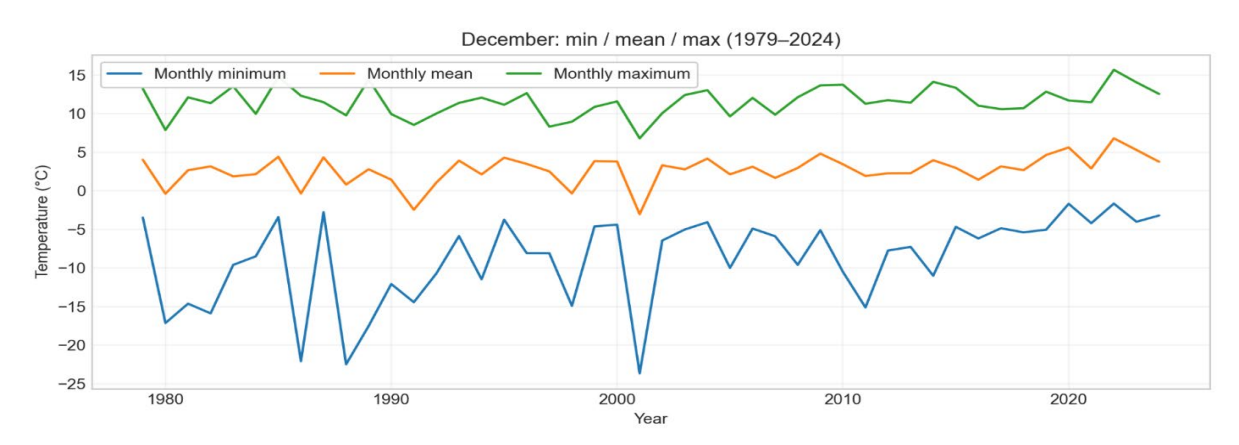


Figure 2.31: December temperature summary

The plot represents the air temperature series for December months from 1979 to 2024 for the Vjosa basin. The three curves represent the maxima minima and the monthly mean. The monthly mean lies between 1 to 6 °C but after 2005 and onward there is a light increase. This increase indicates that winter have gotten milder. The minima are more variable, most years fall from -10 to 2 °C but in mid-1980 and 2001 there were some extreme events with temperatures -20 to -24 °C. The maxima vary from 10 to 15 °C with some higher peaks in the last decades. In the last decade the coldest nights tend to stay -10 °C and upward showing that there is a trend of warmer nights and milder winter.

2.6 Seasonal anomalies

This section describes how surface air temperature has changed across the four seasons—DJF, MAM, JJA, SON—from 1979 to 2024 over the Vjosa basin. Through monthly, the average basin temperature was extracted using the and aggregate it to seasonal means.

DJF (Winter) — Seasonal minimum / mean / maximum (1979–2024)

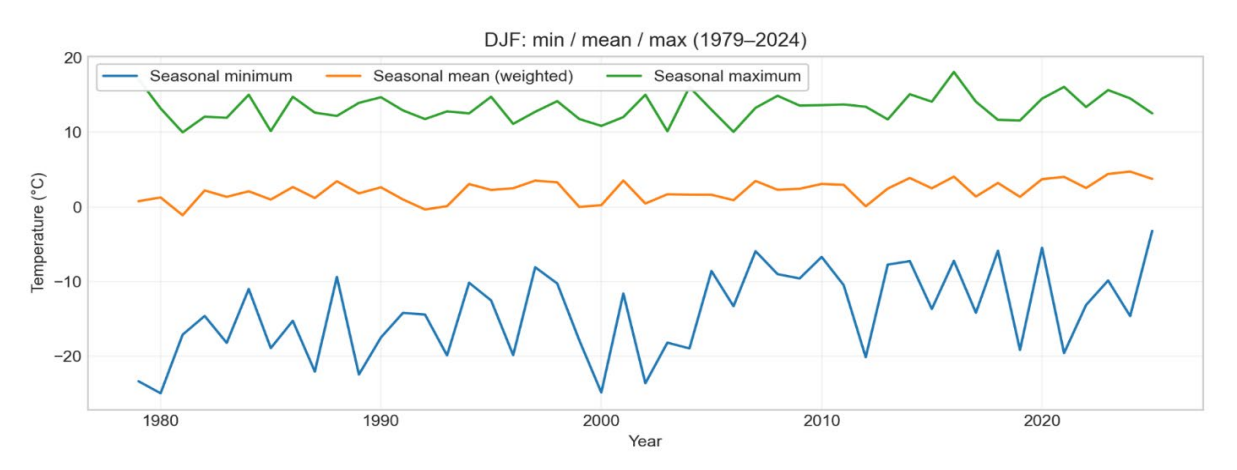


Figure 2.32: DJF (Winter) seasonal temperature summary

The plot summarizes the winter season from 1979 to 2024 through the air temperatures over the basin. The orange curve shows the seasonal mean and it ranges between 0 to 4°C and after the 1990 it shows a little increase which means milder winters. The green curve represents the seasonal maxima and it reaches 10 to 17°C. It displays higher peaks after 2003 which shows again the presence of milder winters. The blue curve shows the seasonal minima where in the 1980 there were some extreme events with temperatures below -20 °C. In the last years the temperatures have dropped till 15°C. In general, the three curves show that winters have become warmer with less extreme events.

MAM (Spring) — Seasonal minimum / mean / maximum (1979–2024)

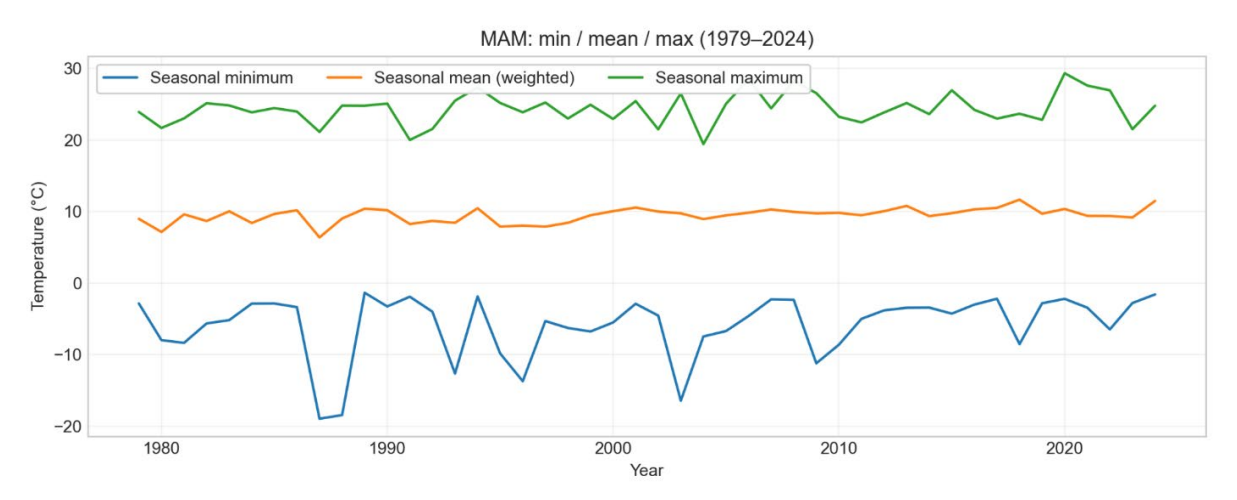


Figure 2.33: MAM (Spring) seasonal temperature summary

The figure represents the spring from 1979 to 2024 through the air temperatures. The orange curve shows the seasonal mean and it ranges between 8 to 11°C and after the 1990 it shows a little increase which means milder springs. The green curve represents the seasonal maxima and it reaches 22 to 28°C. The blue curve shows the seasonal minima where in the 1980 there were some extreme events with temperatures below -18 °C. In general, the spring indicates a warming with high warm days and a decrease of temperature during the night. This last is important for river thermal regimes.

JJA (Summer) — Seasonal minimum / mean / maximum (1979–2024)

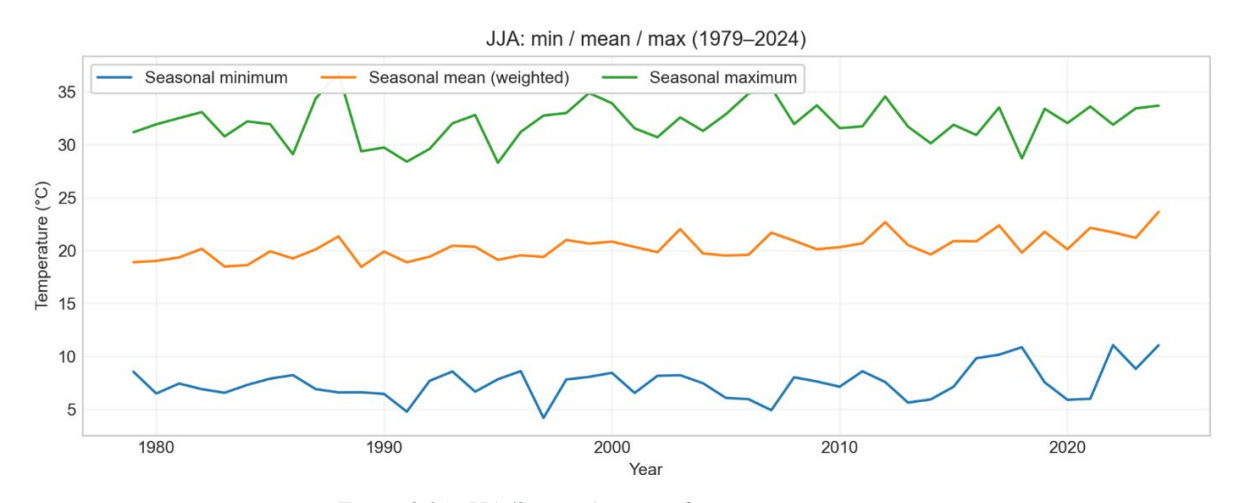


Figure 2.34: JJA (Summer) seasonal temperature summary

The figure represents the summer from 1979 to 2024 through the air temperatures. The orange curve, seasonal mean varies around 19-22°C. The maxima which are the green curve is quite high 35°C also showing that heat waves are present every year. The seasonal minima rise from 8°C in the 80s, 90s till 9-11°C after 2010. This last change indicates fewer cool nights. All three curves show long hotter summers with very little nocturnal cooling which increase the thermal loads on rivers.

SON (Autumn) — Seasonal minimum / mean / maximum (1979–2024)

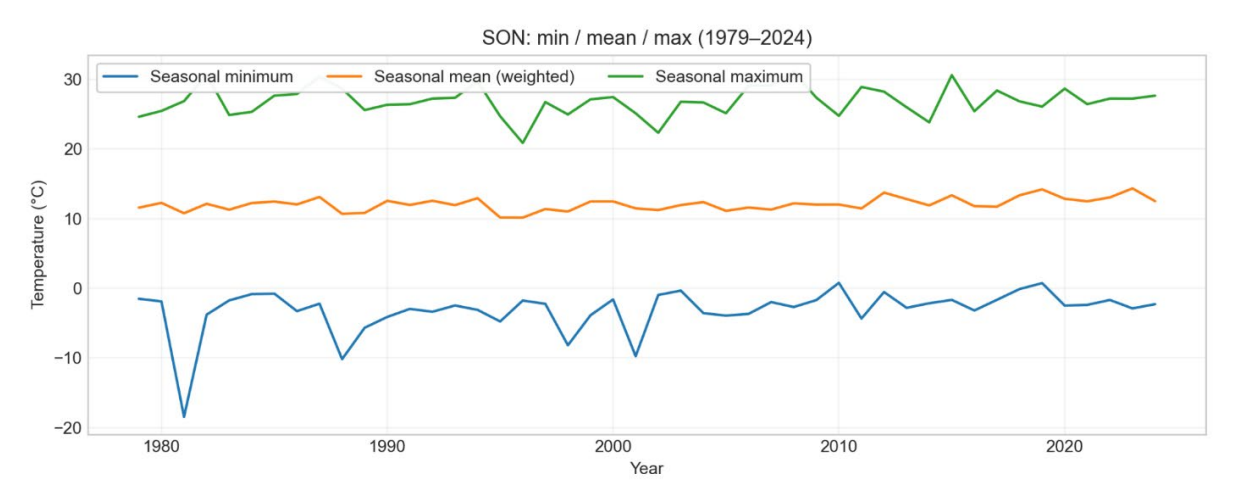


Figure 2.35: SON (Autumn) seasonal temperature summary

The figure shows autumn seasonality through air temperatures from 1979 to 2024. The seasonal mean varies from 10 to 13°C and there is a light rise after the 2005 toward 12-14°C. The maxima are high and vary from 24 to 30 °C showing that usually summer days extend until October. The seasonal minima move from -6 to 0 °C with some cold events in 1980 with temperatures near -18 °C. Autumn seasonality points out delayed transitions from summer.

2.7 12- Month moving average

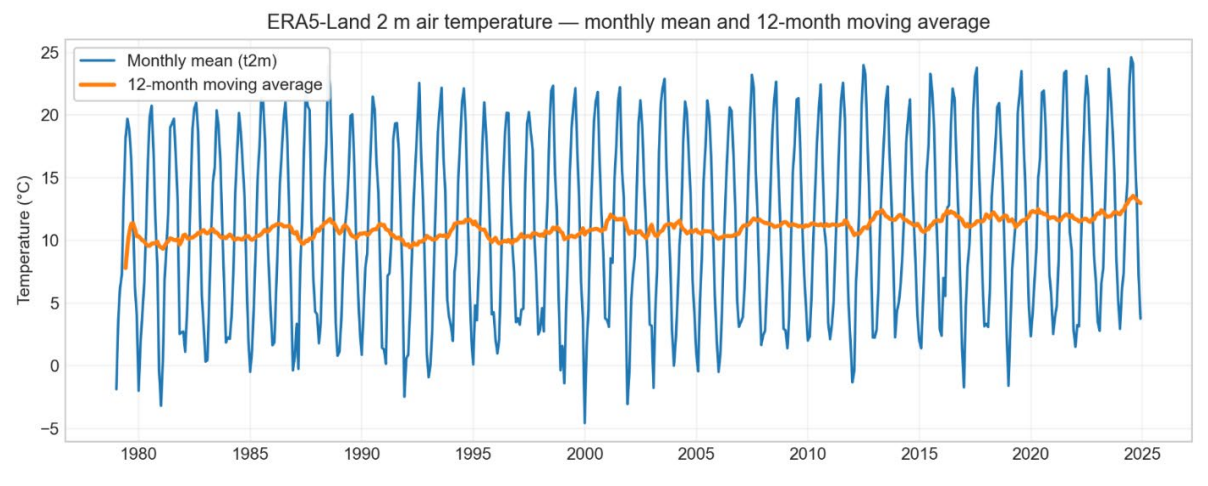


Figure 2.36: Monthly mean and moving average

The figure shows the air temperature as monthly means and a 12-month moving average. The blue curve is the monthly means instead the orange is the 12-month moving average. The blue series show the annual cycle with the minima and maxima and the orange series reveals the background climate signal. The series temperature increases about 10 °C in the beginning of 1980 and reach 13°C by 2024. This indicates a rise of 2-3 °C in the mean air temperature.

A cooler phase is present in the late 1980 and 1990 followed by a rise toward 2015 with the warmest multi-year period since 2018. The plot confirms a persistent warming that elevates the baseline for summer and autumn and automatically implicates also higher river temperatures.

2.8 Mann- Kendall Test

A Mann Kendall Test was generated with all the present data from ERA5 because it is important for cl,imate studes to ujnderstand not only the series but also if the trend is statistically significant. This kind of test is used because is not much sensitive to the extreme events, it is possible to integrate long time series also can evaluate if there are upward or downward trends. [23](IPCC, 2014; Yue & Pilon, 2004).

The test followed the method explained below:

The air temperature downloaded from ERA5 database was converted in $^{\circ}$ C from K and divided into maxima, minima and daily mean. For each series of 46 years was applied the MK test if there was significant upward or downward trend on tmin, tmax and tmean. The two important parameters are tau which represents the positive values and the p values that shows if the trend is significant, usually when < 0.05. The statistic was computed:

$$S = \sum_{i=1}^{n-1} \sum_{j=i+1}^{n} sgn(x_j - x_i), \quad sgn(x_j - x_i)$$

{+1 if xj > xi 0 if xj = xi - 1 if xj < xi

A normal score Z and a P value were obtained from S variance. After a Sen slope was calculated which is a median to all slopes:

$$\beta = median \left(\frac{xj - xi}{j - i} \right)$$
, where j>i

Annual slopes are represented in °Cyr-1 instead monthly ones are represented in °Cdecade-1 *10. (Hamed & Rao, 1998; Yue & Pilon, 2004).

Variable	N (<u>years</u>)	Kendall's tau	p-value	Sen slope (°C/year)	Sen slope (°C/decade)	Trend (α=0.05)
TMAX	46	0,426	0,0000	0,039	0,387	increasing
TMEAN	46	0,658	0,0000	0,045	0,447	increasing
TMIN	46	0,542	0,0000	0,069	0,689	increasing

Table 2.1: Mann Kendall Test

The table shows the results of Mann Kendell Test where there is a significant warming trend with p < 0.001. The Kendell tau is a correlation coefficient that shows the direction of the trend and in our case since there are positive values it means rising temperatures. The p-value is the probability that the results are due to chance but since in our case p value is < 0.001 it means that the results are statistically correct. The Sen's slope represents how much do the temperatures change every year. All the three variables indicate a warming trend where the minimum increases faster than the maximum which is another pattern of the Mediterranean climate.

Month	N (years)	Kendall's tau	p-value	Sen <u>slope</u> (°C/decade)
Jan	46	0,202	0,0478	0,476
Feb	46	0,243	0,0175	0,520
Mar	46	0,198	0,0523	0,417
Apr	46	0,252	0,0135	0,436
May	46	0,223	0,0287	0,270
Jun	46	0,324	0,0015	0,476
Jul	46	0,461	0,0000	0,592
Aug	46	0,380	0,0002	0,627
Sep	46	0,109	0,2847	0,142
Oct	46	0,144	0,1583	0,181
Nov	46	0,345	0,0007	0,531
Dec	46	0,217	0,0331	0,440

Table 2.1 Monthly Tmin Mann Kendall Test

A positive tau during all the months shows a warming trend. Overall, the table shows a warming year by also reducing the winter low temperatures.

Month	N (<u>years</u>)	Kendall's tau	p-value	Sen <u>slope</u> (°C/decade)
Jan	46	0,181	0,0766	1,321
Feb	46	0,090	0,3786	0,356
Mar	46	0,144	0,1583	0,432
Apr	46	0,295	0,0039	0,557
May	46	0,268	0,0087	0,502
Jun	46	0,121	0,2366	0,245
Jul	46	0,328	0,0013	0,581
Aug	46	0,509	0,0000	0,793
Sep	46	0,096	0,3486	0,188
Oct	46	0,142	0,1640	0,319
Nov	46	0,171	0,0938	0,352
Dec	46	0,331	0,0012	1,976

Table 2. 2 Monthly Tmax Mann Kendall Test

The table show that the temperatures indicate a general warming trend. There is a strong increase in summer and in December. These values indicate extreme heat events during summer and less cold events during winter.

Month	N (<u>years</u>)	Kendall's tau	p-value	Sen <u>slope</u> (°C/decade)
Jan	46	0,252	0,0135	0,503
Feb	46	0,217	0,0331	0,532
Mar	46	0,136	0,1819	0,345
Apr	46	0,299	0,0034	0,860
May	46	0,105	0,3021	0,292
Jun	46	0,308	0,0025	0,762
Jul	46	0,202	0,0478	0,437
Aug	46	0,190	0,0621	0,428
Sep	46	0,098	0,3389	0,202
Oct	46	-0,125	0,2219	-0,312
Nov	46	0,237	0,0204	0,734
Dec	46	0,150	0,1422	0,352

Table 2. 3 Monthly Tmean Mann Kendall Test

The table show that the mean temperatures indicate a general warming trend. Most months are warm and the mean temperature increases more during in late spring.

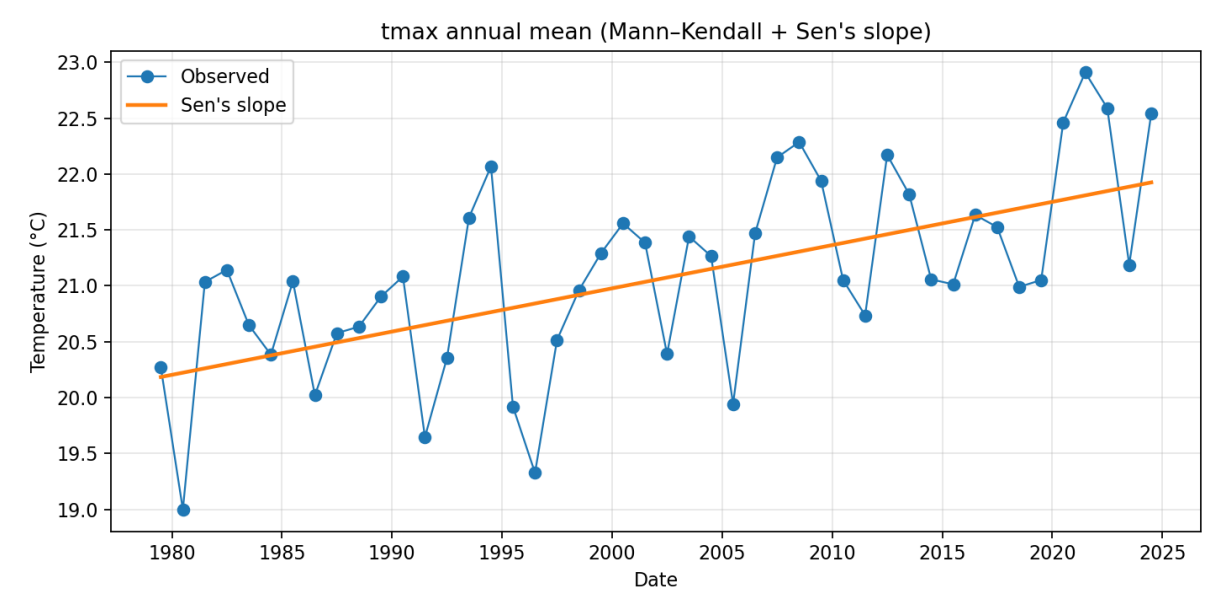


Figure 2.37: Tmax annual mean MK Test

The figure shows the result of the Mann - Kendall Test and how the maxima has evolved during the years. The blue curve indicates the max daily temperatures and the orange line indicates the Theil-Sen median slope. There is an increase tendency where the Theil-Sen slope is $+0.39^{\circ}$ C for each decade where: p < 0.001; N = 46, $\tau = 0.426$ also an increase in order of magnitude of $+1.8^{\circ}$ C across the years. Higher daytime peaks increase the possibility of higher summer thermal threshold which will have effects on the river thermal regime.

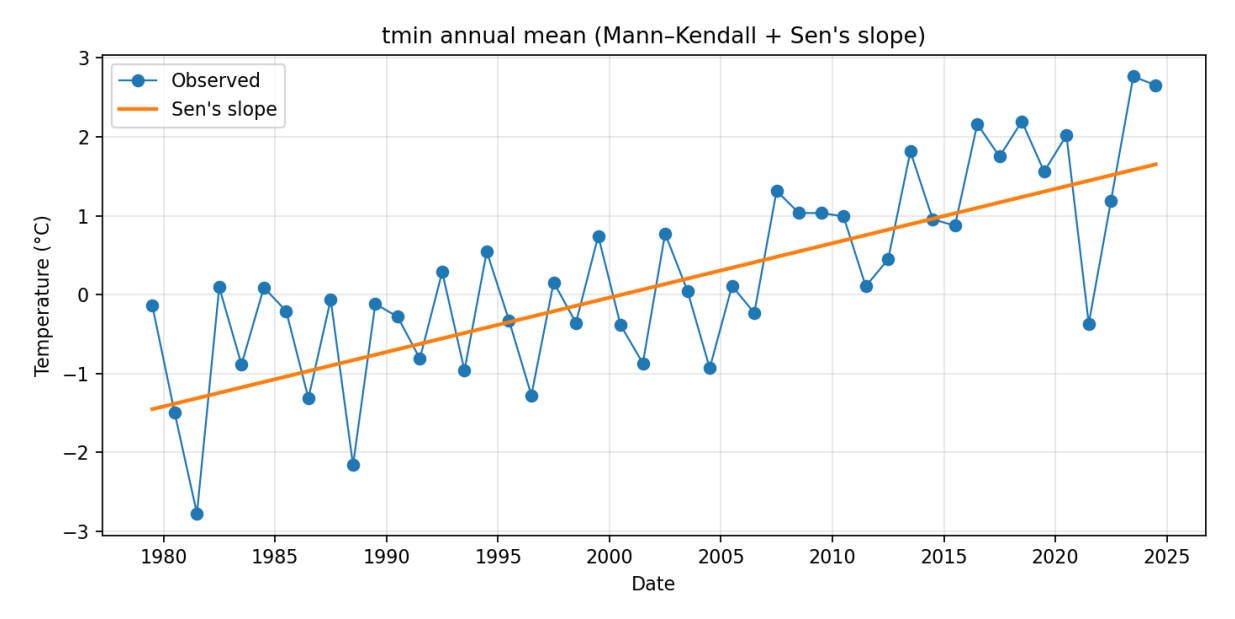


Figure 2.38: Tmin annual mean MK Test

The figure shows the result of the Mann - Kendall Test and how the minima has evolved during the years. The blue curve indicates the min daily temperatures and the orange line indicates the Theil-Sen median slope. There is an increase tendency where the Theil-Sen slope is $+0.07^{\circ}$ C for each decade where: p < 0.001; N = 46, $\tau = 0.542$ also an increase in order of magnitude of $+3.2^{\circ}$ C across the years. A warmer average minimum temperature increases the baseline water temperatures impacting the river conditions and its thermal regime.

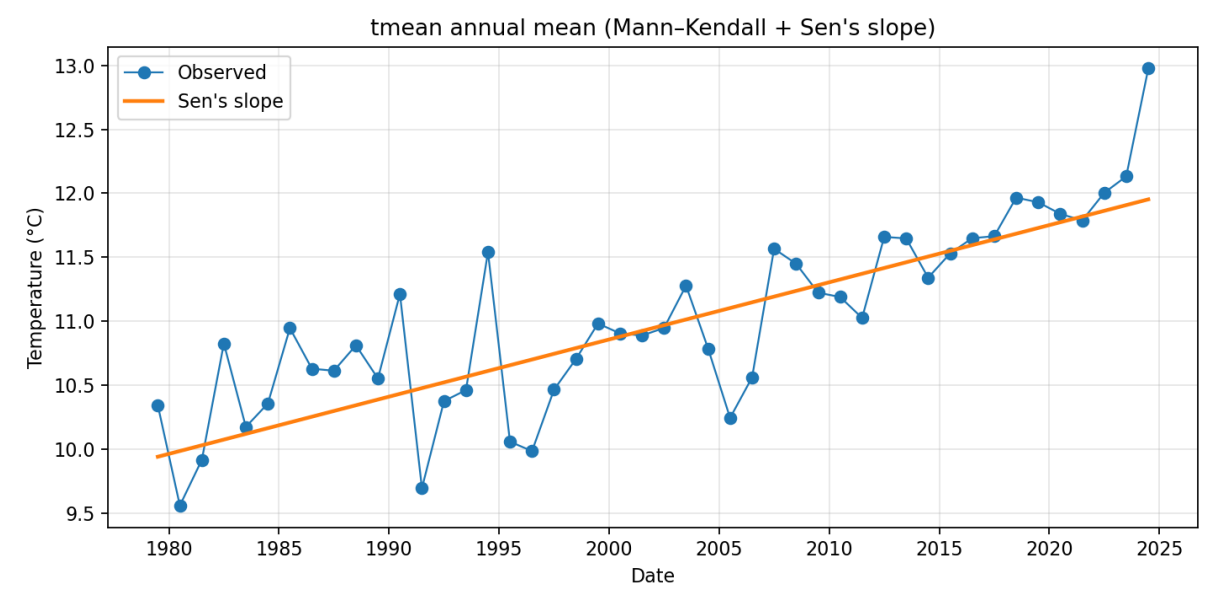


Figure 2.39: Tmean annual mean MK Test

The figure shows the result of the Mann - Kendall Test and how the minima has evolved during the years. The blue curve indicates the mean annual daily temperatures and the orange line indicates the Theil-Sen median slope. There is an increase tendency where the Theil-Sen slope is +0.45°C for each decade where: p < 0.001; N = 46, $\tau = 0.658$ also an increase in order

of magnitude of $+2^{\circ}$ C across the years. With a slope value of $+0.45^{\circ}$ C is expected a warmer water temperature and an increase of the heat stress.

2.9 Data approach and evaluation: ERA5, in-situ loggers, local bulletins

ERA5 are downloaded from the CDS and converted from NetCDF to csv format. Time is harmonized to local time. With the downloaded data daily statistics (mean/min/max) is calculated and compared with the data of the station and logger. Linear Bias Correction and Quantile Mapping are implemented for the downstream analysis so the reanalysis temperature matches observations without erasing long-term change signals. Results are showed through bias, RMSE, MAE, and R² pre/post-correction.

The plots represent the comparison of ERA5's data air temperature and the meteorological station's data for the months of August 2022,2023,2024. In the scatter plots with the minimum and maximum temperature comparison, the 1:1-line represents the perfect agreement.

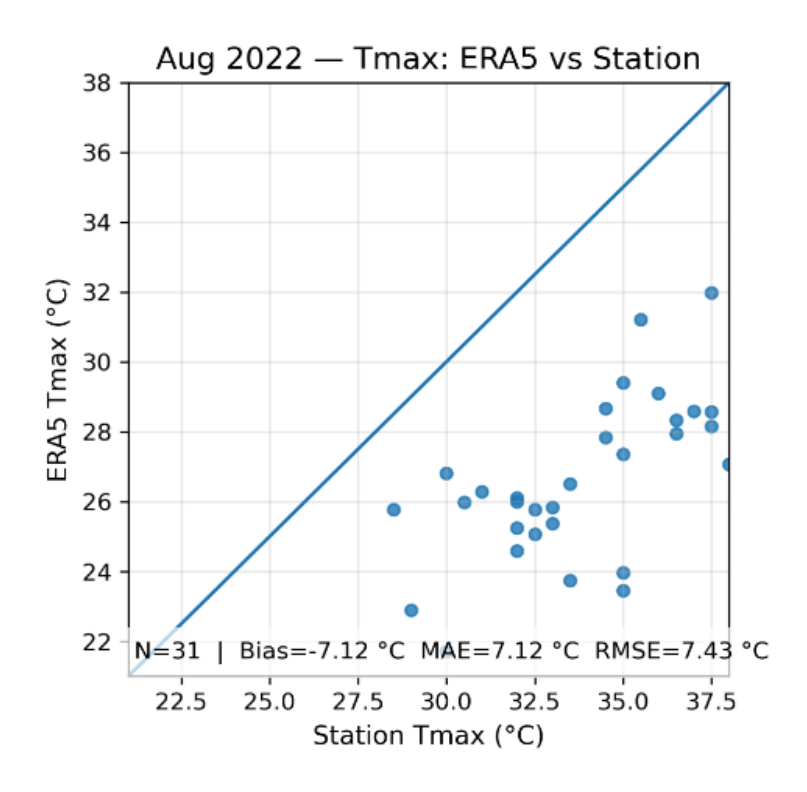


Figure 2.40, a: Comparison of ERA5 and Station Daily Maximum Temperatures (Tmax) — August 2022

In the T max scatter plot, most of the points are below the diagonal, which means that ERA5 data rap resents the temperature lower that the one measured from the station. The average bias, which is the mean difference between ERA5 values and station's values, is a negative value (-7.12 °C). This means that the model (ERA5) systematically underestimates the true values. MAE (mean absolute error), is the average of the absolute differences between ERA5

data and station data. In simpler words it tells how on a typical day, how far off the model is from the right values. For august 2022, MAE is 7.1 °C showing that in a typical august day, ERA5 Tmax is 7.1 °C away from the observed value. The RMSE (Root Mean Square Error) is about 7.4 °C and is close to the Bias. This indicates the underestimation is uniform in one direction, always too cold.

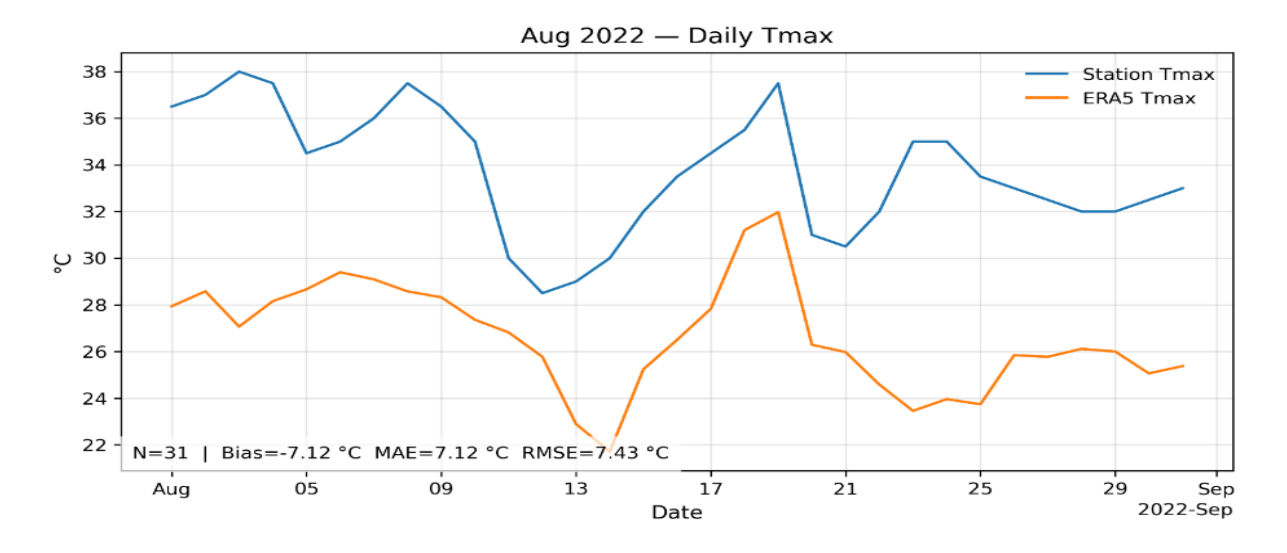


Figure 2.40, b: Comparison of ERA5 and Station Daily Maximum Temperatures (Tmax) — August 2022

In the Tmax series plot, the orange curve represents ERA5 data and the blue one represents the station data. We can notice that both curves go up and down at the same times but the orange curve stays about 5–10 °C lower most days.

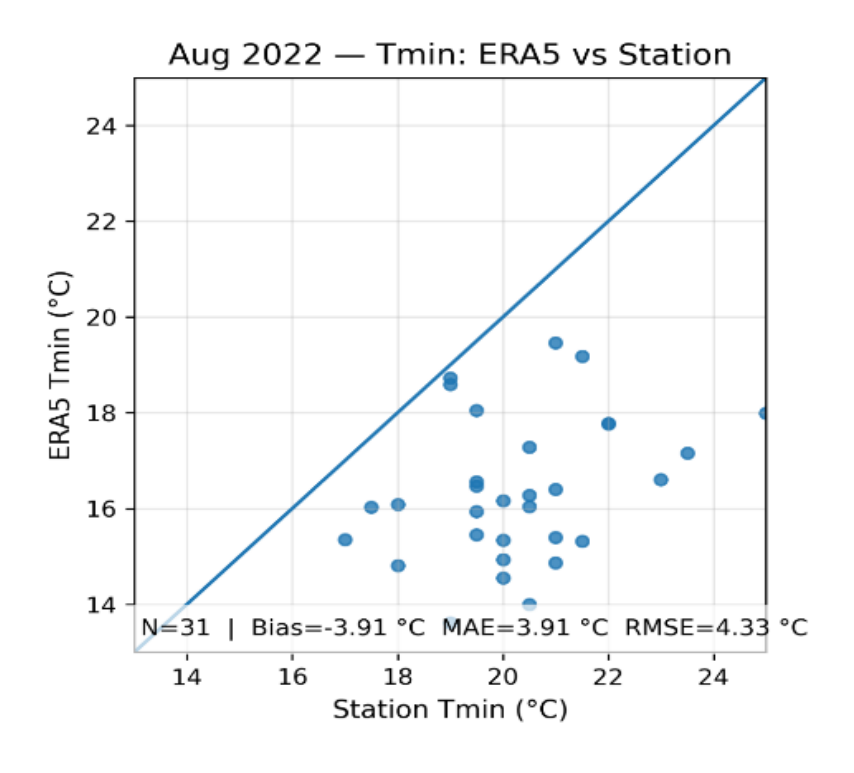


Figure 2.41, a: Comparison of ERA5 and Station Daily Minimum Temperatures (Tmin) — August 2022

In the Tmin scatter plot, most of the points are again below the line, which means that ERA5 also underestimates the temperature during the nights. Bias is -3.91 °C, which means that nights in ERA5 are almost 4 °C colder. MAE is 3.91 °C, which means that ERA5 Tmin differs from station with this value. Also is equal to the Bias which means that the error is almost one sided.

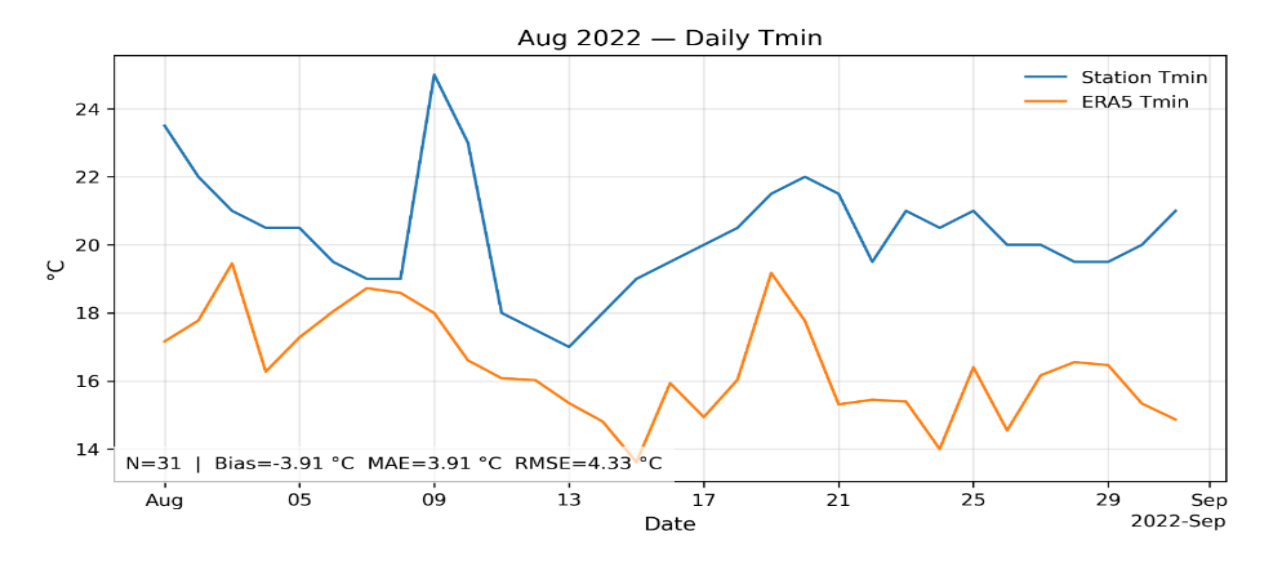


Figure 2.41, b: Comparison of ERA5 and Station Daily Minimum Temperatures (Tmin) — August 2022

In the Tmin series plot, the orange curve rapresent ERA5 data and the blue one rapresent the station data. ERA5 underestimates the magnitude of variations, for example on August 8–10, station Tmin spikes above 24 °C, but ERA5 only reaches 19 °C.

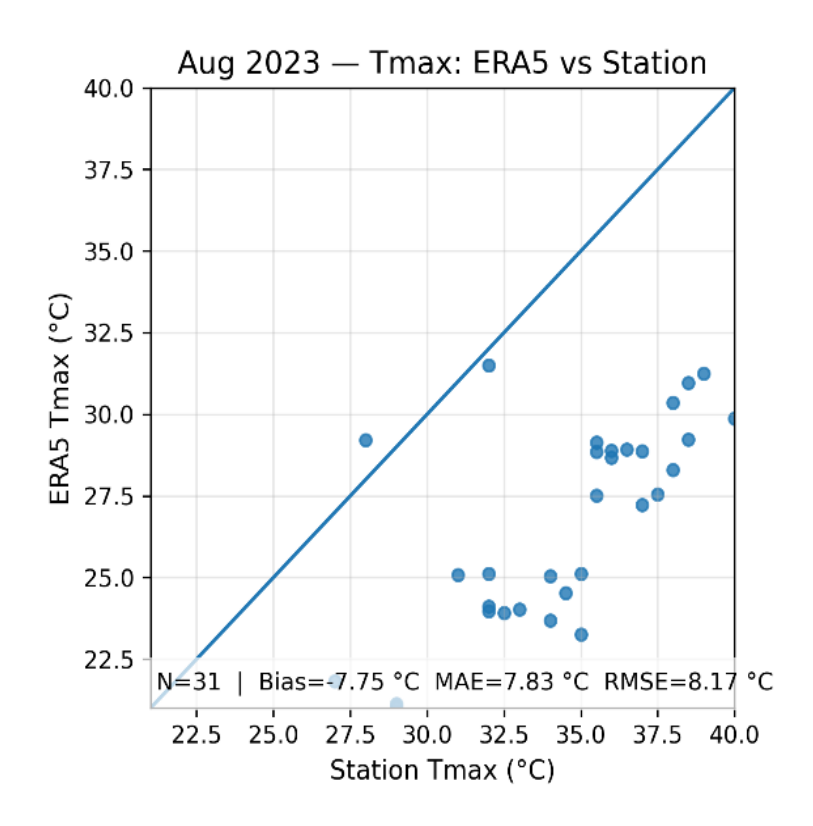


Figure 2.42, a: Comparison of ERA5 and Station Daily Maximum Temperatures (T max) — August 2023

In the T max scatter plot, most of the points are below the diagonal, which means that ERA5 still underestimates the values of T max. The average bias is a negative value (-7.75 °C) and reconfirms what was underlined before. MAE is 7.83 °C and RMSE is about 8.17 °C. This indicates the underestimation is uniform in one direction, always too cold. The values above reconfirm a consistent bias but worse than in August 2022 for T max.

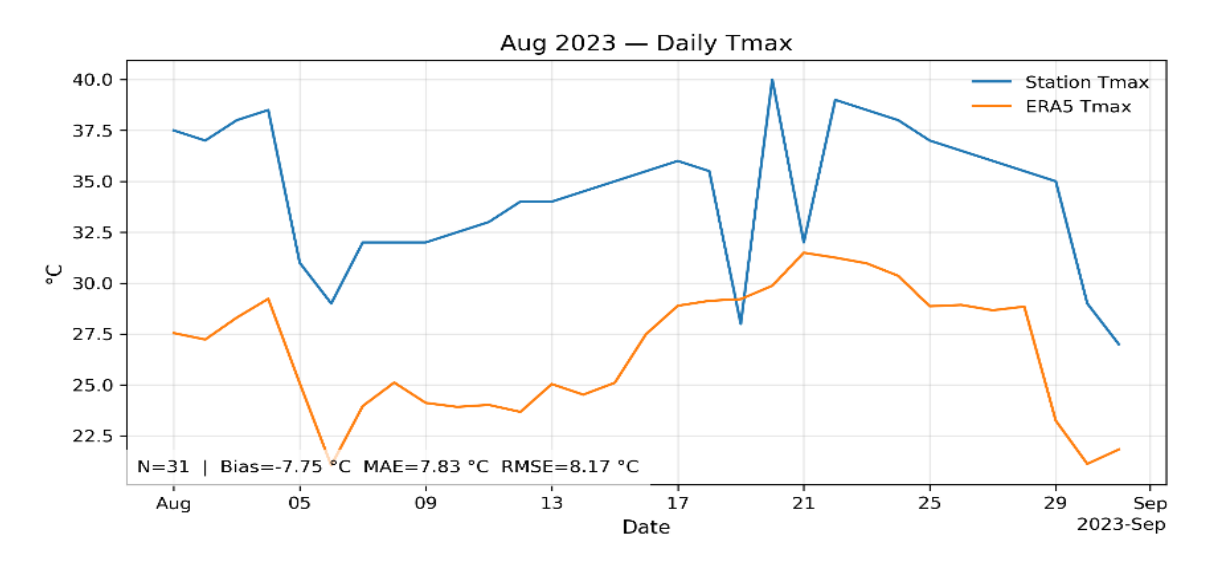


Figure 2.42, b: Comparison of ERA5 and Station Daily Maximum Temperatures (T max) — August 2023

In the T max series plot, both ERA5 and the station show peak and troughs almost at the same time but the ERA5 curve is always a little lower especially on early august.

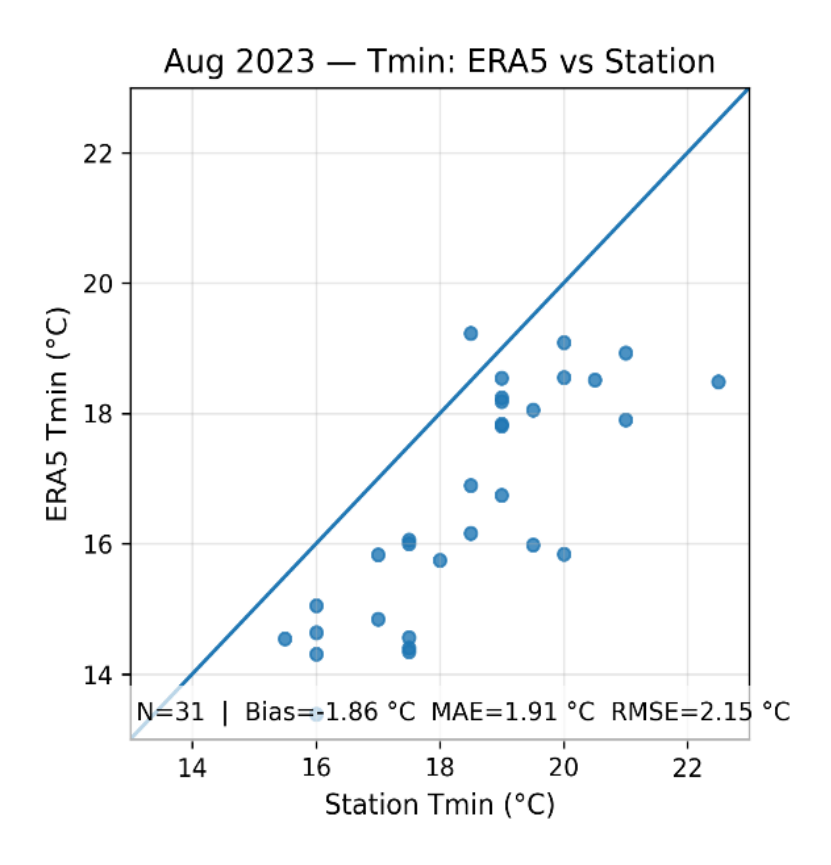


Figure 2.43, a: Comparison of ERA5 and Station Daily Minimum Temperatures (T min) — August 2023

In the T min scatter plot, almost most of the points are closer to the line with a small bias -1.86 °C, which means that nights in ERA5 are still cooler but the error according to MAE 1.91 °C; RMSE 2.15 °is much smaller than for the daytime.



Figure 2.43, b: Comparison of ERA5 and Station Daily Minimum Temperatures (Tmin) — August 2023

The T min timeseries shows how ERA5 follows the day-to-day pattern and always stays on a slightly cooler baseline.

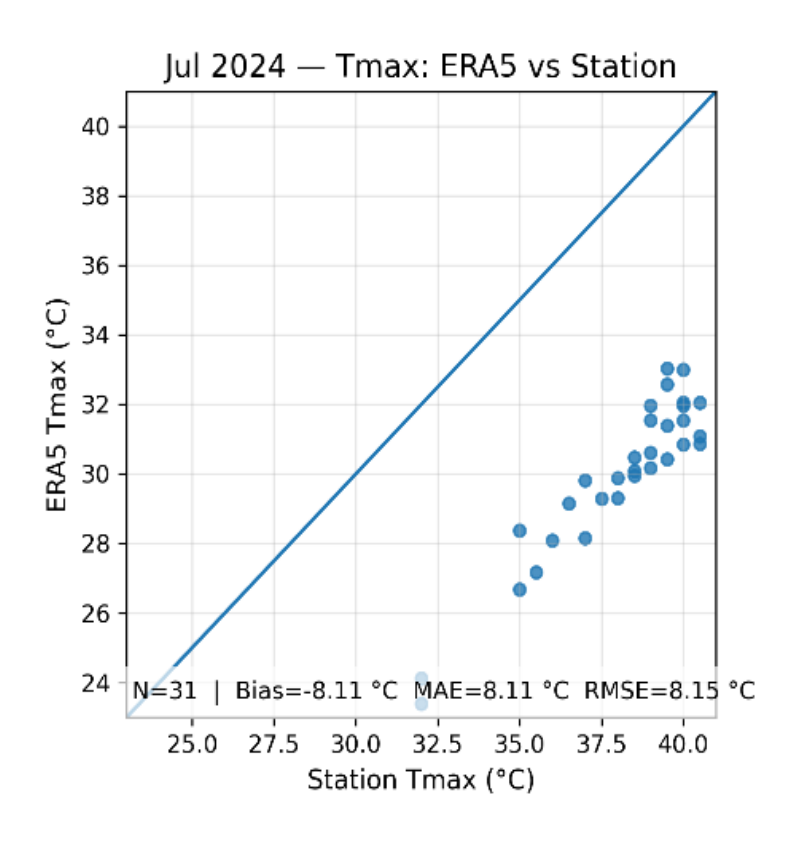


Figure 2.44, a: Comparison of ERA5 and Station Daily Maximum Temperatures (T max) — July 2024

Tmax scatter plot shows that the diagonal is below all the points (ERA5 compared to the station). This means that ERA5 is colder that the station on the days with the highest temperatures. The Bias -8.1° C shows that ERA5 is about 8 °C colder than the station. The daily errors (MAE 8.1 and RMSE 8.2) are large and very close in value, meaning underestimation is systematic.

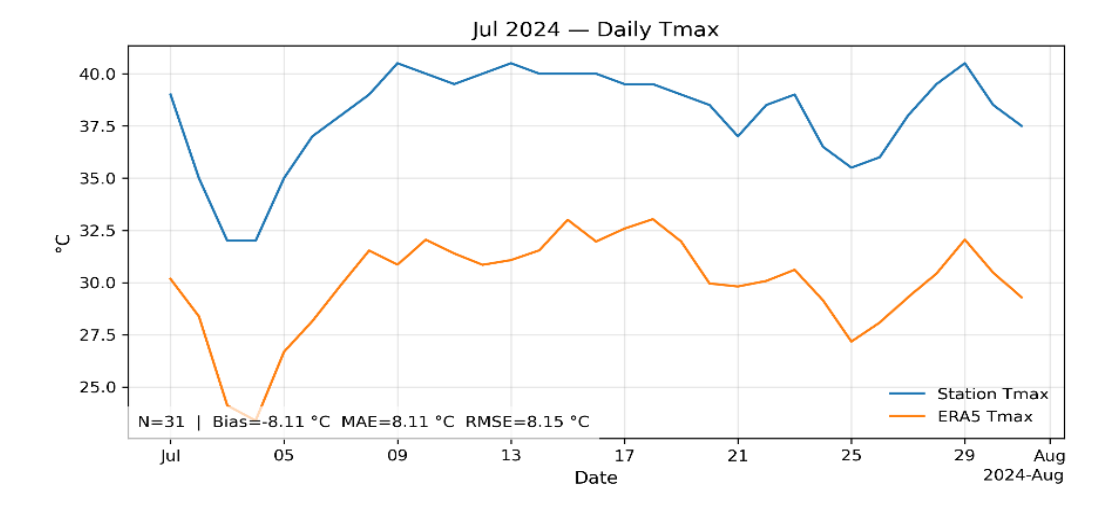


Figure 2.44, b: Comparison of ERA5 and Station Daily Maximum Temperatures (T max) — July 2024

The timeseries shows that ERA5 remains steady under the station's curve which again confirms the cold bias.

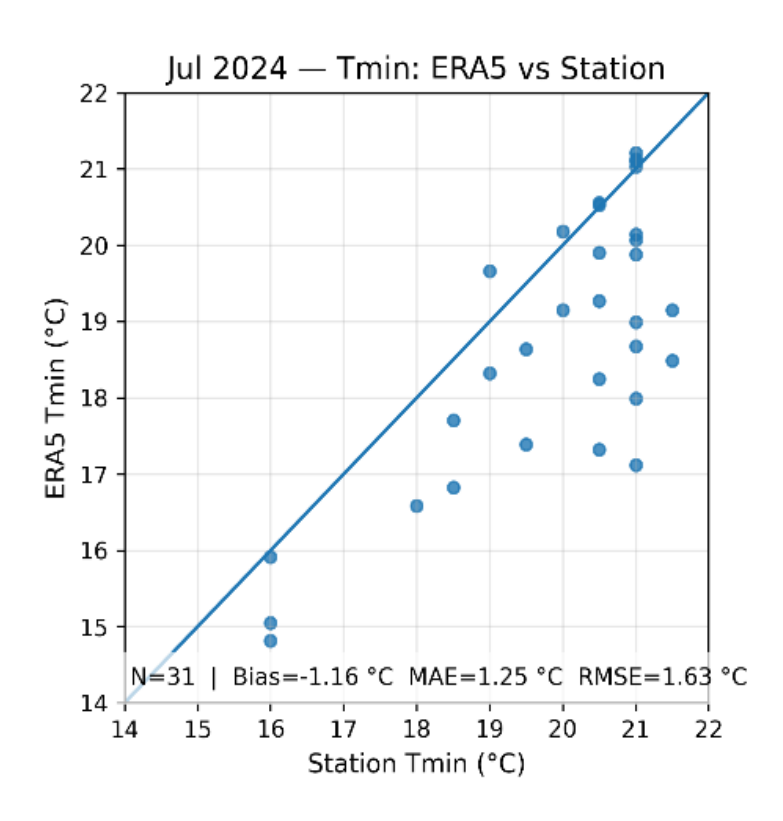
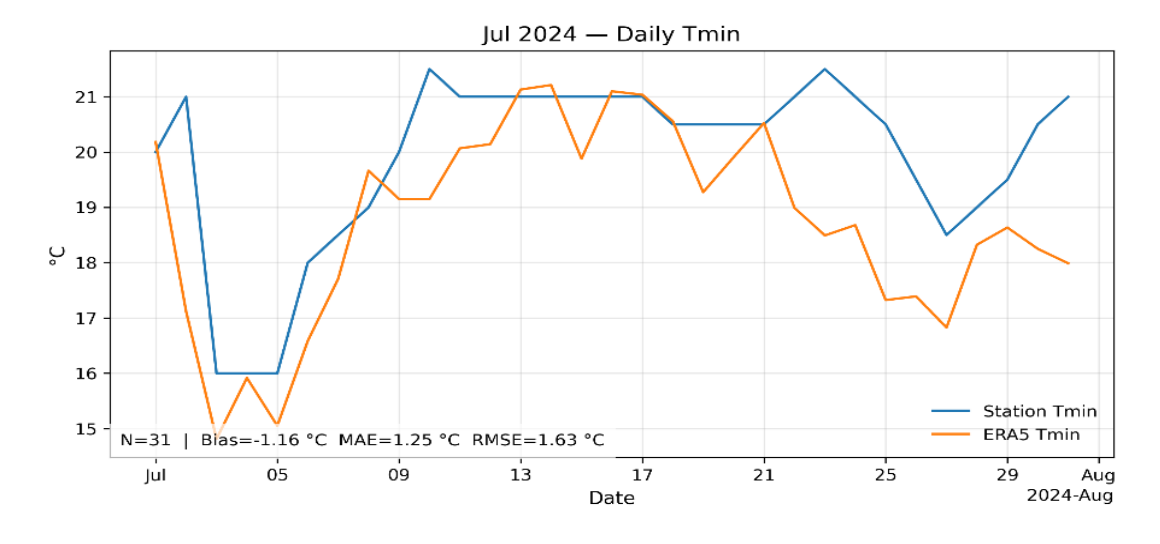


Figure 2.45, a: Comparison of ERA5 and Station Daily Minimum Temperatures (T min) — July 2024

The Tmin scatter plot again shows that ERA5 is colder that the station but the bias is smaller than for the Tmax, (about -1.16°C). It is represented also in the plot since the dots sit close to the diagonal. The errors MAE = 1.25 °C and RMSE = 1.63 °C are small and tell that the nights are shown better compared to the days from ERA5.



 $\textit{Figure 2.45, b: Comparison of ERA5 and Station Daily Minimum Temperatures (T min) -- \textit{July 2024}}$

The T min time series shows the general shape of ERA5 curve, but it's a little cooler most days and below the station. At the beginning of the month, it drops too low; in the middle of the month, it matches better; and at the end of the month, it stays below the station.

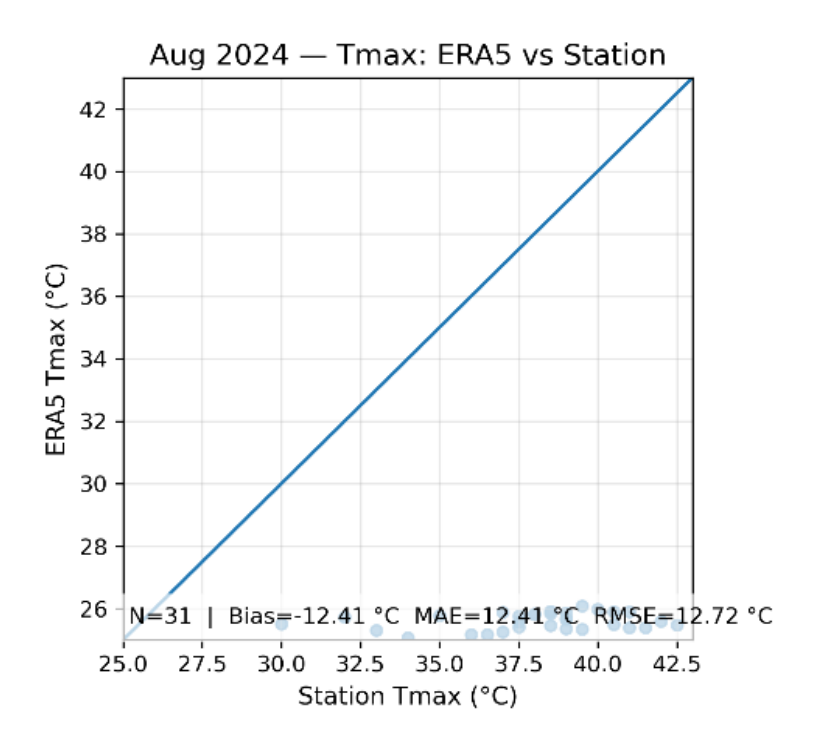


Figure 2.46, a: Comparison of ERA5 and Station Daily Maximum Temperatures (T max) — August 2024

T max scatter plot shows that the points are very far and below the diagonal and we can notice that they are grouped around 25-26°C. The bias is -12.4 °C, a very cold one that means that ERA5 does not catch the daytime heat.

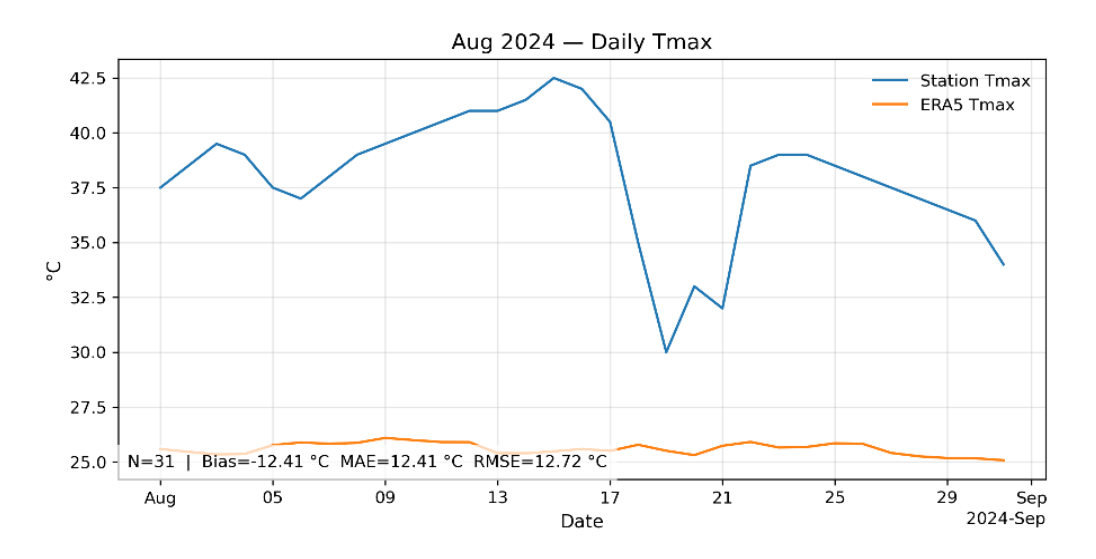


Figure 2.46, b: Comparison of ERA5 and Station Daily Maximum Temperatures (T max) — August 2024

In the time series, ERA5 is way lower in respect of the curve of the station. The temperatures of the station go from 37 to 42 °C, with a big drop in the middle of the month. Instead, the ERA5 temperatures stay almost flat at around 25 to 26 °C.

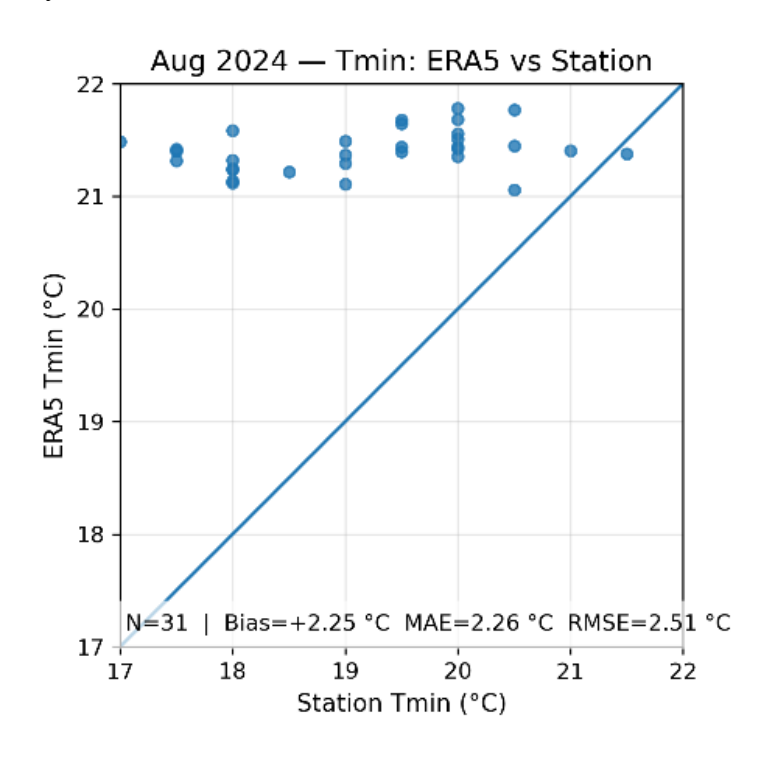


Figure 2.47, a: Comparison of ERA5 and Station Daily Minimum Temperatures (T min) — August 2024

In the T min scatter plot, most of the points are above the line telling us that ERA5 is warmer at night. The bias +2.25 °C is small and positive this time meaning that ERA5 temperatures are warmer than the ones of the station.

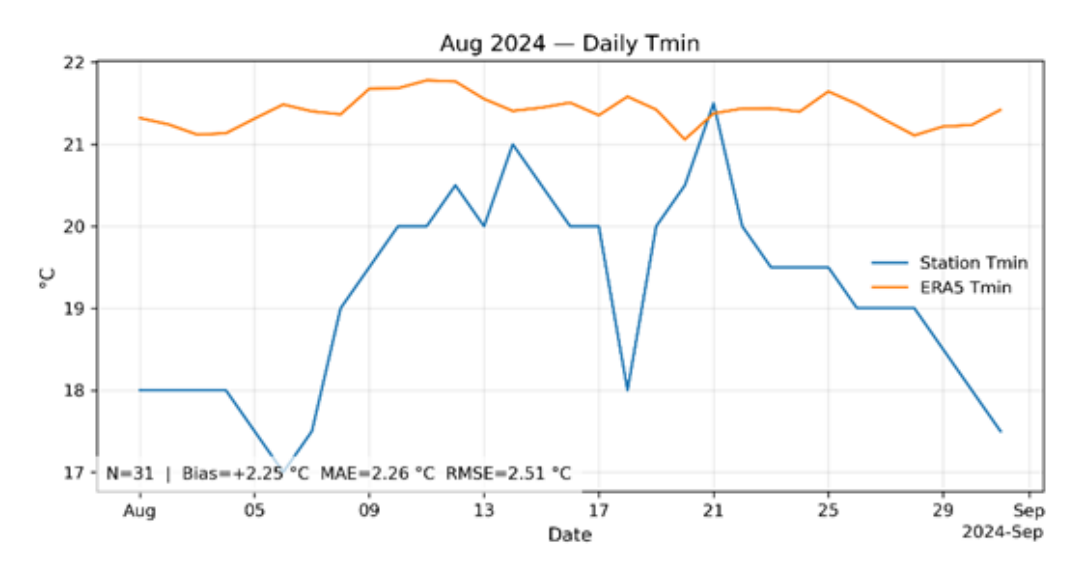


Figure 2.47, b: Comparison of ERA5 and Station Daily Minimum Temperatures (T min) — August 2024

The daily T min time series demonstrates that the ERA5 stays above the observed T min almost every day. The variability of ERA5 curve is low since the curve is almost flat and misses the extremes by not catching the coolest nights as the station does.

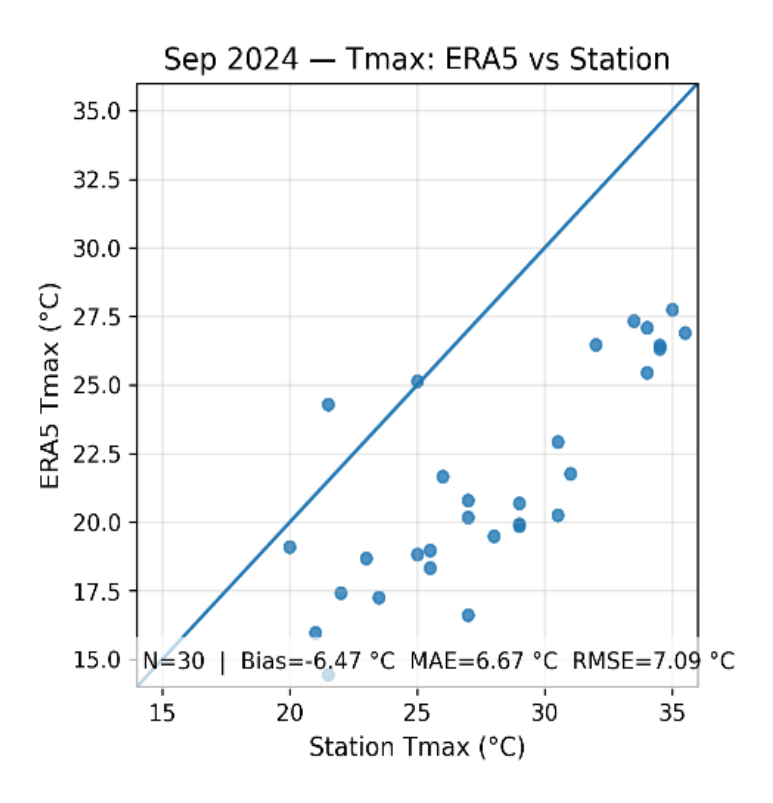


Figure 2.48, a: Comparison of ERA5 and Station Daily Maximum Temperatures (T max) — September 2024

Tmax scatter plot shows that the points well scattered below the diagonal so there is cold bias across the whole month. The bias is -12.4 °C, a very cold one that means that ERA5 does not catch the daytime heat.



Figure 2.48, b: Comparison of ERA5 and Station Daily Maximum Temperatures (T max) — September 2024

The time series plot shows that ERA5 is always below the station's curve and both of the curves show a decline after the beginning of September. Again, ERA5 does not shows the

extremes by smoothing the variability.

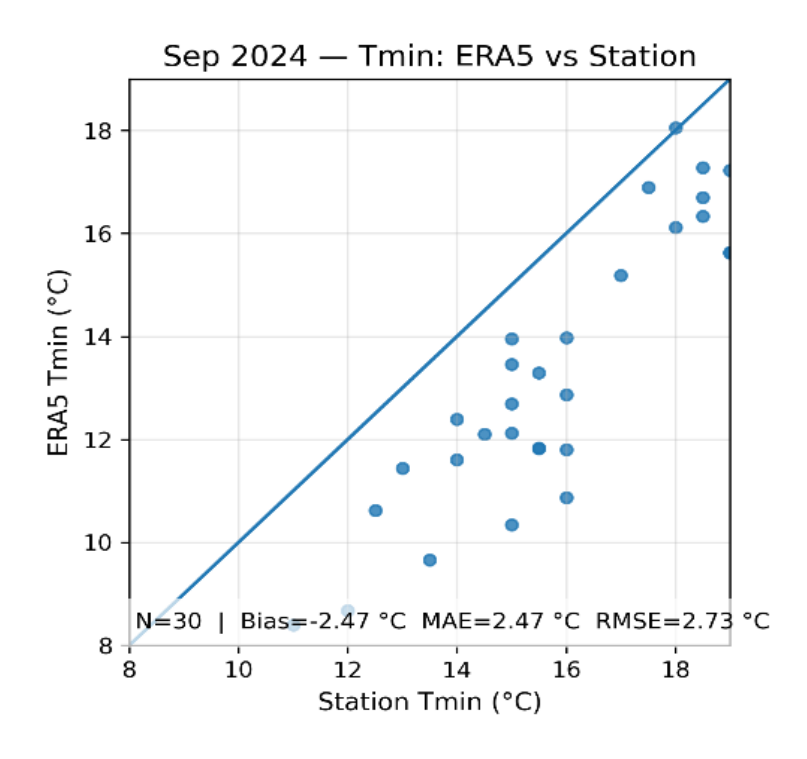


Figure 2.49, a: Comparison of ERA5 and Station Daily Minimum Temperatures (T min) — September 2024

Most point under the diagonal confirm the cold bias on the T min scatter plot. According to bias, ERA5 is about 2.5° C colder than the station. The daily errors, MAE = 2.47° C, RMSE = 2.73° C, are moderate, with RMSE slightly higher than MAE indicating some mismatches.



Figure 2.49, b: Comparison of ERA5 and Station Daily Minimum Temperatures (T min) — September 2024

In the daily time series, the ERA5 curve remains lower respect the station curve, underestimating both peaks and troughs through the whole month.

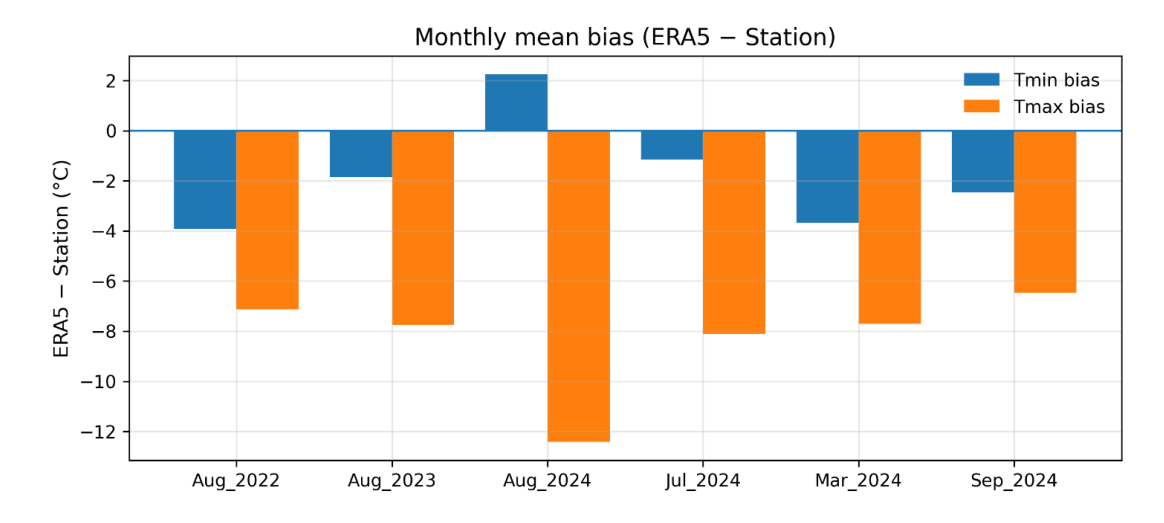


Figure 2.50: Monthly mean bias ERA5 vs Local Station

This bar chart summarizes all the plots explained above by confirming a constant underestimation of T max by ERA5.

The cold bias is persistent, during the summer months and it highlights the inability of ERA5 to capture daytime heat extremes at a local scale. Instead, the T min bias are smaller also on August 2024 is also positive, indicating better model performance for the daily minima during the night time.

These results indicate that ERA5 is more reliable for T min than T max, but both variables require correction before application in a local scale. In our case, we compared the ERA5 data with the local logger data for the months of May, June, July, August 2025. These months were chosen for the main reason that the loggers we installed in the end of May 2025.

To understand better how ERA5 data is positioned respect to the logger data, two methods were used the linear bias correction and the quantile mapping. Both methods help us understand and correct the data and also by comparing them with each other there is a higher chance to retrieve some more correct results. The analysed data is hourly air temperature data. The air logger was registered to measure the temperature every 10 minutes during the installation. Before analysing and comparing both data from logger and ERA5, the logger data was calibrated into hourly data since ERA5 provides only hourly data. Also, extreme temperature values were removed since the logger ends up measuring his own temperature instead of the air temperature because of sun radiation. By taking into consideration the air temperature ranges in Permet, extreme values measured by the logger were removed and the empty cells of the sheets were filled through interpolation. Following this procedure, the plots are more complete and there are no sporadic spaces.

2.9.1 Correction methods: linear bias correction and quantile mapping

2.9.1.a Linear bias correction

A linear bias correction was used to change reanalysis temperatures (like ERA5) to fit local conditions before doing analysis and modelling.

The results are reported by RMSE/MAE and point out that linear correction keeps the timing and rank correlation of events but changes the mean and amplitude. The relationship between the model and observations is mostly linear and stationarity. Linear correction enhances mean levels and variability, but does not rectify distribution tails (extremes). In the plots below the is shown the data confrontation of the Air logger vs ERA5 regarding the months of May, June, July, August 2025. A linear bias correction method was used.

This plot shows how the air temperatures from ERA5 compare to the temperatures from the logger at the end of May 2025, in Permet. The black line is the perfect agreement. The blue dots (ERA5 data) are mostly below that line, this means that ERA5 is too cool and doesn't reach the highest values. The sensor shows 27–29°C, but ERA5 indicates 26°C. Through a linear bias correction, the red squares move up and line up way better with the 1:1 line. In other words, ERA5 doesn't show the heat in Përmet well enough, but a quick linear correction makes it look much better.

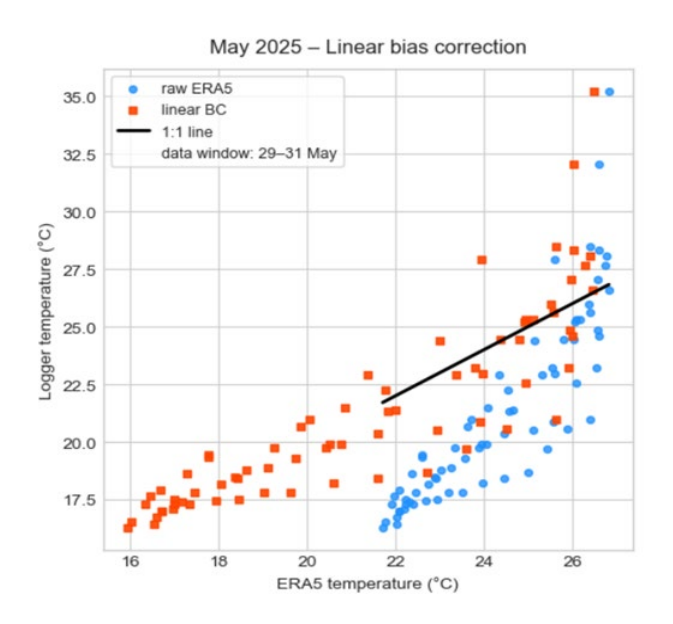


Figure 2.51: LBC of ERA5 Temperatures for May 2025

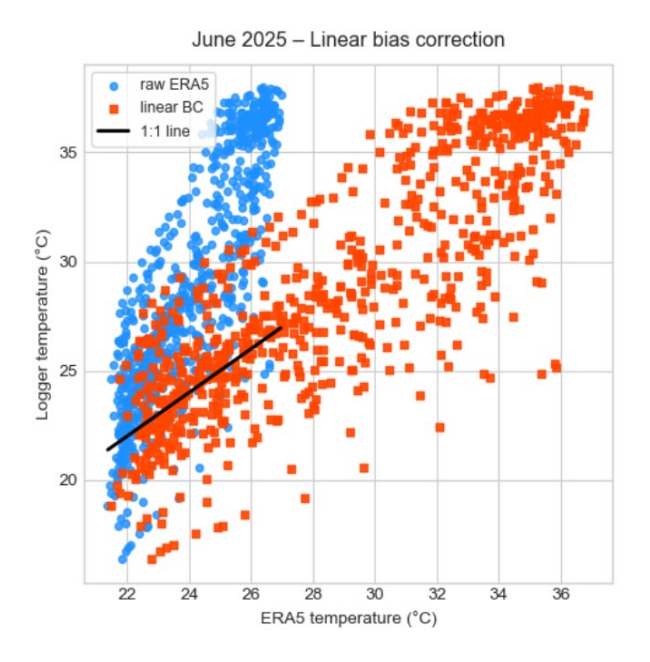


Figure 2.52: LBC of ERA5 Temperatures for June 2025

In the June plot, the blue dots show the raw ERA5 data compared to the logger. The red squares show the ERA5 that has been corrected with LBC. Most of the points in ERA5 are on the left but the logger goes up to about 37°C. ERA5 is cooler and doesn't get to the extremes of the day. After the correction, the points move to the right and spread out. A lot of them land near the diagonal, especially during warm hours. This means that the corrected ERA5 follows the logger much better.

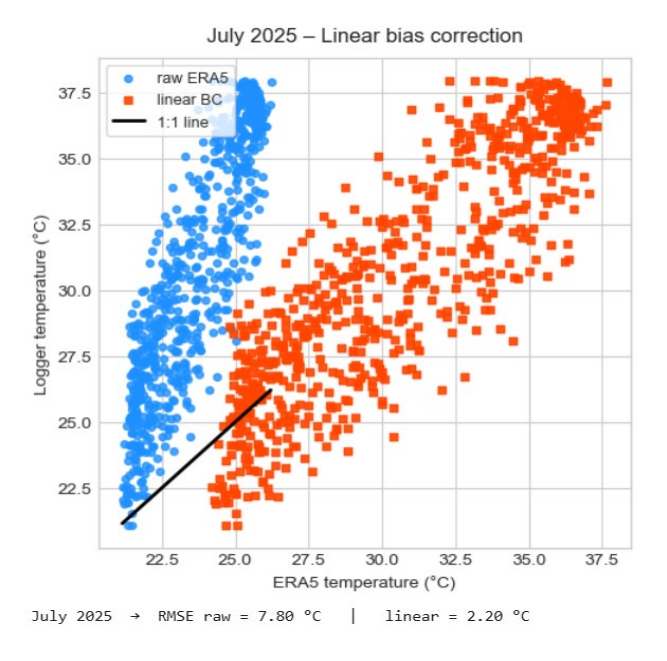


Figure 2.53: LBC of ERA5 Temperatures for July 2025

The July scatter plot compares ERA5 with the logger. The blue dots are positioned on the cool side according to the temperatures while the logger reaches up to 38 °C. ERA5 is clearly too

cold and misses the extremes. After applying the LBC, points shift to the right and align much closer to the diagonal. The error drops from RMSE 7.8 °C to 2.2 °C and there is about a 72% improvement. There's still some scatter at the extremes, but the linear fix removes most of the cold bias.

The application of Linear Bias Correction method shows a lot of improvement across different thermal regimes. Even under extreme summer conditions, the method reduced the errors showing that is an acceptable method to be applied across seasons.

2.9.1.b Quantile Mapping Method

Quantile mapping (QM) is a method for correcting bias that uses the full distribution of a model variable and matches it to the local observations. QM changes not only the mean, but also the variability and tails extremes.

The plot represents the quantile mapping for the last days of May 2025. The grey dots represent the raw ERA5 data and most of them are below the diagonal. This means that ERA5 is too cold. The points move up and spread after quantile mapping and they move closer to the diagonal. The error goes down from RMSE 4.06 °C to 1.34 °C, it shows 67% improvement. The QM differently from the LBC, corrects not only the mean but also the distribution of the values.

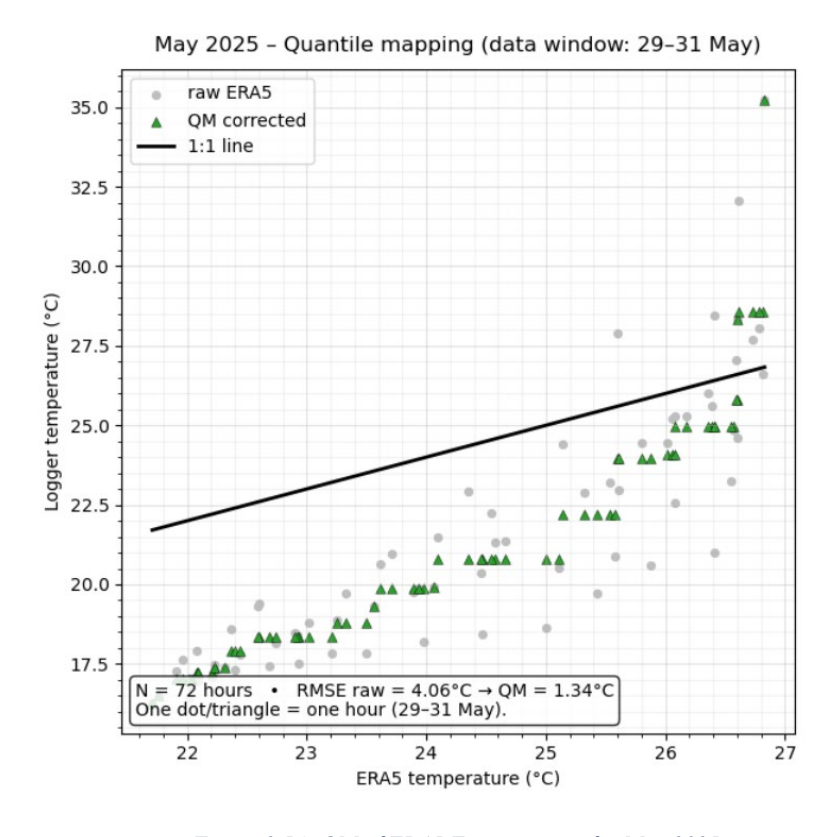


Figure 2.54: QM of ERA5 Temperatures for May 2025

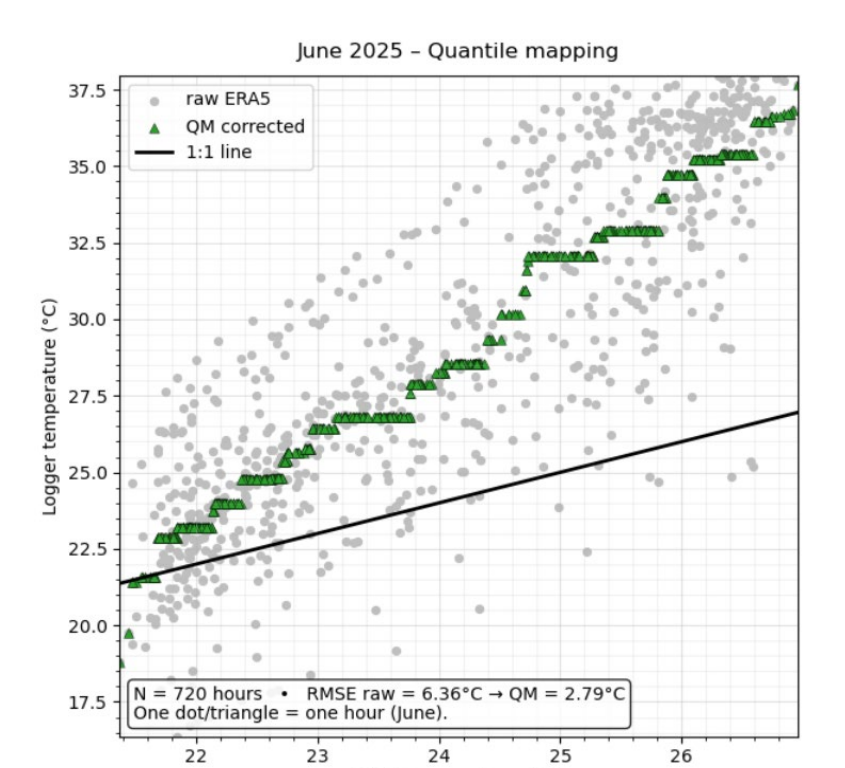


Figure 2.55: QM of ERA5 Temperatures for June 2025

ERA5 temperature (°C)

In the QM plot for June 2025, we notice that when the ERA5 values are warmer they are positioned near and below the diagonal. The total error goes down from RMSE 6.36°C to 2.79°C, which is a 56% improvement. Again, the QM method corrects not only the mean values but also the extremes.



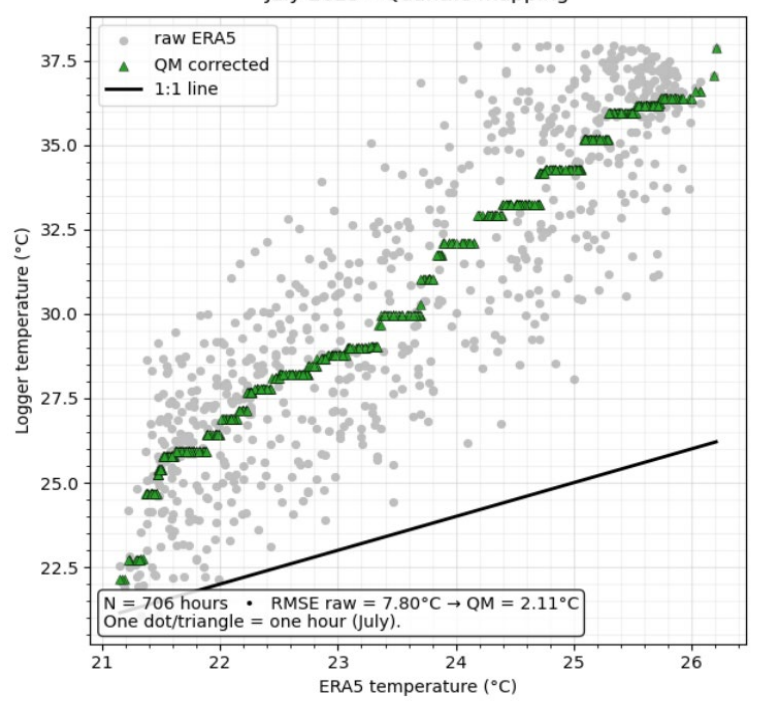


Figure 2.56: QM of ERA5 Temperatures for June 2025

In the QM plot for July, the ERA5 dots are lower than the diagonal because the logger gets to 38°C and ERA5 to 26°C. This means that the cold bias is strong and the range is small. The points move up and follow the logger distribution much better after using quantile mapping. The error drops from RMSE 7.80°C to 2.11°C, which is about 73% better.

The plots that we described above reveal that the raw ERA5 data is colder than the temperature measured from the air logger, for example ERA5 reveals a temperature of 26°C but the logger registers 27–29°C. The LBC moves the ERA5 data to line it with the diagonal, instead the quantile mapping improves the alignment of the data not only to the diagonal but also across the whole range of values, basically it stretches the data by taking into consideration also the tails (extremes).

On all the plots the RMSE has been lowered a lot with 56%-72% of improvement.

2.9.2 Water Temperature Analysis

The plot shows the water temperature trend in the Langarica river for the las 3 days of May 2025. The blue curve shows the temperature of water measured every hour from our logger. If we follow the curve alteration, we can notice that the water's temperature becomes warmer during the day and colder during the night as in a normal temperature cycle in 24 hours.

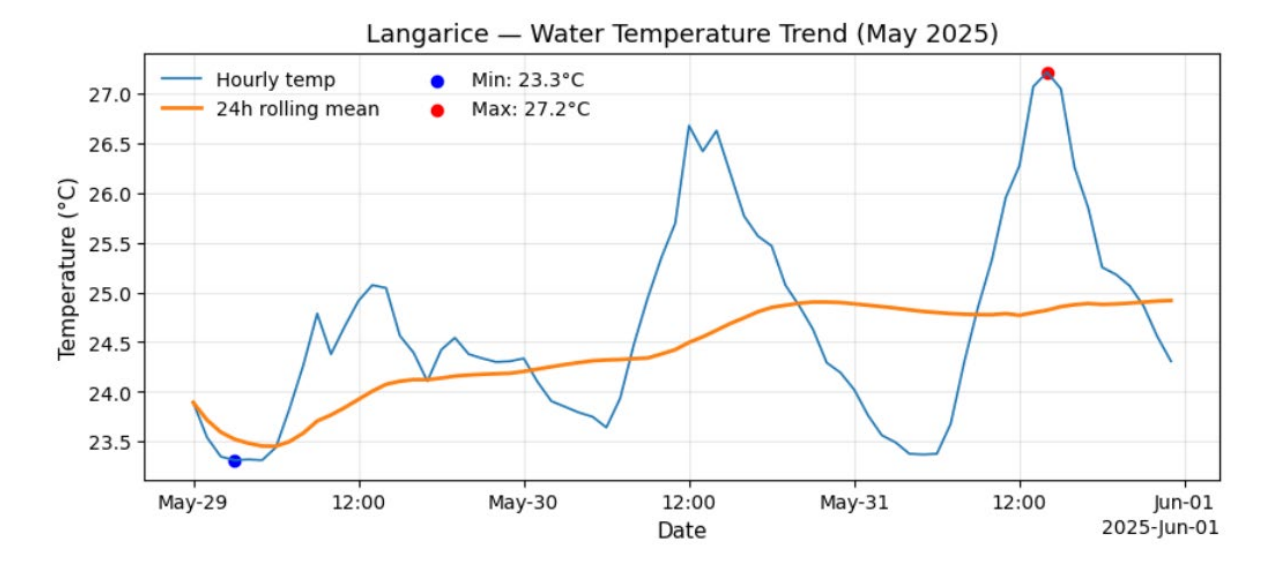
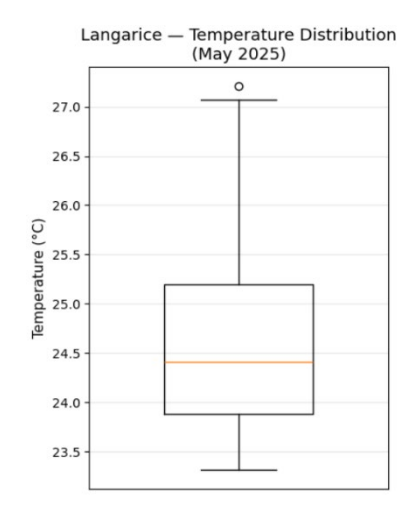


Figure 2.57: Langarica water temperature trend, May 2025

The orange curve shows the average temperature of these last four days of May. Also, in this case the curve tends to raise approaching June as normally should be since June is a hotter month than May. The blue and orange dots show the minimal and maximal temperatures for these four days.

From the timeseries, the maximum is reached on 31 May, after midday where the sun is at its peak, with a value of 27°C. The minimum temperature is 23°C measured at the early hours of morning, approximately at 8:00. Also, in this case the measured data was analysed and modified. Similar to our air logger which was explained, the water logger was calibrated to measure the temperature every 10 minutes.

Through mathematical modifications, the registered data was modified into hourly. Also values above 27°C were removed manually since they are not correct for these river normal temperatures. The empty data after the removal was fixed by interpolation to provide smoother and uninterrupted curves that represent better the temperatures situation in Langarica.



The boxplot for the last days of May shows that in these days the water temperature in Langarica was constant between 24-25 °C and it corresponds to the interquantile range. The orange line is the median and is about 24.4 °C. As we know in a boxplot the box represents the middle of the data which in our case is 23.9–25.2 °C. Instead, the whiskers show the normal range which varies between 23 to 27 °C. The circle represents the warm outlier which is about 27°C. In the end of May there was at least one warm spike.

During June 2025 we were able to measure the water temperature every day of the month. Again, the registered data was modified into hourly and the missing ones were replaced through interpolation. From the curves we can notice that June was a calm month and most of the days were the same following also the peak and troughs of the blue curve.

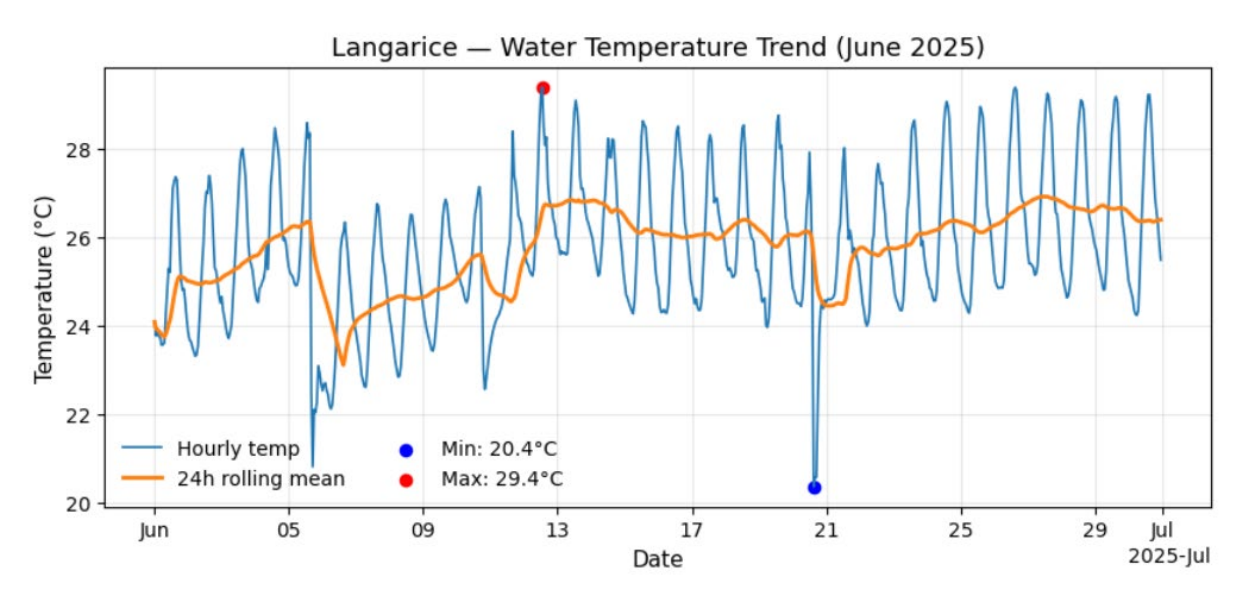
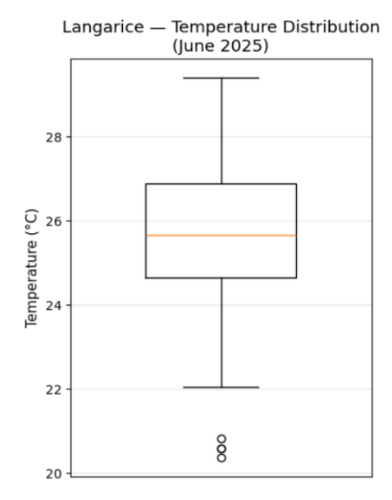


Figure 2.59: Langarica water temperature trend, June 2025

Although there are two breaks, one around 6 June and one sharp temperature drop on 21 June. The warmest day of the months was 13 June where the temperature reached 29.4°C. The coldest one was on 21 June which is the same day of the sharp drop of the temperature. Approximately the last week of June seems the warmest of the month.

The mean curve shows a smooth rose during the month following of course the trend of the hourly timeseries with a mean monthly temperature approximately 26°C.



In the boxplot of June, it is noticed that most days were around 25°C according to the median. The box which shows the 50% of values shows that the temperatures are stable and they range from 25-27°C.

The whiskers range from 22°C (minimum) to 29°C (maximum) and it represents a normal day-night cycle. Below the lowest whiskers are three circles below 22°C that show a decrease in temperature.

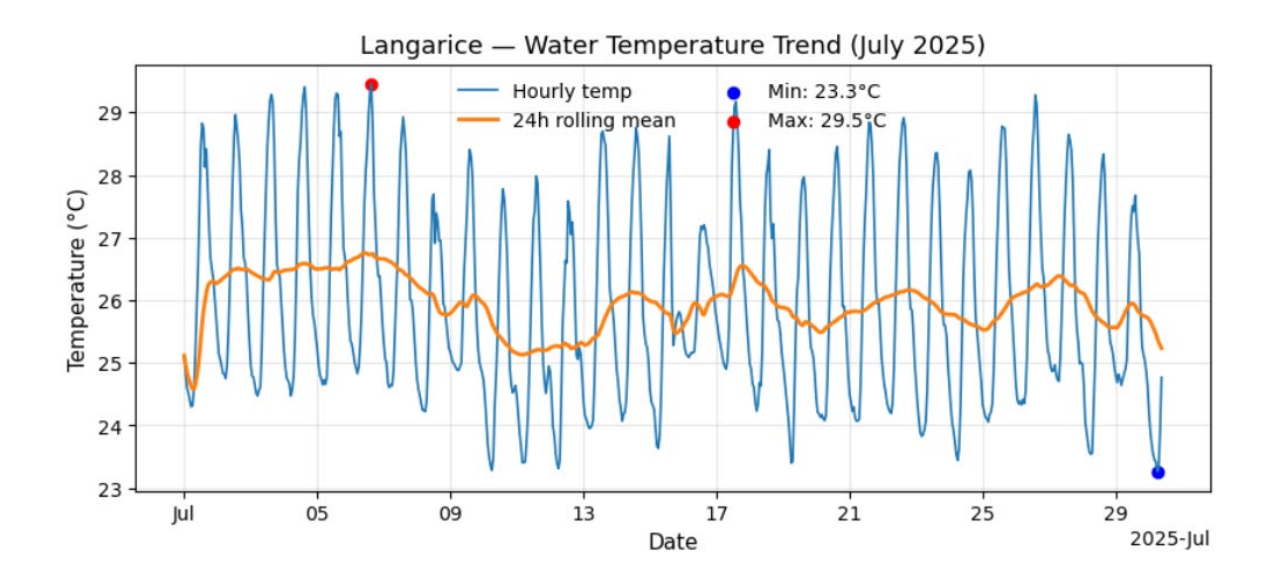
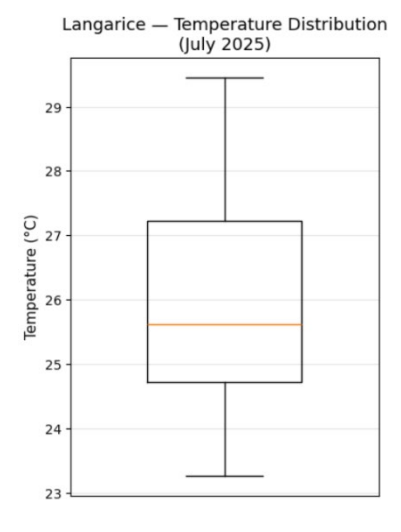


Figure 2.61: Langarica water temperature trend, July 2025

Also, for July, the data was measured for the whole month. According to the plot, the pattern of the trend is quite regular where the temperatures oscillate from high values most in the afternoons to low ones on overnight. We can tell confidently from the timeseries that the first week of the month is the warmest. The warmest day is on 7 July with a temperature value of 29.5°C and the coldest day is on 30 July with a measured temperature of 23.3°C.



Again, the orange curve follows the hourly trend by showing the gradual variations with the highs and lows in the background.

For the month of July, the boxplot shows that the median is around 25.5°C. The middle 50% of values, goes from about 25 to 27°C. The whiskers range from 23 to 29.5 °C which is a normal range for the month.

The upper one is longer than the lower one and this means the spikes of temperature were more frequent. There is no presence of outlier since all the temperatures values are considered within the range.

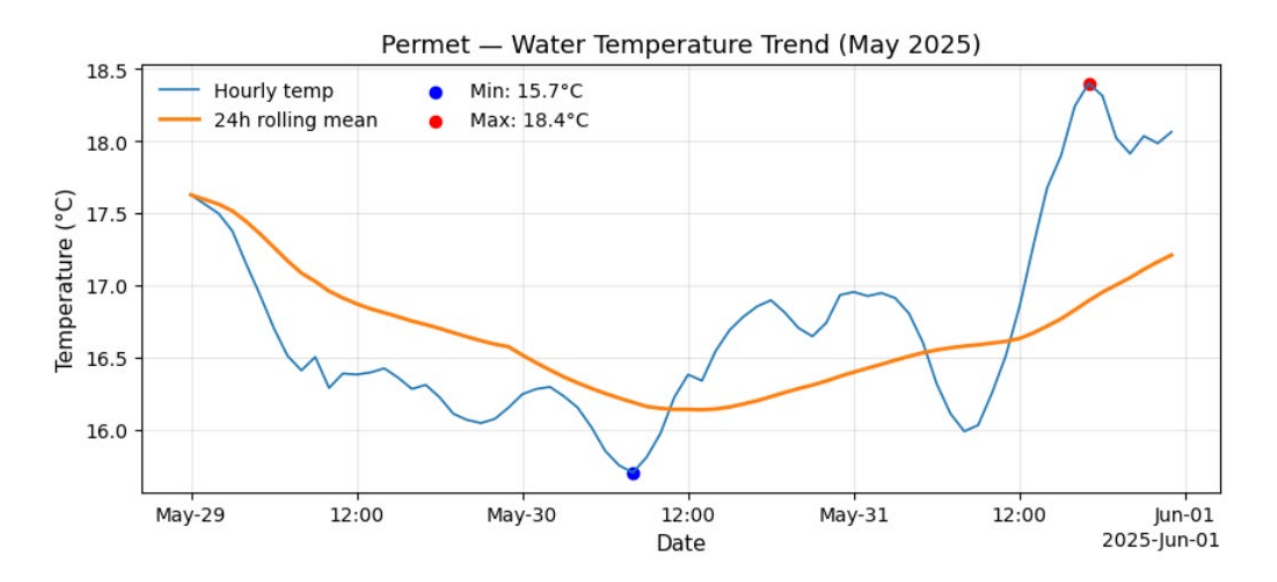
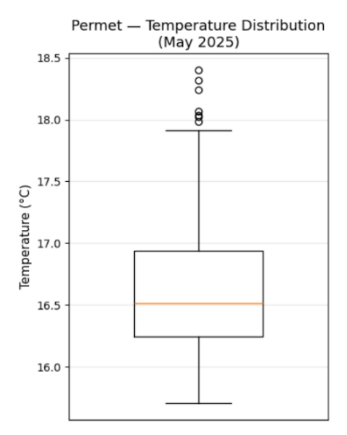


Figure 2.63: Vjosa, Permet water temperature trend, May 2025

The same process as in Lanagrica was followed to analyse the data measured from Vjosa. The last four days of May seems calmer and colder than in Langarica. There is a noticeable drop of temperature between 29-30 May and the lowest point is 15.7°C.

On the last day of May there is a sharp rise of the temperature till the first day of June with a measured temperature 18.4°C. The orange curve is smoother that the one of Langarica following accordingly the hourly trend.



The boxplot for the last days of May shows a median of 16.5°C. Also, according to the box, half of the readings is between 16.2 - 16.9°C. The whisker's values range from 15.5°C for the coldest hour till 17.8°C for the warmest one.

There are a few outliers that represent the warm spikes and they range from 17.8 °C to almost 18.5 °C.

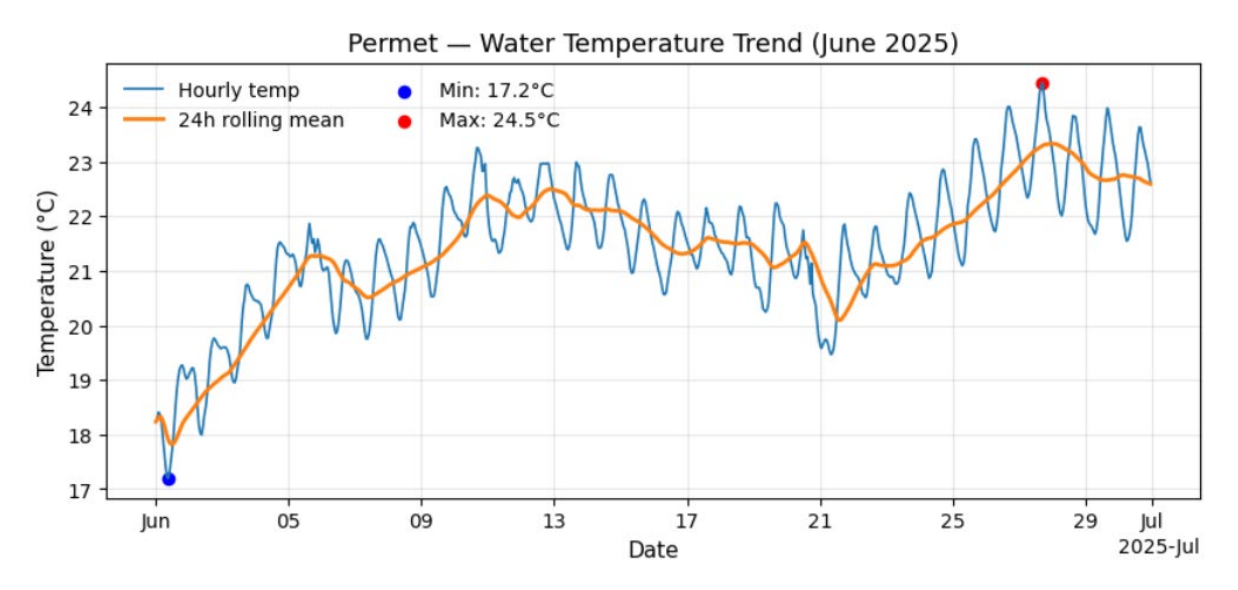
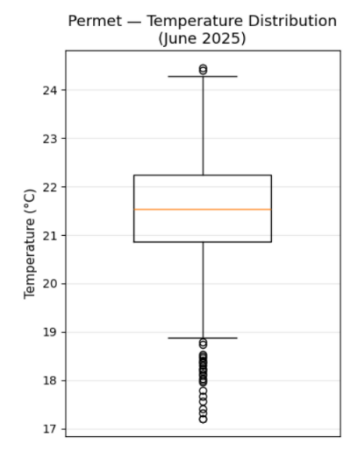


Figure 2.65: Vjosa, Permet water temperature trend, June 2025

June starts with a sharp drop of temperature on the 1st which is also the coldest day of the month with a measured temperature of 17.2°C. Also, the first week of the month is the coldest one.

The middle June seems stable with temperatures variating from 21-22°C finishing with a smooth drop on 21st. The drop is quickly recovered by an increase of temperature during the last week, reaching the maximum on 28th June with a measured value of 24.5 °C.

The mean curve follows the hourly curve trend starting from 18 °C at the beginning of the month to about 23 °C by the end of the month.



The boxplot for June 2025 shows that the most daily temperature in Vjosa ranges between 21-22.2°C. The median temperature is almost 21.5°C.

The whiskers range is from 19°C to 24.5°C. There are a high number of outliers, cold ones, between 19 to 24°C which show the short spells of cold and also there is a warm outlier which represents the warm spike above 24°C. Juna was a warm month but with a long cold tail.

During July 2025 the temperatures in Vjosa oscillate between 22-24 °C during the daytime.

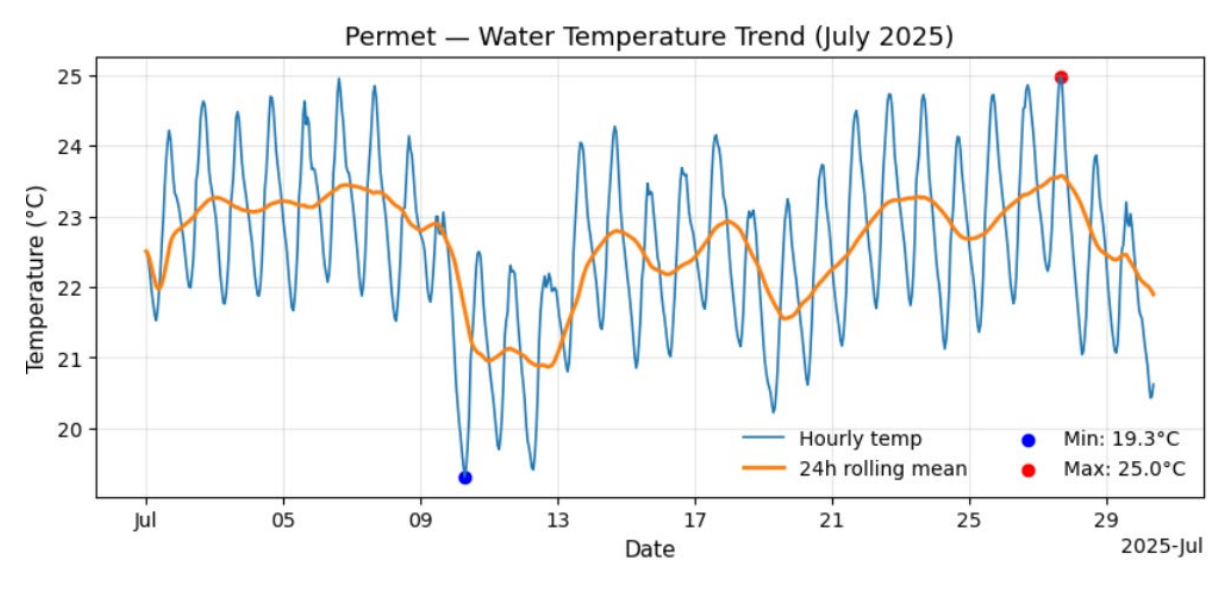
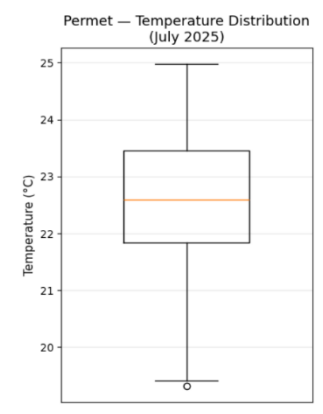


Figure 2.67: Vjosa, Permet water temperature trend, July 2025

After the middle of the month the river gets warmer with the increase of the temperatures. There is again a smooth drop on 18-21 July being overpassed by an increase of temperature till reaching the warmest day on the 28th with a measured value of 25°C. The orange curve is not as smoother as the one of June and shows that the mean temperature stays between 22-23 °C during the whole month.



The boxplot of July 2025 shows that most of the temperatures stayed in the low 20s and the median was about 22.5°C. The IQR varies between 21.9°C to 23.5°C.

The whisker's range is from 19.5°C to 25°C and there is only one outlier, a cold one around 19.7°C. Almost all the values are 1°C warmer than in June and the stretched whiskers show the stronger sun on the late summer.

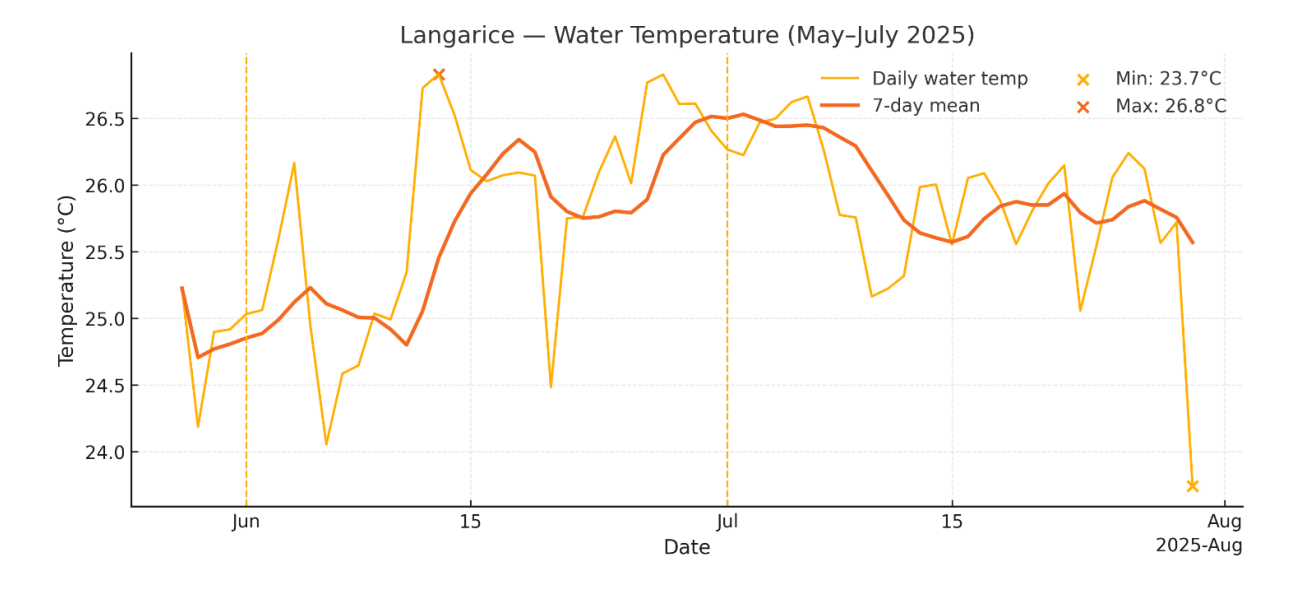


Figure 2.69: Langarica Water Temperature

The May–July plot for Langarica shows the daily water temperature (gold) and the 7-day mean (red). From late May to the end of July 2025, the yellow line shows the daily water temperature at Langaricë. The orange line shows the 7-day mean, which smooths out noise from day to day. The 7-day mean starts at about 24.5–25.0 °C at the end of May and rises steadily until it reaches a warm plateau of about 26.2–26.6 °C in late June to early July. In the middle of June, the warmest day is 26.8 °C, and at the end of July, the coolest day is 23.7 °C. After the peak in early July, the temperature drops a little and stays between 25.5 and 26.0 °C until the middle or end of July. There is a smooth rise from late spring to mid-summer and a small cool pulse at the very end.

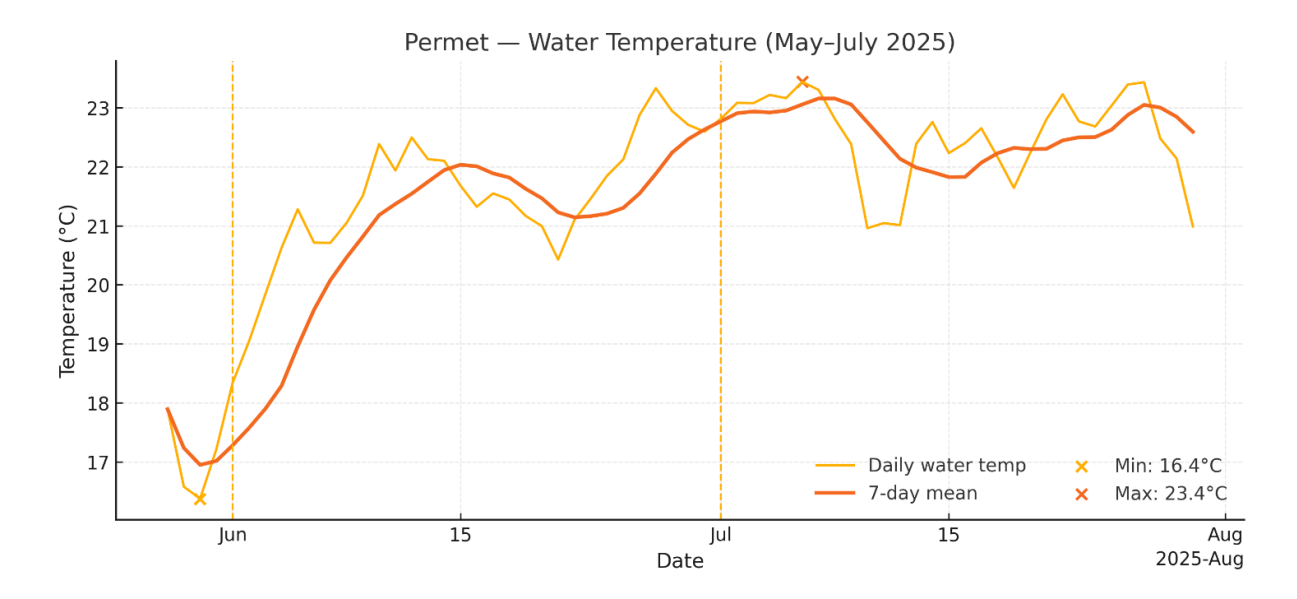


Figure 2.70: Vjosa Water Temperature

The May–July plot for Vjosa shows the daily water temperature (gold) and the 7-day mean (red). The dashed lines show the 1st of June and the 1st of July. The beginning of the period is cool, with temperatures reaching 16.4 °C at the end of the month. By mid-June, the 7-day mean has risen from about 17 °C to about 22 °C.

From late June to July, the temperature stays on a high, stable plateau of about 22.5–23.1 °C. There are small changes from day to day (about 0.5–1.0 °C), and there may be a few short dips that are probably caused by short weather or flow events. The highest temperature during this time is 23.4 °C in late July. Vjosa is about 3–4 °C cooler than Langaricë from June to July. The plot shows a warm-up from spring to summer, followed by a steady warm period with no long periods of extreme heat.

Chapter 3 – Thermal Impact Assessment on fish biodiversity

3.1 Introduction

The Vjosa river declared also a Wild River National Park has a high ecological and cultural value. It is characterized of a high biodiversity of habitats and species where are documented more than thirty fish species, 27 of them are native and 8 of them are endemic species in the Balkan region. (Shumka et al., 2018; Inception Report EU4N, 2025).

As all the Mediterranean water bodies, Vjosa also is threatened by climate change specially because of the frequent warming seasons. The increase of air and water temperature affects the thermal regime as was explained in the chapter above but also the habitats and the organisms since they are very close co related and co-dependent with the water temperature for their growth, reproduction and survival. A representation of changes in temperature gives us also a possible change of the river habitats in the future by taking into consideration the thermal tolerance of the species.

3.2 Target Species

The freshwater species especially fishes are organisms whose longevity depends a lot on the temperature of their environment. Thermal thresholds affect and define their growth, survival and reproduction. For example, in the Mediterranean the fish species are used to cold water temperatures and with the warming temperatures they are threatened. In this chapter there is a small analysis regarding some threatened species to the water temperatures of summer 2025. There are five target fish species that represent conservation concerns in the Vjosa river and those are: *Chondrostoma vardarense*, *Chondrostoma vardarense*, *Gobio, Salmo farioides*, *Gobio scadarensis*. These species cover different groups like dwelling cyrpinids, cold water salmonids ecc.



Figure 3.1: Gobio



Figure 3.2: C. vardarense



Figure 3.3: Salmo farioides



Figure 3.4: G. scadarensis

Gobi scadarensis is more threatened since it is an endemic species in a limited range and also is listed as endangered species in the IUCN red list. Since this species of fish lives in cold waters and is very sensitive to temperature oscillations the warming seasons are for sure a threat for it. Instead, the barbel and nase are more tolerant to temperature oscillations but still need a high-level oxygen environment. [24] (Shumka et al., 2018).

3.3 Analysis

For the analysis were used water temerature data registered from the water loggers. It was taken into consideration the daily mean by retaining it from the minimun and maximun data. The thermal threshold is a critical limit during summer for the target taxa. In this case they were obtained by Bayat et al., 2025, Scientific Data which is a global database for freshwater thermal tolerances covering > 900 species. In the rare cases some species are not available it is used the data of the closest congener.

For each of our targes a table was created containing the type of species, the life stage the Ctmax ecc. The exceedance calculations used daily mean water temperaure but in cases also the tmax could be used if it is necessary to study the case when more stress is applied. For each species s which is the "specific species and θs which is the critical temperature threshold for that specific species was choosen. The binary exceedance indicator and magnitude were calculated:

Binary exceedance indicator: $I(d,s) = \{1 \text{ if } X(d) > \theta_s \text{ 0 otherwise } \}$

Exceedance magnitude: $\Delta T(d,s) = max[0,X(d) - \theta_s]$

The EED shows both how long and far were the measured temperatures from the threshold.

$$EDD(s) = \sum_{d \in D} \Delta T(d, s)$$
 [°C· days

For the detection of possible heatwaves it was took into consideration that a heat event is run > 3 consecutive days with I(d,s) = 1. Usually for marine environments the heat events are 3-5 days.

For the detected event were computed: the star and end date, number of days and the mean intensity:

$$\overline{\Delta T}_e(s) = \frac{1}{L_e} \sum_{d \in e} \Delta T(d, s)$$

Le is the event duration.

After for each species is calculated the frequency if events, the length and EDD (${}^{\circ}\text{C} \cdot \text{days}$): sum of $\Delta T(d,s)$ over all the days and the % days over the threshold:

% days =
$$100 \times \frac{\sum_{d \in D} I(d,s)}{|D|}$$

As was mentioned above working with t mean and not t max prevents the increase of exceedance and events statistics.

3.3.1 Thermal stress indicators

To understand better the thermal stress that our target fish species experience during the studied season were computed and analysed some thermal indicators for Vjosa and Langarica. Through the combination of the season and daily dynamics it is possible to analyse the intensity and the distribution of temperature exceedance above the ecological threshold. The results on the tables and on the plots explain better the analysis. Using the Exceedance Degree Days which measures the magnitude of temperature exceedance over the studied season. After, through a heatmap it is studied the frequency of this exceedance and represented through percentage. The mentioned indicators give e general picture of how the vulnerability if the species from high water temperatures.

The table represents the exceedance episodes detected when the T mean of water was above 24 °C which is our species threshold.

Site	Species	Start Date	End Date	Duration D	Mean Intensity	Peak Intensity	Edd Cdays
		Date	Date		C	C	Cuays
Lengarica	Salmo	2025-06-	2025-07-	59	1.89	2.83	111.24
	Farioides	01	29				
Lengarica	Salmo	2025-07-	2025-08-	6	0.98	1.64	5.91
	Farioides	31	05				
Lengarica	Salmo	2025-08-	2025-08-	20	0.94	1.8	18.71
	Farioides	07	26				

Table 2. 4 Heat-wave events

Consecutive-day exceedance episodes detected when daily mean water temperature was above the species threshold (24 °C). For each event the start/end date, duration (days), mean and peak exceedance intensity (°C above threshold), and cumulative burden expressed as Exceedance Degree-Days (EDD; °C·days) are reported. The signed events are related to the fish species Salmo farioides in Langarica. The mean exceedance is +1.89 °C for 59 days than +0.98 °C for 6 days and +0.94 °C for 20 days. This means that the water temperature stayed above the threshold for almost 60 days procuring an intense long heat wave which might have been very stressful for the species. These kind of values of the exceedance increase the disease risk, decreases the aerobic scope and the growth.

For the mainstream Vjosa there are no heat wave events since the species thresholds are not exceeded in summer 2025. It is important to outline that Langarica a smaller stream, with and a low discharge and shallow waters in the summer season due to upstream hydropower derivation, thus, the considered river reach is more responsive to atmospheric changes and has less thermal inertia compared to the Vjosa river.

The table number 2.5 shows a seasonal summary of the exceedance for summer season of 2025. Also, here it is highlighted that the thermal stress affects only Salmo farioides in Lengarica for 59 days which is a long heat wave event and stressful. The total EED value 135.85 °C·days is enough to imply stress and growth repression for this type of cold-water salmonid. The recovery windows were limited since most of the summer was over the

tolerance.

All the other species present in the table have zero values meaning that the thresholds were not exceeded. Langarica acts like a thermal bottleneck for Salmon farioides, instead Vjosa was stable during summer season for all the taxa.

Site	Species	N Events	Max Duration D	Total Edd Cdays	Pct Days Over Thr
Lengarica	Barbus Barbus	0	0	0	0
Lengarica	Barbus Meridionalis	0	0	0	0
Lengarica	Chondrostoma Vardarense	0	0	0	0
Lengarica	Gobio Gobio	0	0	0	0
Lengarica	Gobio	0	0	0	0
	Scadarensis				
Lengarica	Salmo Farioides	3	59	135.85	96.59
Vjosa	Barbus Barbus	0	0	0	0
Vjosa	Barbus Meridionalis	0	0	0	0
Vjosa	Chondrostoma Vardarense	0	0	0	0
Vjosa	Gobio Gobio	0	0	0	0
Vjosa	Gobio Scadarensis	0	0	0	0
Vjosa	Salmo Farioides	0	0	0	0

Table 2. 5 Seasonal summary of EDD

Lengarica River Results:

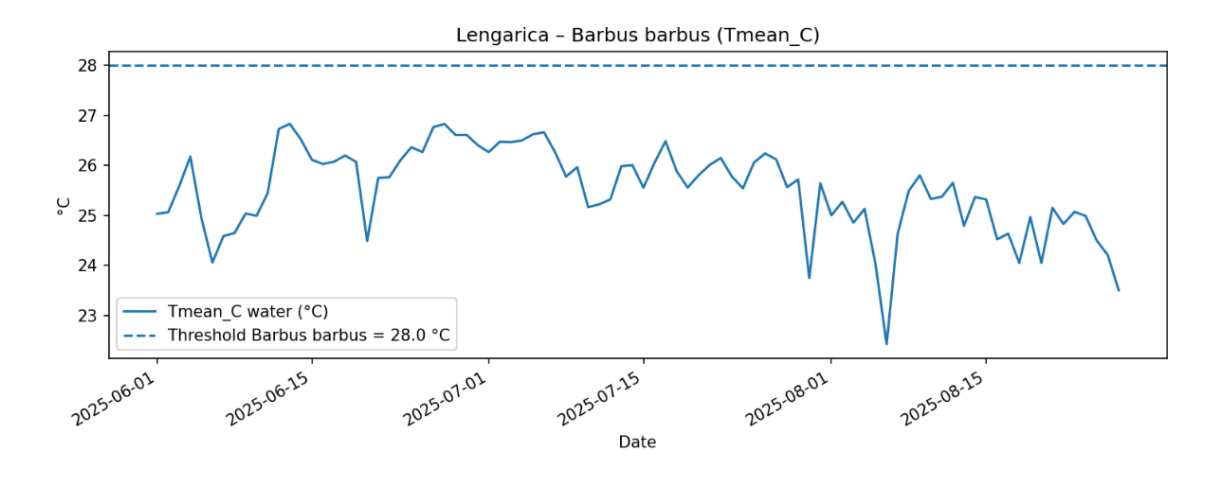


Figure 3.5: T mean and species threshold of Barbus

The graph shows the progression of the daily mean water temperature in Lengarica during the summer season June-August 2025 for the fish species *Barbus barbus*. The blue curve represents the daily water temperature and the blue dashed line represent the species threshold which in this case is 28°C and above this limit the fish species start to experience the heat stress. From the plot it is more than clear that the water temperature is always lower than the spices threshold so for this species it did not occur a thermal exceedance during the summer period.

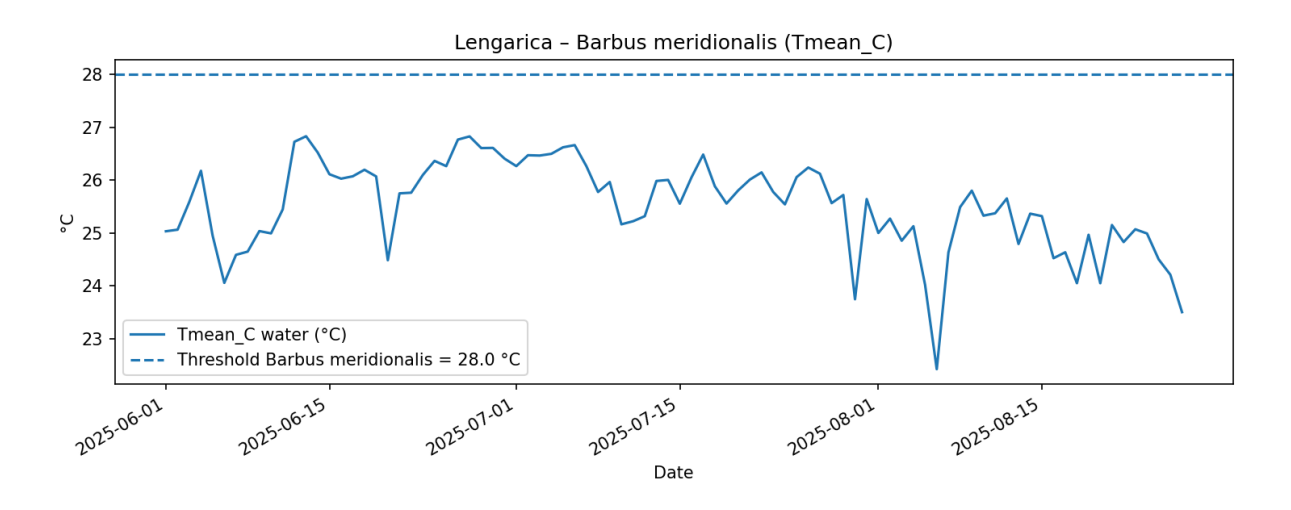


Fig3.6: T mean and species threshold of Barbus meridionalis

The graph shows the progression of the daily mean water temperature in Lengarica during the summer season June-August 2025 for the fish species *Barbus Meridionalis*. The blue curve represents the daily water temperature and the blue dashed line represent the species threshold which in this case is 28°C and above this limit the fish species start to experience the heat stress. From the plot it is more than clear that the water temperature is always lower than the spices threshold so for this species it did not occur a thermal exceedance during the summer period.

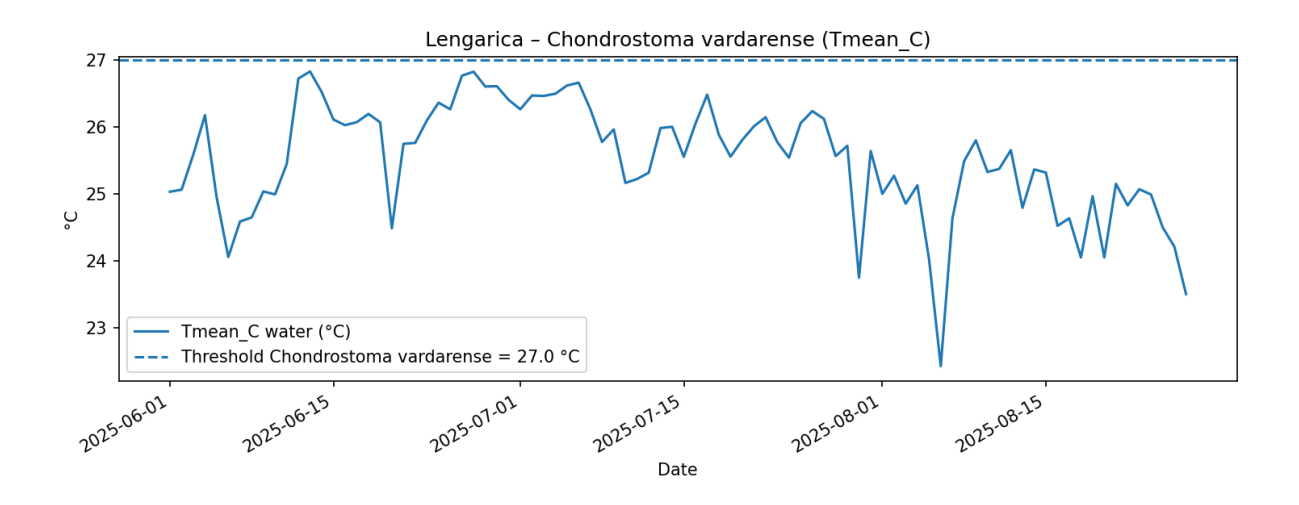


Figure 3.7: T mean and species threshold of Barbus meridionalis

The graph shows the progression of the daily mean water temperature in Lengarica during the summer season June-August 2025 for the fish species *Chondrostoma vardarense*. The blue curve represents the daily water temperature and the blue dashed line represent the species threshold which in this case is 27°C and above this limit the fish species start to experience the heat stress. From the plot we notice that the water temperature event though is lower than the spices threshold sometimes it approaches the threshold slightly between the middle of June and some days during middle of July. The species experience some moments with potential thermal exceedance during the summer period.

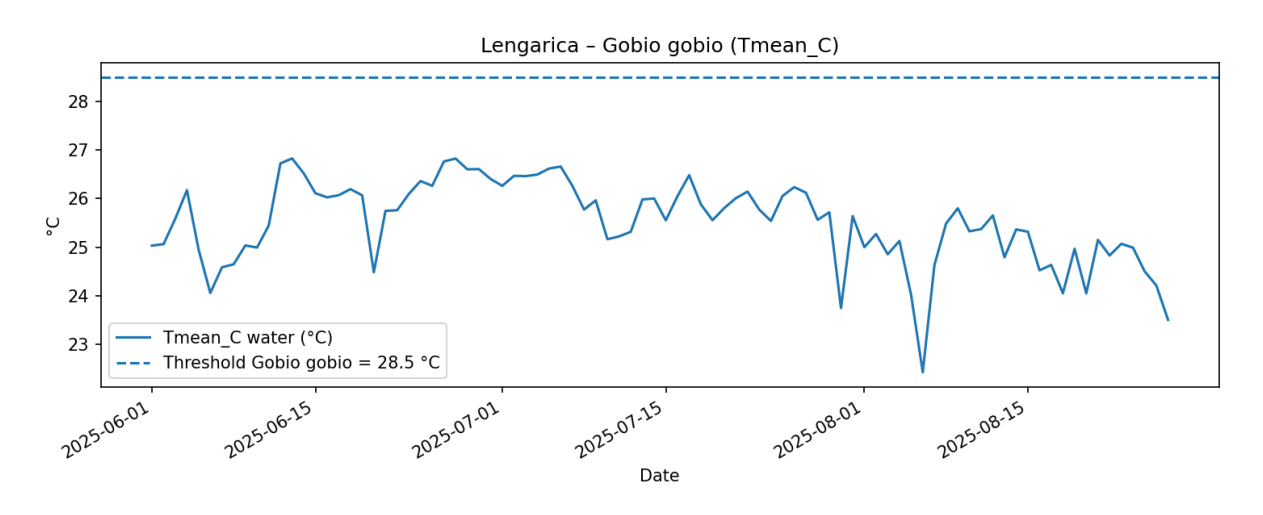


Figure 3.8: T mean and species threshold of Gobio gobio

The graph shows the progression of the daily mean water temperature in Lengarica during the summer season June-August 2025 for the fish species *Gobio gobio*. The blue curve represents the daily water temperature and the blue dashed line represent the species threshold which in this case is 28.5°C and above this limit the fish species start to experience the heat stress. From the plot it is more than clear that the water temperature is always lower than the spices threshold so for this species it did not occur a thermal exceedance during the summer period.

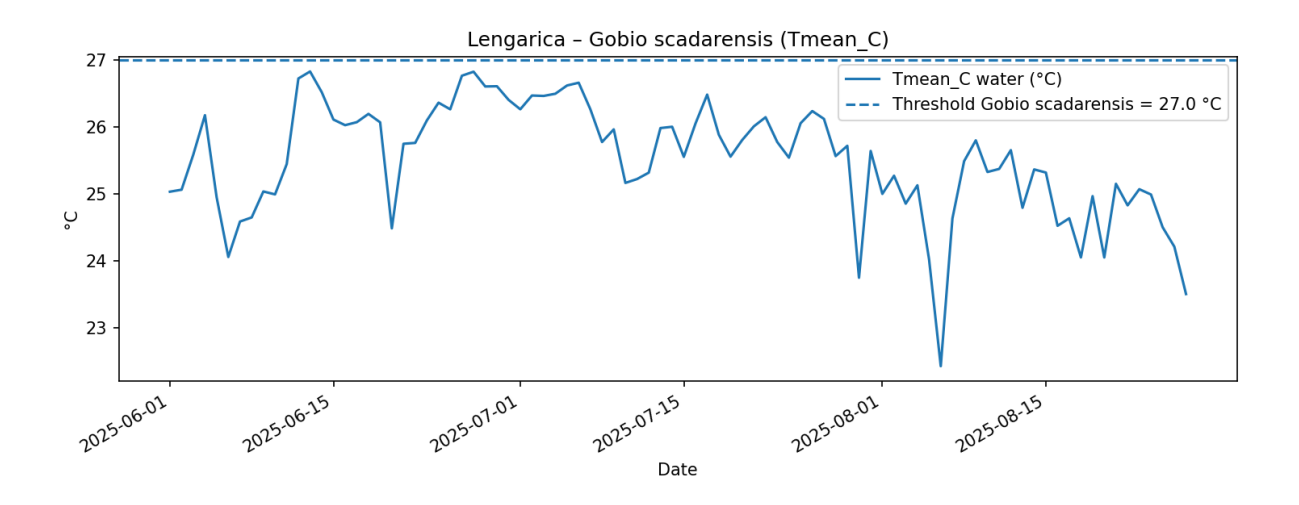


Figure 3.9: T mean and species threshold of Gobio scadarensis

The graph shows the progression of the daily mean water temperature in Lengarica during the summer season June-August 2025 for the fish species *Gobio scadarensis*. The blue curve represents the daily water temperature and the blue dashed line represent the species threshold which in this case is 27°C and above this limit the fish species start to experience the heat stress. From the plot we notice that the water temperature event though is lower than the spices threshold sometimes it approaches the threshold slightly between the middle of June and some days during middle of July. The species experience some moments with potential thermal exceedance during the summer period.

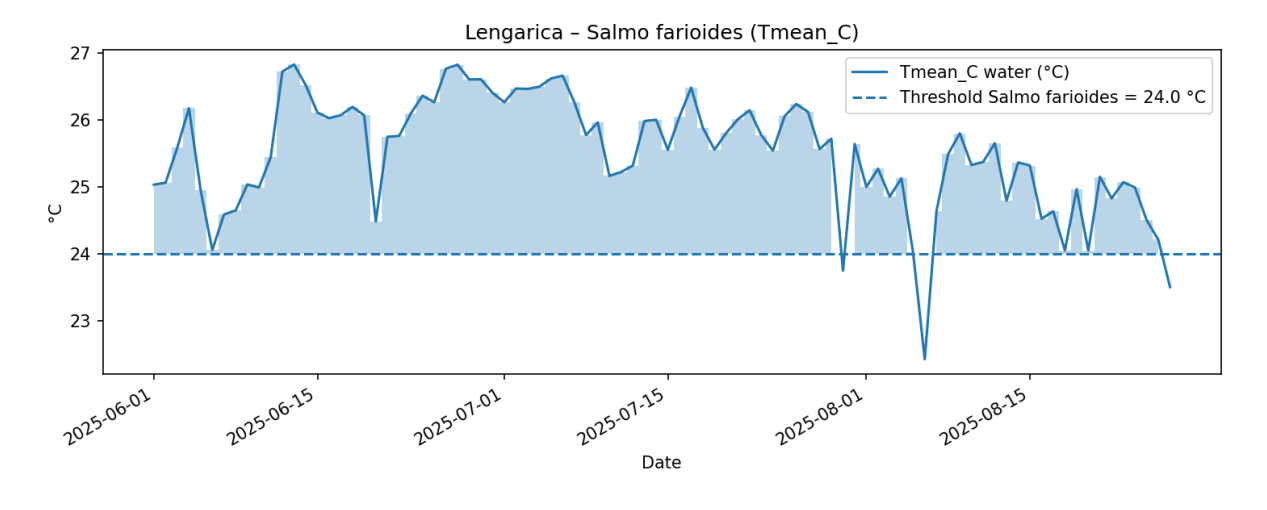


Figure 3.10: T mean and species threshold of Salmo farioides

The graph shows the progression of the daily mean water temperature in Lengarica during the summer season June-August 2025 for the fish species *Salmo farioides*. This kind of fish species is a cold-water salmonid and is very sensitive to warming temperatures. The blue curve represents the daily water temperature and the blue dashed line represent the species

threshold which in this case is 24°C and above this limit the fish species start to experience physiological stress.

In this plot differently from the others the water temperature has exceeded the threshold during the whole summer season and it is represented through the blue shaded area. The exceedance has started from the beginning of June till the end of august with a drop in the first week of august. The warmest period is mid-June until the end of July which shows a very prolonged heat period. The fish species experienced continuous and prolongedheat stress during the summer season according to the results. This kind of exposure can affect salmonid growth and metabolism especially in the delicate life stages.

Vjosa River Results

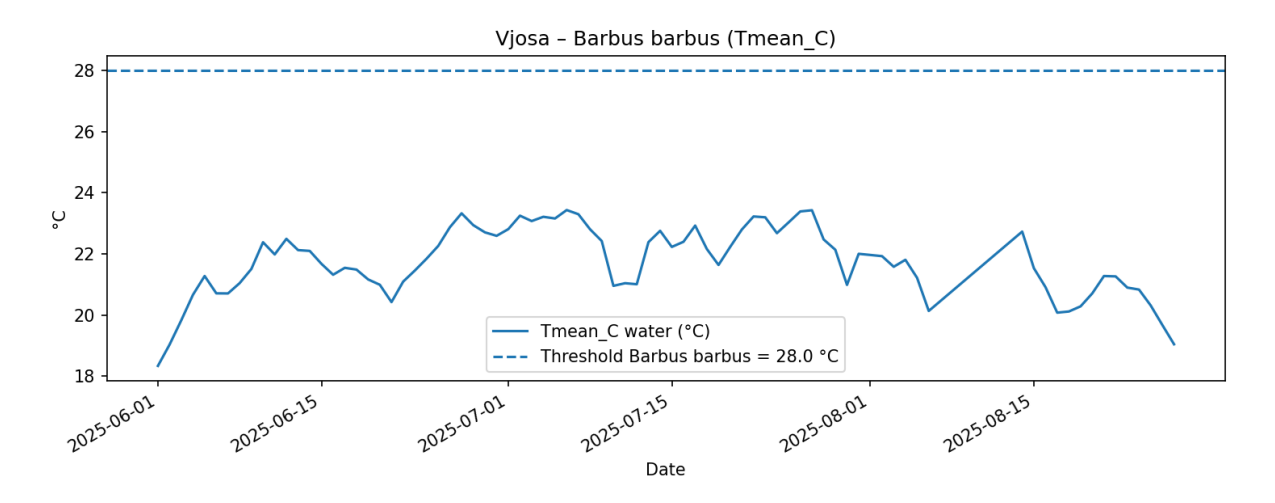


Figure 3.11: T mean and species threshold of Barbus barbus

The graph shows the progression of the daily mean water temperature in Vjosa during the summer season June-August 2025 for the fish species *Barbus barbus*. The blue curve represents the daily water temperature and the blue dashed line represent the species threshold which in this case is 28°C and above this limit the fish species start to experience the heat stress. From the plot it is more than clear that the water temperature is always lower than the spices threshold varying from 18-24°C so for this species it did not occur a thermal exceedance during the summer period. The main Vjosa channel has colder water conditions and is a good refuge compared to Langarica.

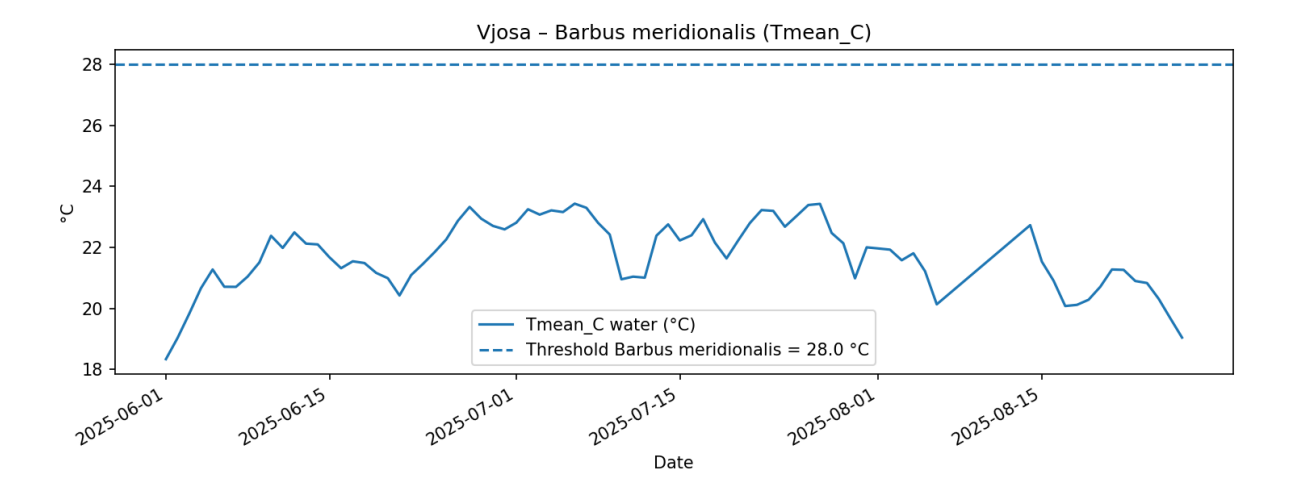


Figure 3.12: T mean and species threshold of Barbus meridionalis

The graph shows the progression of the daily mean water temperature in Vjosa during the summer season June-August 2025 for the fish species *Barbus Meridionalis*. The blue curve represents the daily water temperature and the blue dashed line represent the species threshold which in this case is 28°C and above this limit the fish species start to experience the heat stress. From the plot it is more than clear that the water temperature is always lower than the spices threshold so for this species it did not occur a thermal exceedance during the summer period.

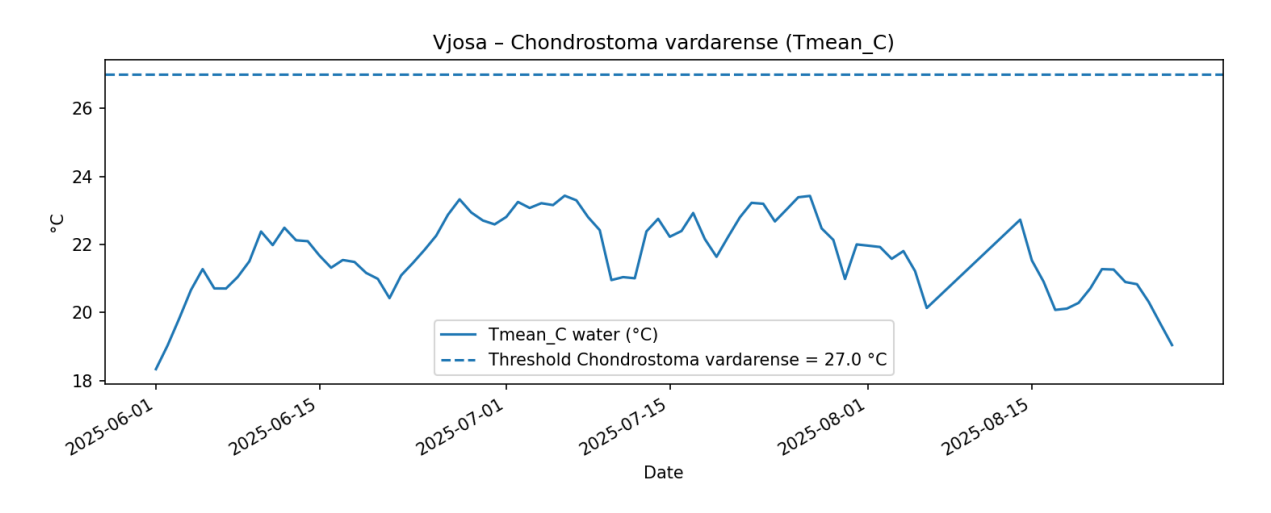


Figure 3.13: T mean and species threshold of Chindrostoma vardarense

The graph shows the progression of the daily mean water temperature in Vjosa during the summer season June-August 2025 for the fish species *Chondrostoma vardarense*. The blue curve represents the daily water temperature and the blue dashed line represent the species threshold which in this case is 27°C a above this limit the fish species start to experience the heat stress. From the plot it is more than clear that the water temperature is always lower than the spices threshold so for this species it did not occur a thermal exceedance during the summer period.

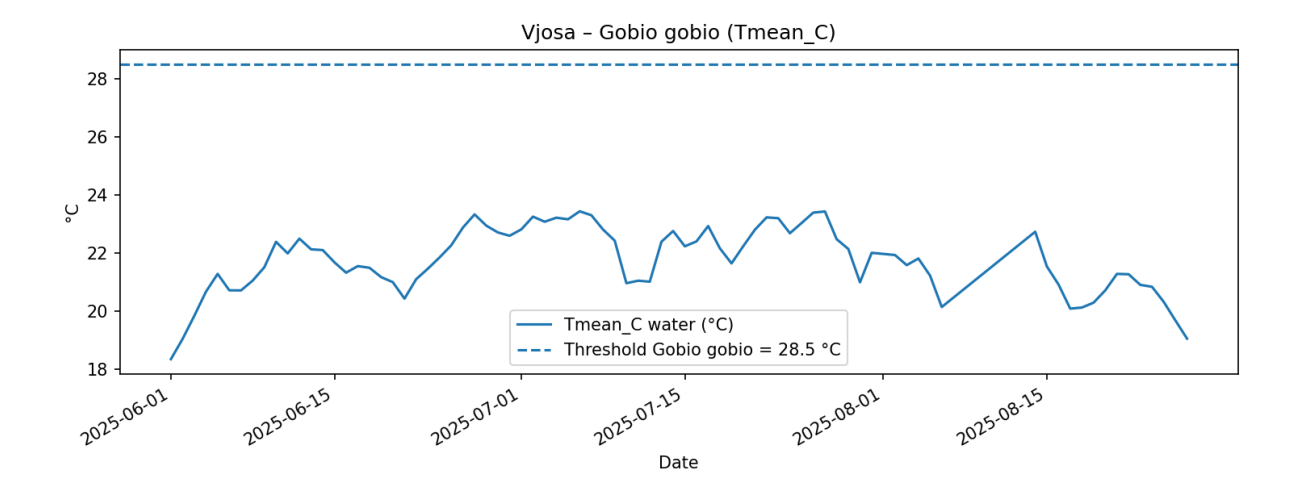


Figure 3.14: T mean and species threshold of Gobio gobio

The graph shows the progression of the daily mean water temperature in Vjosa during the summer season June-August 2025 for the fish species *Gobio gobio*. The blue curve represents the daily water temperature and the blue dashed line represent the species threshold which in this case is 28.5°C and above this limit the fish species start to experience the heat stress. From the plot it is more than clear that the water temperature is always lower than the spices threshold so for this species it did not occur a thermal exceedance during the summer period. The cool hydrological system of Vjosa is suitable for cyprinid species.

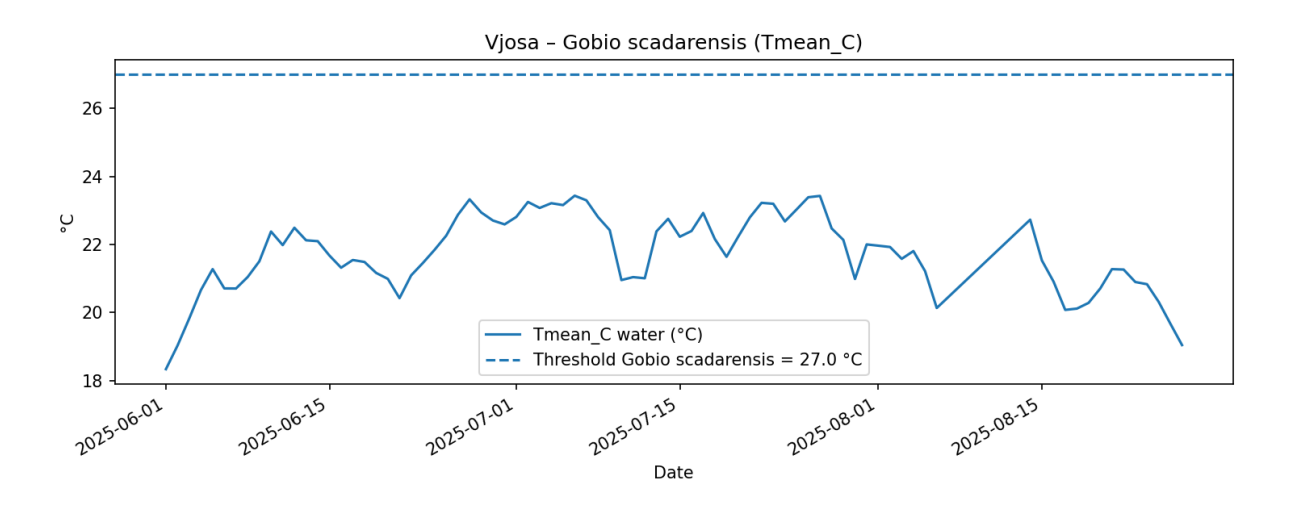


Figure 3.15: T mean and species threshold of Gobio scadarensis

The graph shows the progression of the daily mean water temperature in Vjosa during the summer season June-August 2025 for the fish species *Gobio scadarensis*. The blue curve represents the daily water temperature and the blue dashed line represent the species threshold which in this case is 27°C and above this limit the fish species start to experience the heat stress. From the plot it is more than clear that the water temperature is always lower than the

spices threshold so for this species it did not occur a thermal exceedance during the summer period.

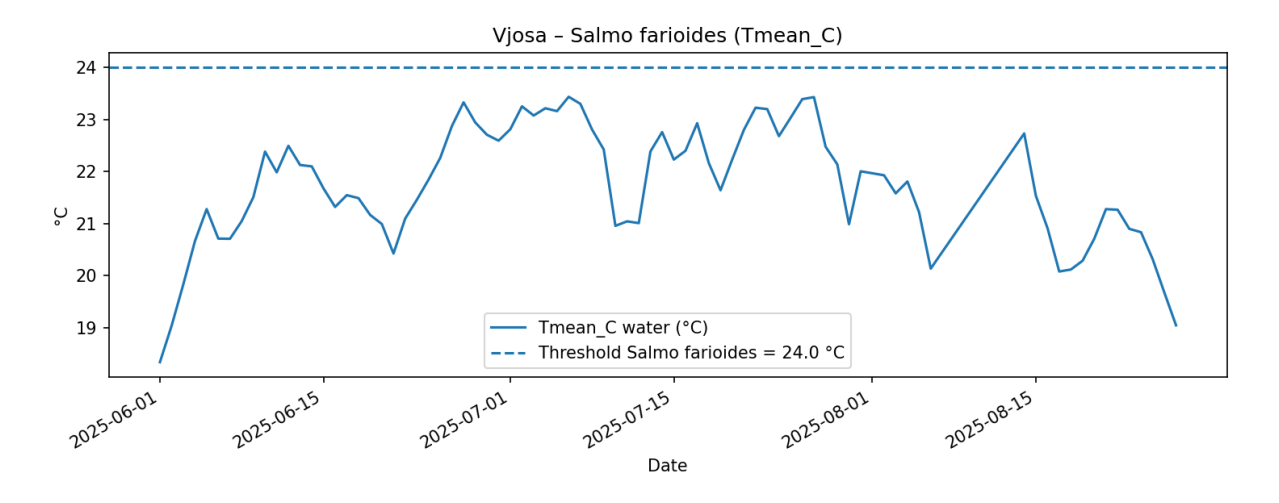


Figure 3.16: T mean and species threshold of Salmo farioides

The graph shows the progression of the daily mean water temperature in Vjosa during the summer season June-August 2025 for the fish species *Salmo farioides*. The blue curve represents the daily water temperature and the blue dashed line represent the species threshold which in this case is 24°C and above this limit the fish species start to experience the heat stress. From the plot it is more than clear that the water temperature is always lower than the spices threshold so for this species it did not occur a thermal exceedance during the summer period.

If this plot is compared with the Lengarica we can notice that Vjosa provides cooler thermal conditions and a more stable habitat for the salmonids.

3.3.2 Frequency of Threshold Exceedance (Heatmap)

Through a heatmap the frequency of the threshold exceedance was analysed and evaluated. The map helps to create a general idea of the studied case by representing the species their thermal tolerances also the percentage of the threshold exceedance in case there are some.

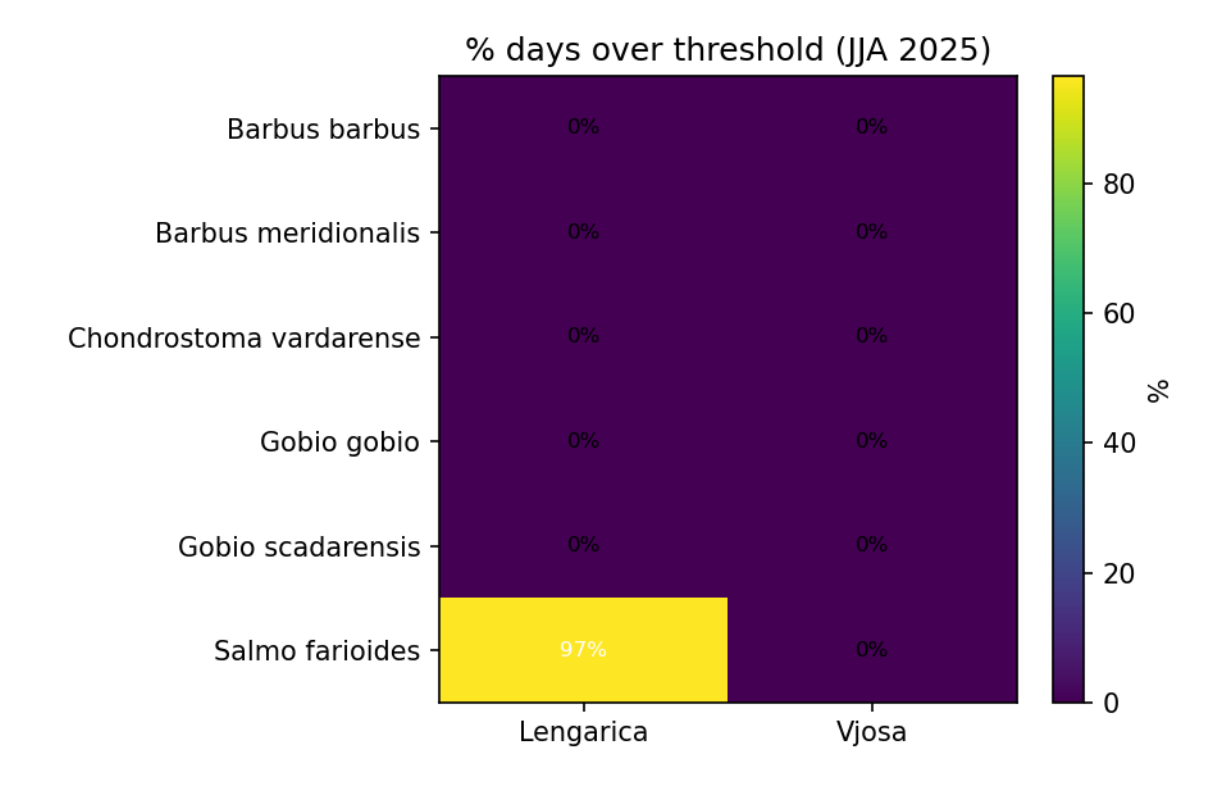


Figure 3.17: Threshold Exceedance Heatmap

The map shows the % of the days where water temperatures exceeded the thermal thresholds in both rivers. The purple cells represent the 0% of days above the threshold where there was no exceedance. Instead, the yellow cell represents the % of days where there was exceedance and in this case is 97%. The heatmap result is consistent with the series plots where expect *Salmo farioides* none of the other species experienced thermal heat stress during summer season.

3.3.3 Exceedance Degree Days

Exceedance Degree Day which measures the total amount of accumulated heat above species threshold was used in this subchapter to analyse and explain the thermal stress. This type of variable provides a general overview about the intensity of the thermal stress that different fish species experience.

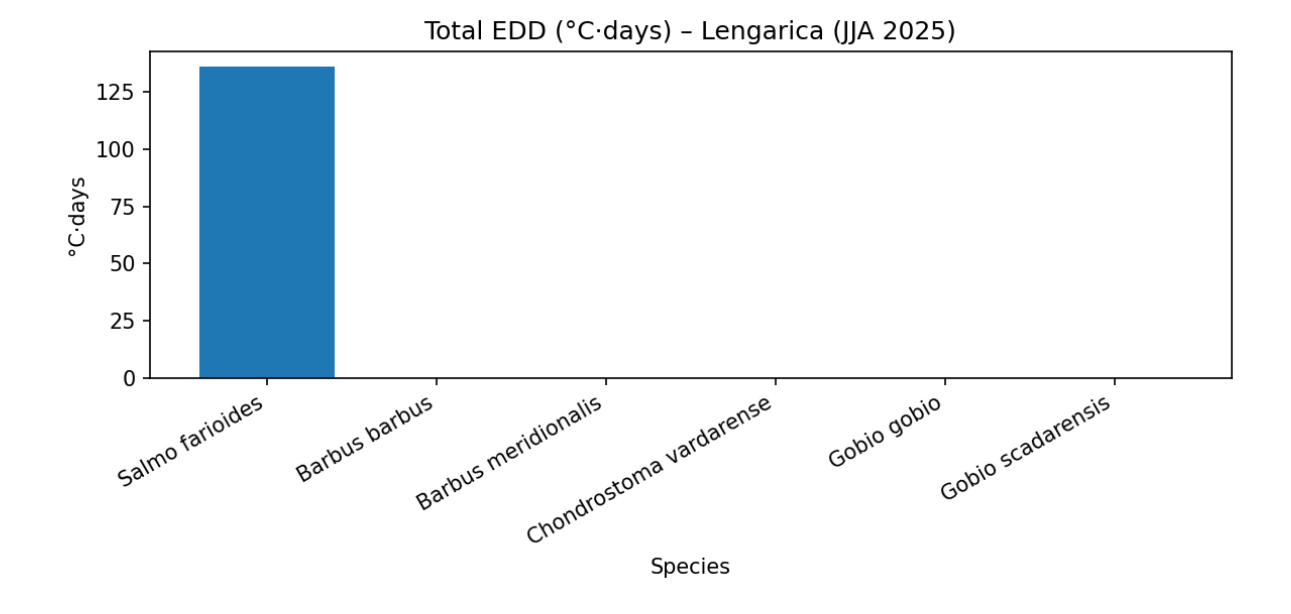


Figure 3.18 EED Lengarica river

The figure represents an EED analysis for the Lengarica tributary for the summer season. The most affected species is *Salmo farioides* which accumulated a heat stress about 135°C·days which means that the temperature stayed above the threshold for almost 2 months. All the other species were not influenced from the temperature oscillation since the mean temperatures remained under the species respective thresholds. There is also another detail in the plot which is the different responsive behaviour of different fish species toward thermal oscillations.

During the summer season of 2025, water temperatures in Vjosa did not exceed the species threshold showing that Vjosa acts as a better habitat form the thermal point of view.

The results indicate that in this case there is a higher chance that thermal risk is concentrated in the tributaries instead of the main stream as Vjosa. If the comparison between salmonids and cyrpinids is made it is clear that the first ones are very sensitive to the thermal oscillations and they occupy the lower end of the thermal spectrum tolerance. Rivers of the Mediterranean are projected to warm 2-3 degrees by 2100 according to [24] (MedECC, 2020) and this prediction also suggests that exceedance frequency will increase by threating the cold-water species and the biodiversity. It should be important to manage or take prevention by prioritizing the refugia through riparian

The results of this chapter request also some possible solutions in case that the heatwaves will be more frequent and longer in the future. According to [25] (Isaak & Young, 2023) connecting cold water refugia can create excellent conservation zones since salmonids use this type of habitats during the heatwaves. Also, through setback buffers and native canopy restoration can be reconstructed the riparian shades which smooth the maxima during the warm seasons. [26] (Bowler et al., 2012).

3.3.4 Sub-Lethal Thermal Stress Thresholds

In addition to the critical upper thermal threshold of 24°C, it is essential to consider lower sub-lethal thresholds that can also compromise fish health. Research indicates that for salmonids like *Salmo farioides*, disease risk, immune suppression, and increased parasite load often commence at temperatures significantly below lethal limits. For instance:

- Stress threshold (~19–20°C): Fish metabolism and aerobic scope begin to decline, especially with prolonged exposure.
- Disease vulnerability threshold (~21–22°C): Immune function weakens, making individuals more susceptible to infections.
- Critical threshold (≥24°C): Prolonged exposure becomes physiologically unsustainable, leading to high mortality risk.

The analogous procedure can be thus applied also to stress and disease vulnerability thresholds, that of course woul shown higher exposure of fish communities, being 20° and 22°C often found as water temperatures both in theVjosa and Lengarica rivers. By incorporating these graduated thresholds into the analysis, it could be possible to capture not only direct lethal stress but also sub-lethal, chronic stresses that significantly increase the risk of disease outbreaks, reduced growth, and long-term population decline.

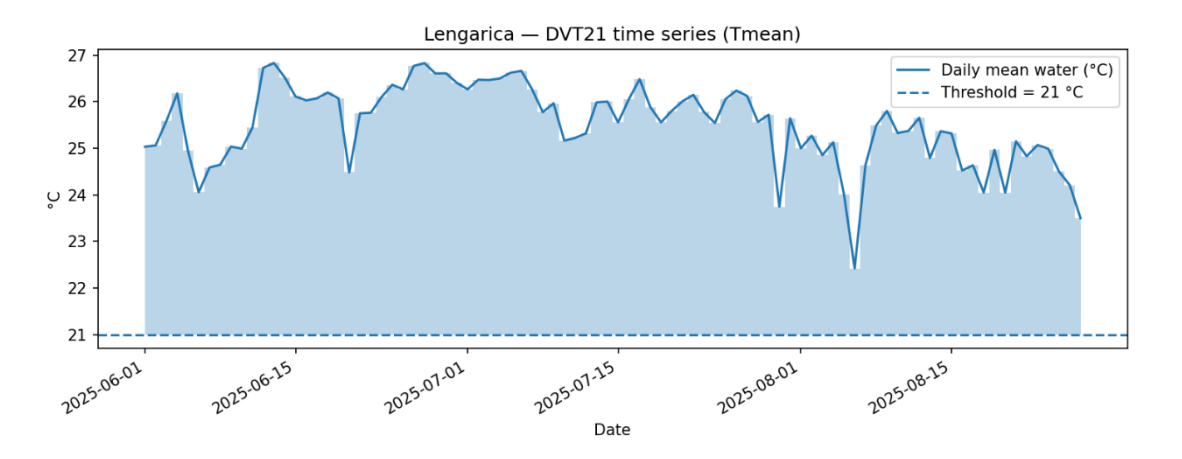


Figure 3.20: T mean and species DVT in Langarica

The figure 3.20 represents the disease vulnerability threshold (21°C) of the species in Lanagarica river during the summer season of 2025. The blue dashed line is the disease vulnerability threshold beyond which the risk of species disease is very high and the physiological stress increases a lot. The blue curve is the daily mean water temperature which varies from 22 to 27°C. The plot indicates that disease vulnerability was permanent during summer and every day the species were under such conditions.

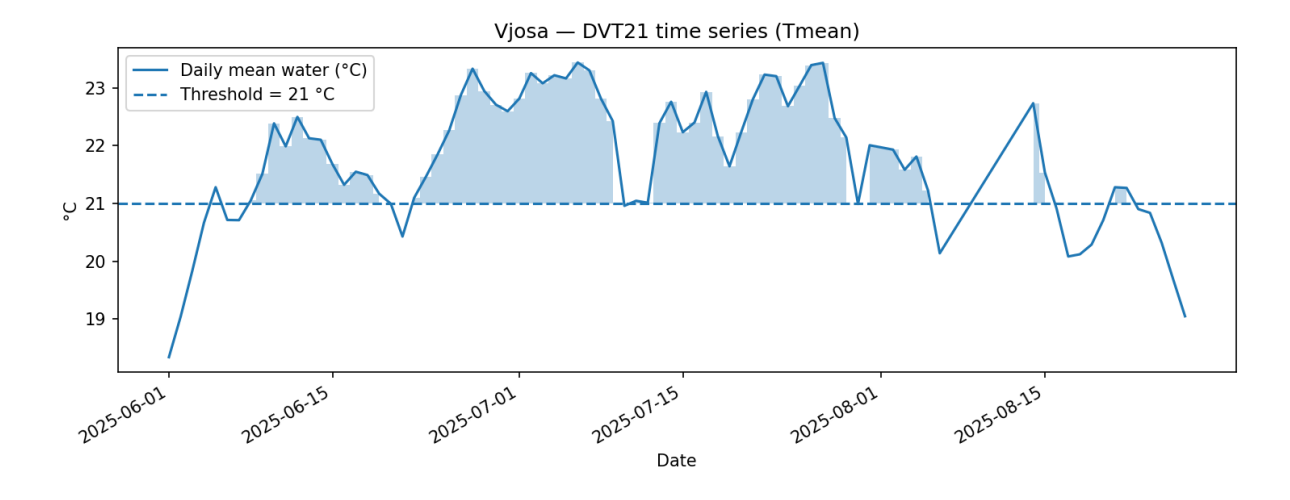


Figure 3.21: T mean and species DVT in Vjosa

The figure represents the disease vulnerability threshold of the species in Vjosa river during the summer season of 2025. The blue dashed line is the desease vulnerability threshold beyond which the risk of species disease is very high and the physiological stress increases a lot. The blue curve is the daily mean water temperature which varies from 19 to 24°C. Vjosa also shows some under threshold days at the beginning of June and at the end of August. In this case the exceedance is not continuous but frequent and intermittent. Even though Vjosa was exposed to periods of disease stress there were also days to cool off and for the habitat to recovery.

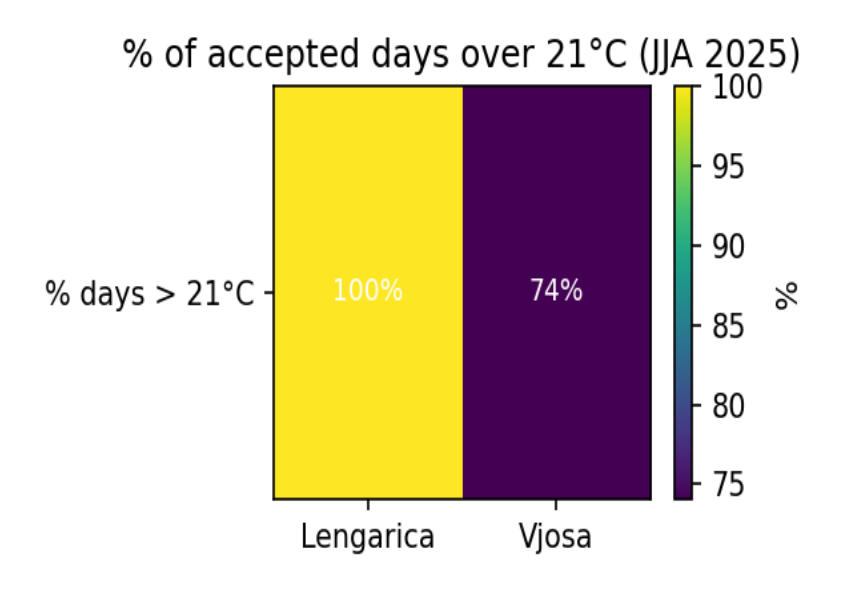


Figure 3.21: Heatmap DVT

The figure shows the percentage of summer days above 21°C disease vulnerability threshold in Vjosa mainstream and Lanagarica tributary. In Lanagrica in 100% of the days, the temperature was above 21°C without any recovery period. Instead in Vjosa, 74% of the days were above the threshold leaving almost one quarter of the time below it and securing a

window of recovery. Langarica differently from Vjosa has experienced a continuous stress related to diseases being a more vulnerable spot of disease for cold water species. Vjosa even though also exposed most of the time has benefited from the cooler days.

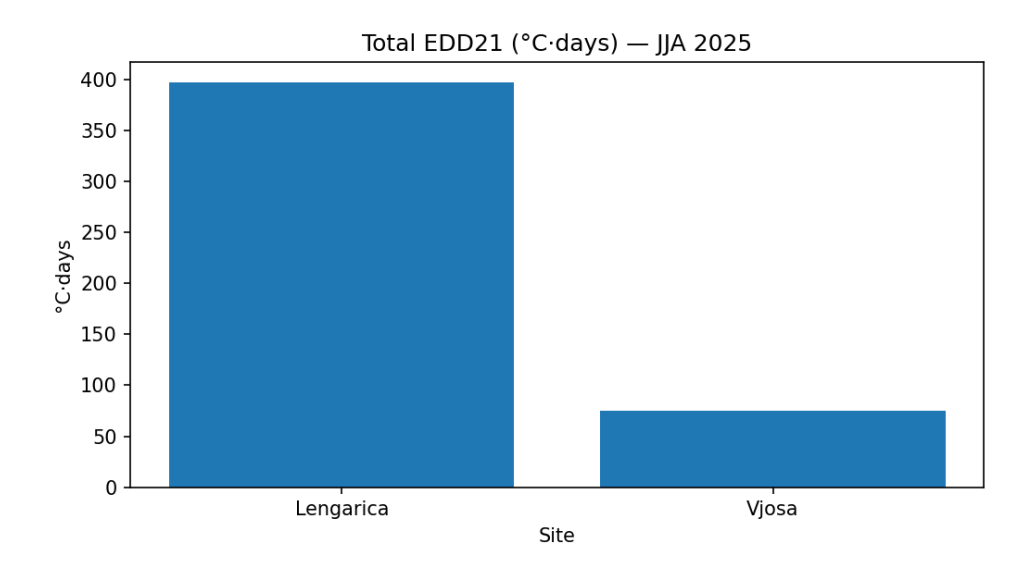


Figure 3.23: EDD 21 in Vjosa and Langarica

The plot is a bar chart that represent the EED above the 21°C disease vulnerability threshold during summer 2025 for Vjosa and Langarica. Both the intensity and the duration are integrated in the plot to give a better understanding of the stress. Langarcia has nearly 400 °C·days meaning that the exceedance was constant and very intense. Vjosa has 75 °C·days meaning that even though there was exceedance there were also some milder periods.

This contrast between Vjosa and Langarica indicates that Vjosa experiencing also milder windows has a greater buffering capacity probably due to larger flows and channel morphology.

4.1 Possible climate scenarios in Vjosa Basin

In the Mediterranean climate change is expected to led to more long and persistent warming seasons with milder and shorter cold seasons and hotter and longer warm seasons [24](Gao et al., 2021). Also, the redistribution of the precipitation towards "the shoulder seasons" which are the periods between high to low season [25](Zittis, 2018). Also, for river habitats as for the basin of Vjosa, the high temperatures are expected to increase the evaporation and the thermal stress on the biota, as was analysed also in the previous chapter. The baseflows (groundwater, lakes, snowmelt etc) are getting smaller because of the dry hot summers. Moreover, the order of storms is changing and this last affects the sediment transport system of the rivers [26] (Ran et al., 2018). In some calculated climate scenarios like RCP4.5 or RCP 8.5 - which are the intermediate and the worst case - there is a very high potential of erosion [27](Marko et al., 2023).

The most problematic areas might be the headwaters and the steep hills. Since the weather pattern will change it is expected longer drier periods with sudden bursts of thunderstorms, which when hit the steep hills will cause flash floods since the soil there is very dry. High erosivity due to the geology of the Vjosa catchment (high proportion of flysch, [28]Schiemer 2020) will be then exacerbated. It is expected that river flow will become increasingly unpredictable, with more frequent floods and longer low-flow periods. As flows oscillate and diverge from current patterns, the sediment budget will also change significantly. These shifts in river morphology will inevitably affect biodiversity and habitat conditions. As highlighted in the previous chapter, rising temperatures will further reduce the availability of thermal refugia, creating a high risk that many fish species will not be able to adapt [27](Marko et al., 2023).

The Vjosa, as one of the last free-flowing rivers in Europe, maintains a strong connection between water and sediment transport along its course. Its near-intact state makes it an ideal natural laboratory to study how climate change influences water–sediment interactions and reshapes rivers. The presence of multiple interwoven channels, constantly shifting, demonstrates the system's natural capacity to mobilize sediment. Climate change will not stop the river from evolving, but the modes of change are likely to shift, becoming more abrupt and chaotic. As [29]Schiemer et al. (2018) note, it is not sufficient to focus only on rising temperatures or increased flooding; it is equally important to understand the mechanisms through which the river transports and reorganizes its gravel and fine sediments.

4.1.1 Possible impacts on the ecosystem

Vjosa, being a free-flowing river with a high sediment mobility, has a high variety of habitats. The habitat is composed of riffle, braid islands, side channels ecc depending on the continuous exchanges of water and sediment. The warming climate impacts the low-flow seasons, increase the flow variability and this way there is a high risk that in the riparian shade, bottlenecks will be more frequent. [30](ERC2017).

From the ecological point of view spawings and nursery habitats are always moving and in the warmer years the cold water refugia are less stable because of the impactys of climate. As [31]Bizzi et al. (2021) underline, one of the most effective ways to maintain a river's climate resilience is to preserve its ability to shift laterally and to sustain intact long-lateral connections. The designation of Vjosa as a River National Park has given a new point of view to the river management. If years ago, there was a tendency to protect by isolating just fragments instead now the trend is to protect its natural habitats integrating lateral and

longitudinal continuity and connectivity. Adaptation strategies should not be strict but flexible enough to let the river move freely and focusing on protecting the small cool streams, restoring riparian forest, maintaining the barrier free continuity.

4.1.2 Adaptation and mitigation strategies through EU policy frameworks

The EU's Water Framework Directive provides frameworks for the management of the Vjosa basin. This framework allows that the ecological flows of the river can be defended legally and always incorporate nature-based solutions.

On the other side the WFD is not always capable of managing different stressors like it is requested for the river status. It is important to integrate different and combined threats like pollution, habitat fragmentation with thermal risk indicators like EDD so in case of a detected warming trend initiates riparian campaigns. At the site scale every decision taken should be in line with the mitigation hierarchy which means avoiding impacts before starting the restoration process. (Voulvoulis et al., 2017). [32]

The recently adopted **EU Nature Restoration Law** complements the WFD by setting binding targets for ecosystem recovery. It requires Member States to restore a minimum share of degraded river systems, reconnect free-flowing rivers, and enhance biodiversity through measures such as riparian reforestation and floodplain reconnection. For rivers like the Vjosa, this legislation reinforces the priority of safeguarding ecological flows while ensuring that restoration actions enhance resilience to climate change rather than constrain natural river dynamics.

For **Albania**, advancing on its path towards EU accession, alignment with the WFD and the Nature Restoration Law represents both a challenge and an opportunity. On one hand, it calls for strengthening governance, monitoring capacities, and enforcement mechanisms to meet EU environmental standards. On the other, it provides a roadmap for sustainable river basin management that positions the Vjosa as a flagship example of how natural heritage can be integrated into European environmental policy. The designation of the Vjosa as Europe's first Wild River National Park already anticipates these EU directives, demonstrating how national conservation priorities can align with European frameworks.

By integratingtogether WFD, Nature Restoration Law, EU accession path and the mitigation hierarchy to implement a series of measures like maintaining the barrierfree longitudinal continuity, reconnecting floodplains, expanding the riparian canopy to improve shading effect, ecc. This way the management exploits the river connectivity and dynamism as the mechanism that ensures the adaptation of the ecosystem (WFD).

Chapter 5 – Discussion and Conclusions

The objective of this thesis was to evaluate the thrmal regime impacts of climate change on the thermal regime of the Vjosa River basin, specifically concentrating on the sub-catchments of Përmet and Langarica, and to discuss possible impacts of climate change. The project was planned to combine long-term climate reanalysis datasets (ERA5 and ERA5-Land) with records collected in the field to create a multi-scale picture of past changes, current problems, and possible ecological effects. The main research questions were whether we can see global

climate signals at the basin level, how well reanalysis products show local microclimates, and what this means for local cold-water species and aquatic ecosystems in the Vjosa system.

A clear and systematic bias was found when comparing ERA5 outputs to station measurements. ERA5 usually overestimates daily minimum temperatures by about 0.5 to 3 °C and underestimates maximum temperatures by 3 to 7 °C, especially during the hottest months of the year. These differences are due to the well-known smoothing that happens with gridded reanalysis products, which average across different types of terrain within a 30 km cell [1](Hersbach et al., 2020). Consequently, local phenomena such as valley inversions, radiative cooling, and extreme daytime heating are not entirely represented. Even so, ERA5 accurately reproduced the seasonal cycle, showing that it is good for trend and anomaly analyses at climatological scales. Performance metrics corroborated this interpretation: for minimum temperatures, the RMSE was approximately 1 °C with a R² of about 0.78, whereas for maximum temperatures, the RMSE surpassed 3 °C and the R² was negative, signifying inadequate predictive capability without adjustment.

Using these calibrated datasets, the thesis created a baseline climatology for the years 1991 to 2020 and compared it to more recent data from 2022 to 2025. The analysis demonstrated that summers in 2024 surpassed the baseline by over +2 °C in mean air temperature, a deviation aligned with regional Mediterranean warming indicators [37](Lionello & Scarascia, 2018). These anomalies are not only statistically significant but also ecologically significant, as they elevate water temperatures to and beyond established tolerance thresholds for various species. The study converted raw thermal signals into biologically significant stress metrics by figuring out exceedance days, heatwave events, and cumulative exceedance degree-days (EDD).

The findings indicate that the frequency and severity of exceedance events have risen in recent summers, especially in the Langarica tributary, which is more susceptible due to diminished summer flows, shallow depths, and elevated solar exposure. Exceedances above generic thresholds, like 21 °C for disease vulnerability, are now common. The tributaries are very important to get monitored even separately from the mainstream because they are most vulnerable to hat stress and climate. In EED plots another important thing that was noticed was that stress does not happen only when there are big heat spikes but also in the case of small spikes that last for weeks without any cool period.

From an ecological point of view these results are also important if we look at the fish species like Salmo farioides, Chondrostoma vardarense, which are cold water species and rheophilic cyprinids highly sensitive to high temperatures.

Another significant result of this thesis is the implementation of a hybrid measurement that integrates logger data with continuous reanalysis products. Through this method was recognized that each of the dataset has its own weaknesses when used isolated. For example, the loggers gave in-situ ground truth but the time period they cover is not long enough. Instead ERA5 cover decades and contains historical data but in the local range it needs to be validated and corrected. By comparing and rectifying both sources continuously during this

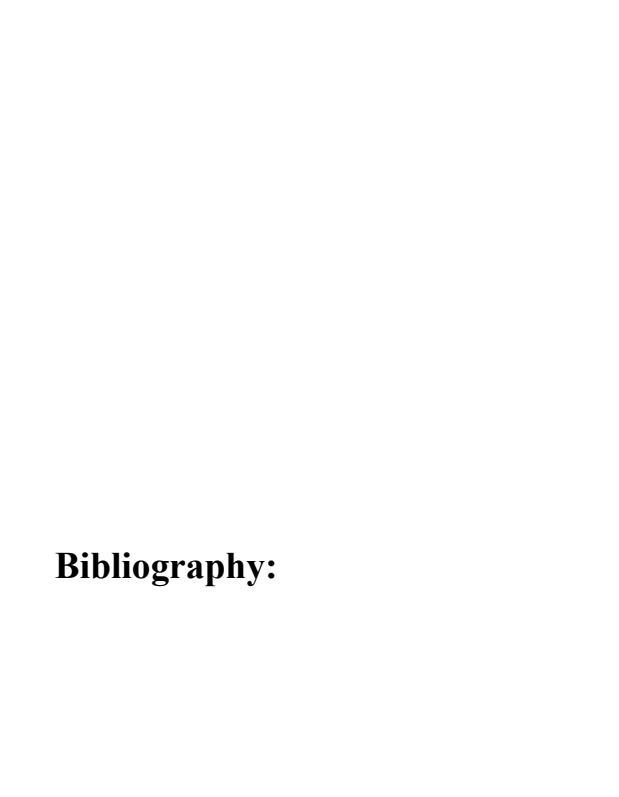
study it was provided a more comprehensive characterization of the thermal regime.

On the other side there are present the limitations of the data and of each method. In our case the short length if the recoded data from the loggers made it impossible to create a direct connection between the air temperatures and the water conditions. ERA5 resolution is not enough to indicate local thermal inversions. Also, the ecological thresholds were taken as fixed values even though in reality they change depending on the stage of life and on flow conditions. It is important that in successive research aim to investigate and enhance the methodological simplification that were done in this study in order to obtain a more effective implementation.

To improve the investigation and study of a thermal regime alteration, more years and tributaries can be added to monitor better the local scale. The data obtained would be helpful it builds strong calibration and study trends. For example, through discharge and radiation data heat models could be build more complete. Modelling downscaling tools like Air2stream [33](Toffolon M., and S. Piccolroaz (2015) show good potential for resolving one of the main gaps in this study, just by using air temperature and discharge data to create water temperature scenarios under different climate projections.

In conclusion, this thesis offers clear evidence that Vjosa basin is undergoing considerable thermal stress which is also aligned with the climate change patterns. ERA5 data were useful to set the scene and finding the anomalies as long as bias correction were made, even though they are not perfect in local scale. All the different patterns like the increase of the exceedance days, heatwaves events, thermal stress are a serious problem for the taxa sensitive to these patterns. The management should focus more on taking care of the summer flows, protecting the cold refugia and always protecting the riparian shading. This work shows that by combining local monitoring, reanalysis data and exceedance metrics it is a good strategy to predict ecological risks in free-flowing rivers by climate change.

In a more general sense, this work shows that combining reanalysis data, local monitoring, and exceedance-based metrics is a strong way to predict ecological risks in free-flowing rivers affected by climate change.



Hersbach, H., Bell, B., Berrisford, P., Biavati, G., Horányi, A., Muñoz Sabater, J., Nicolas, J., Peubey, C., Radu, R., Rozum, I., Schepers, D., Simmons, A., Soci, C., Dee, D., Thépaut, J-N. (2023): *ERA5 hourly data on single levels from 1940 to present. Copernicus Climate Change Service (C3S) Climate Data Store (CDS)*, DOI: 10.24381/cds.adbb2d47 (Accessed on 13 June 2025)

WWF (2021) *WWF Annual Report 2021*. Gland, Switzerland: World Wide Fund for Nature (WWF). https://files.worldwildlife.org/wwfcmsprod/files/FinancialReport/file/7g37j96psg_WWF_AR2021_spreads.pdf (Accessed:13 March 2025).

Caissie, D. (2006) 'The thermal regime of rivers: a review', *Freshwater Biology*, **51**(8), pp. 1389–1406. Available at: https://onlinelibrary.wiley.com/doi/10.1111/j.1365-2427.2006.01597.x (Accessed: 29 May 2025).

Schiemer, F., Drescher, A., Hauer, C. and Schwarz, U. (2018) 'The Vjosa River corridor: a model of natural hydro-morphodynamics and a hotspot of highly threatened ecosystems of European significance', *Landscape Ecology*, **33**(6), pp. 923–938.

Available at: https://link.springer.com/article/10.1007/s10980-018-0650-8 (Accessed: 30 May 2025).

Schinegger, R., Trautwein, C., Melcher, A. and Schmutz, S. (2013) 'The challenge of establishing an ecological reference status for large rivers—A case study of the Austrian Danube', *Hydrobiologia*, **704**(1), pp. 357–375.

Available at: https://link.springer.com/article/10.1007/s10750-012-1253-8 (Accessed: 30 May 2025).

Poole, G.C. and Berman, C.H. (2001) 'An ecological perspective on in-stream temperature: natural heat dynamics and mechanisms of human-caused thermal degradation', *Environmental Management*, **27**(6), pp. 787–802.

Available at: https://link.springer.com/article/10.1007/s00267-001-0188-0 (Accessed: 29 May 2025).

Caissie, D. (2006) 'The thermal regime of rivers: a review', *Freshwater Biology*, **51**(8), pp. 1389–1406. Available at: https://onlinelibrary.wiley.com/doi/10.1111/j.1365-2427.2006.01597.x (Accessed: 29 May 2025).

Poole, G.C. and Berman, C.H. (2001) 'An ecological perspective on in-stream temperature: natural heat dynamics and mechanisms of human-caused thermal degradation', *Environmental Management*, **27**(6), pp. 787–802.

Available at: https://link.springer.com/article/10.1007/s00267-001-0188-0 (Accessed: 29 May 2025).

Schiemer, F., Drescher, A., Hauer, C. and Schwarz, U. (2018) 'The Vjosa River corridor: a model of natural hydro-morphodynamics and a hotspot of highly threatened ecosystems of European significance', *Landscape Ecology*, **33**(6), pp. 923–938.

Available at: https://link.springer.com/article/10.1007/s10980-018-0650-8 (Accessed: 30 May 2025).

Schinegger, R., Trautwein, C., Melcher, A. and Schmutz, S. (2013) 'The challenge of establishing an ecological reference status for large rivers—A case study of the Austrian Danube', *Hydrobiologia*, **704**(1), pp. 357–375.

Available at: https://link.springer.com/article/10.1007/s10750-012-1253-8 (Accessed: 23 April 2025).

Marcos-Garcia, P., Pulido-Velazquez, M., Garcia-Molla, M. et al. (2017) 'Combined use of relative drought indices to analyze climate change impact on meteorological and hydrological droughts in a Mediterranean basin', *Journal of Hydrology*, **553**, pp. 444–456.

Available at: https://www.sciencedirect.com/science/article/abs/pii/S0022169417306327 (Accessed: 3 June 2025).

Yavuz, V.S., [insert co-authors if applicable] (2025) 'Impact of temperature and flow rate on oxygen dynamics and water quality in major Turkish rivers', *Scientific Reports*, **15**, Article 22830.

Available at: https://www.nature.com/articles/s41598-025-06433-8 (Accessed: 3 June 2025). nature.com

Papadaki, C., Kavvadias, A., Zogaris, S. & Dimitriou, E. (2022) 'Human interventions to natural streamflow: flow regime, habitat and hydraulic modelling for environmental flows', in *Marine and Inland Waters Research Symposium 2022 Proceedings*. Hellenic Centre for Marine Research.

Available at: https://flowtech.hcmr.gr/wp-content/uploads/2023/02/Papadakietal2022 Proceedings Marine-and-Inland-Waters-Research-Symposium-2022.pdf (Accessed: 3 June 2025).

Žganec, K. (2012) 'The effects of water diversion and climate change on hydrological alteration and temperature regime of karst rivers in central Croatia', *Environmental Monitoring and Assessment*, **184**(9), pp. 5705–5723.

Available at: https://doi.org/10.1007/s10661-011-2376-7 (Accessed:3 June 2025).

Zajkov, M., Gjoni, V., Stafilovska, P., Stojkoska, E. & Slavevska-Stamenković, V. (2023) 'Contribution to the Knowledge of the Benthic Invertebrate Fauna of the Vjosa River (Albania) and Its Tributaries', *Diversity*, **15**(3), 444.

Available at: https://doi.org/10.3390/d15030444 (Accessed: 3 June 2025).

Estrela-Segrelles, C., Gómez-Martínez, G. & Pérez-Martín, M.Á. (2023) 'Climate Change Risks on Mediterranean River Ecosystems and Adaptation Measures (Spain)', *Water Resources Management*, **37**, pp. 2757–2770.

Available at: https://doi.org/10.1007/s11269-023-03469-1 (Accessed:3 June 2025). link.springer.com+1

Carlson, E.A., Melathopoulos, A. & Sagili, R. (2024) 'The power to (detect) change: Can honey bee collected pollen be used to monitor pesticide residues in the landscape?', *PLoS ONE*, **19**(9), e0309236. Available at: https://doi.org/10.1371/journal.pone.0309236 (Accessed: 3 June 2025).

Carlson, E.A., Melathopoulos, A. & Sagili, R. (2024) 'The power to (detect) change: Can honey bee collected pollen be used to monitor pesticide residues in the landscape?', *PLoS ONE*, **19**(9), e0309236. Available at: https://doi.org/10.1371/journal.pone.0309236 (Accessed: 7 June 2025).

Pease, A.A., Matthews, M.S., Linke, S. and Gido, K.B. (2011) 'Thermal heterogeneity and groundwater discharge in a karst river system', *Freshwater Science*, **30**(4), pp. 1165–1176. Available at: https://doi.org/10.1899/10-149.1 (Accessed: 7 June 2025).

Milošević, **D.**, **Maric**, **D.**, **Pešić**, **V.** and **Pavicević**, **A.** (2016) 'Length-weight relationship and condition factor of two sympatric *Rutilus* species in Lake Skadar (Montenegro)', *Archives of Biological Sciences*, **68**(1), pp. 177–184.

Available at: https://doi.org/10.2298/ABS150420038M (Accessed: 7 June 2025).

Crivellaro, M., Ragno, N., Tubino, M. & Bonanomi, R. (2024) 'Evidences of permafrost signatures in the planform shape of Arctic meandering streams', *Geophysical Research Letters*, **51**(17). Available at: https://doi.org/10.1029/2024GL109410 (Accessed: 3 March 2025).

Viviroli, D., Kummu, M., Meybeck, M., Kallio, M. & Wada, Y. (2020) 'Increasing dependence of lowland populations on mountain water resources', *Nature Sustainability*, **3**, pp. 917–928. Available at: https://doi.org/10.1038/s41893-020-0559-9 (Accessed: 7 June 2025).

Crivellaro, M., Serrao, L., Bertoldi, W., Bizzi, S., Vitti, A., Hauer, C., Skrame, K., Cekrezi, B. and Zolezzi, G. (2024) 'Multiscale morphological trajectories to support management of free-flowing rivers: the Vjosa in South-East Europe', Journal of Environmental Management, 370, 122541.

Available at: https://doi.org/10.1016/j.jenvman.2024.122541 (Accessed: 3 March 2025).

Isaak, D.J., Wollrab, S., Horan, D. and Chandler, G. (2011) 'Climate change effects on stream and river temperatures across the northwest U.S. from 1980–2009 and implications for salmonid fishes', *Climatic Change*, 113, pp. 499–524.

Available at: https://doi.org/10.1007/s10584-011-0326-z (Accessed: 7 June 2025).

Hersbach, H., Bell, B., Berrisford, P., Hirahara, S., Horányi, A., Muñoz-Sabater, J., Nicolas, J., Peubey, C., Radu, R., Schepers, D., Simmons, A., Soci, C., Abdalla, S., Abellan, X., Balsamo, G., Bechtold, P., Biavati, G., Bidlot, J., Bonavita, M., De Chiara, G., Dahlgren, P., Dee, D., Diamantakis, M., Dragani, R., Flemming, J., Forbes, R., Fuentes, M., Geer, A., Haimberger, L., Healy, S., Hogan, R.J., Hólm, E., Janisková, M., Keeley, S., Laloyaux, P., Lopez, P., Lupu, C., Radnoti, G., de Rosnay, P., Rozum, I., Vamborg, F., Villaume, S. and Thépaut, J-N. (2020) 'The ERA5 global reanalysis', *Quarterly Journal of the Royal Meteorological Society*, 146(730), pp. 1999–2049. Available at: https://doi.org/10.1002/qj.3803 (Accessed: 8 June 2025).

Wanders, N., van Vliet, M.T.H., Wada, Y., Bierkens, M.F.P. & van Beek, L.P.H. (2019) 'High-resolution global water temperature modeling', *Water Resources Research*, **55**(4), pp. 2760–2778.

Available at: https://doi.org/10.1029/2018WR023250 (Accessed: 22 June 2025).

World Meteorological Organization (WMO) (2017) WMO Statement on the State of the Global Climate in 2017. Geneva: WMO.Available at: https://library.wmo.int/doc_num.php?explnum_id=4305 (Accessed: 9 September 2025).

IPCC (2014) Climate Change 2014: Synthesis Report. Contribution of Working Groups I, II and III to the Fifth Assessment Report of the Intergovernmental Panel on Climate Change. Geneva: Intergovernmental Panel on Climate Change.

Available at: https://www.ipcc.ch/report/ar5/syr/ (Accessed: 9 September 2025).

Yue, S. and Pilon, P. (2004) 'A comparison of the power of the t test, Mann–Kendall and bootstrap tests for trend detection', *Hydrological Sciences Journal*, 49(1), pp. 21–37.

Available at: https://doi.org/10.1623/hysj.49.1.21.53996 (Accessed: 9 September 2025).

Hamed, K.H. and Rao, A.R. (1998) 'A modified Mann–Kendall trend test for autocorrelated data', *Journal of Hydrology*, **204**(1–4), pp. 182–196.

Available at: https://doi.org/10.1016/S0022-1694(97)00125-X (Accessed: 9 September 2025).

Yue, S. and Pilon, P. (2004) 'A comparison of the power of the t test, Mann–Kendall and bootstrap tests for trend detection', *Hydrological Sciences Journal*, 49(1), pp. 21–37.

Available at: https://doi.org/10.1623/hysj.49.1.21.53996 (Accessed: 9 September 2025).

MedECC, 2020. Climate and Environmental Change in the Mediterranean Basin – Current Situation and Risks for the Future. First Mediterranean Assessment Report (MAR1). Marseille, France: MedECC Secretariat / Union for the Mediterranean / Plan Bleu / UNEP/MAP.

Available at: https://www.medecc.org/wp-content/uploads/2021/05/MedECC_MAR1_SPM_ENG.pdf (Accessed: 9 September 2025).

Isaak, D.J. & Young, M.K. (2023) 'Elevation-dependent warming of streams in mountainous regions: implications for temperature modeling and headwater climate refugia', *Canadian Water Resources Journal*, **48**(2), pp. 167–188.

Available at: https://doi.org/10.1080/07011784.2023.2176788 (Accessed: 25 September 2025).

Bowler, D.E., Mant, R., Orr, H., Hannah, D.M. & Pullin, A.S. (2012) 'What are the effects of wooded riparian zones on stream temperature?', *Environmental Evidence*, **1**, 3.

Available at: https://doi.org/10.1186/2047-2382-1-3 (Accessed: 25 September 2025). environmentalevidencejournal.biomedcentral.com

Gao, X., Giorgi, F. and Dell'Aquila, A. (2021) 'Projections of future daily temperature and precipitation extremes over the Mediterranean region from a WCRP-CORDEX high-resolution and multi-model ensemble', *Earth System Dynamics*, **12**(4), pp. 1145–1163.

Available at: https://doi.org/10.5194/esd-12-1145-2021 (Accessed:16 September 2025).

Zittis, G. (2018) 'Observed and projected changes in the seasonality of precipitation in the Mediterranean region', *Regional Environmental Change*, **18**(6), pp. 1641–1653.

Available at: https://doi.org/10.1007/s10113-018-1296-3 (Accessed: 18 September 2025).

Ran, Q., Gao, Y., Marx, L. and Perica, S. (2018) 'Does storm temporal pattern matter for sediment transport? An experimental study using a tilting flume', *Journal of Hydrology*, **563**, pp. 889–899. Available at: https://doi.org/10.1016/j.jhydrol.2018.06.064 (Accessed: 26 September 2025).

Marko, O., Gjoka, K., Shkodrani, N., Gjipalaj, J., & Aliu, A. (2023) 'Climate Change Effect on Soil Erosion in Vjosa River Basin', *Journal of Ecological Engineering*, **24**(2), pp. 92–100.

Available at: https://doi.org/10.12911/22998993/156831 (Accessed: 26 September 2025)

Schiemer, F., Beqiraj, S., Drescher, A., Graf, W., Egger, G., Essl, F., Frank, T., Hauer, C., Hohensinner, S., Miho, A., Meulenbroek, P., Paill, W., Schwarz, U. & Vitecek, S. (2020) 'The Vjosa River corridor: a model of natural hydro-morphodynamics and a hotspot of highly threatened ecosystems of European significance',

Landscape Ecology, 35, pp. 953-968.

Available at: https://doi.org/10.1007/s10980-020-00993-y (Accessed: 30 May2025).

European Research Council (ERC) (2017) Annual Report on the ERC Activities and Achievements in 2017. Brussels: ERC. Available at: https://erc.europa.eu/sites/default/files/2022-09/erc_annual_report_2017.pdf (Accessed: 1 October 2025).

Bizzi, S., Tangi, M., Schmitt, R., Pitlick, J., Piegay, H. & Castelletti, A. (2021) 'Sediment transport at the network scale and its link to channel morphology in the braided Vjosa River system', Earth Surface Processes and Landforms, 46(14), pp. 2946-2962. Available at: https://doi.org/10.1002/esp.5225

(Accessed: 1 October 2025).

Voulvoulis, N., Arpon, K.D. & Giakoumis, T. (2017) 'The EU Water Framework Directive: From great expectations to problems with implementation', Science of the Total Environment, 575, pp. 358–366.

Available at: https://www.sciencedirect.com/science/article/pii/S004896971632157X (Accessed: 1 October 2025).

Toffolon M., and S. Piccolroaz (2015), A hybrid model for river water temperature as a function of air temperature and discharge, Environmental Research Letters, under review

Piccolroaz S., M. Toffolon, and B. Majone (2013), A simple lumped model to convert air temperature into surface water temperature in lakes, Hydrol. Earth Sys

Lionello, P. & Scarascia, L., 2018. *The relation between climate change in the Mediterranean region and global warming.* **Regional Environmental Change**, 18(5), pp.1481–1493. https://doi.org/10.1007/s10113-018-1290-1. MedECC

Shumka, S., Bego, F., Beqiraj, S., Paparisto, A., Shuka, L., Kashta, L., Miho, A., Shumka, L. & Mali, S., 2018. *Trading-off freshwater biodiversity and hydropower in a unique Balkan hotspot (Vjosa River watershed, Albania)*. **The Holistic Approach to Environment**, 8(4), pp.114–123. https://doi.org/10.1001/josa.2018.01

EU4Nature – **Inception Report.** The most recent publicly available inception report I can find is: UNDP Albania, 2024. *EU4Nature Action: Inception Report* (June 2024). Available via project trackers. If you need a 2025 edition, I couldn't locate it publicly.

Figure 1.1
Figure 2.1, a, b Air logger installed at CESVI office, Permet May 2025 and the logger model
Figure 2.4, a,b The installation of the water logger in Vjosa and in Langarica (Crivellaro, May 2025)
Figure 2.6 DEM Albania, 10m
Figure 2.8 Permet Catchement
Figure 2.9 Permet Catchment and River Segments in the Study Catchment
Figure 2.10.a, b Slope map of the Permet catchment (left) with legend (right).
Figure 2.11.a, b Slope < 5% map (black) t1 (white); the river reach selected is shown in re
Figure 2.12 Attribute table of river-network metrics
Figure 2.13 Attribute table Flat-terrain proportion
Figure 2.14 Permet Bridge Cross-section
Figure 2.15 Permet Bridge Cross-section distance vs elevation
Figure 2.16 Monthly climatology 1991-2020
Figure 2.17 Monthly mean temperature anomalies (°C) relative the 1991–2020 baseline,
shown separately20
Figure 2.18 Monthly anomalies relative the 1991–2020 baseline (°C)21.
Figure 2.19 Monthly anomalies of 202426
Figure 2.20 January temperature summary27
Figure 2.21 February temperature summary
Figure 2.22 March temperature summary
Figure 2.23 April temperature summary
Figure 2.24 May temperature summary
Figure 2.25 June temperature summary30
Figure 2.26 July temperature summary
Figure 2.27 August temperature summary31
Figure 2.28 September temperature summary
Figure 2.29 October temperature summary
Figure 2.30 November temperature summary
Figure 2.31 December temperature summary
Figure 2.32 DJF (Winter) seasonal temperature summary34
Figure 2.33 MAM (Spring) seasonal temperature summary
Figure 2.34 JJA (Summer) seasonal temperature summary
Figure 2.35 SON (Autumn) seasonal temperature summary
Figure 2.36 Monthly mean and moving average
Figure 2.37 Tmax annual mean MK Test
Figure 2.38 Tmin annual mean MK Test
Figure 2.39 Tmean annual mean MK Test
Figure 2.40, a Comparison of ERA5 and Station Daily Maximum Temperatures (Tmax)—
August 202241

Figure 2.40, b Comparison of ERA5 and Station Daily Maximum Temperatures (Tmax) —
August 202241
Figure 2.41, a Comparison of ERA5 and Station Daily Minimum Temperatures (Tmin) — August 202242
Figure 2.41, b Comparison of ERA5 and Station Daily Minimum Temperatures (Tmin)—
August 2022
Figure 2.42, a Comparison of ERA5 and Station Daily Maximum Temperatures (T max) —
August 202343
Figure 2.42, b Comparison of ERA5 and Station Daily Maximum Temperatures (T max) —
August 202343
Figure 2.43, a Comparison of ERA5 and Station Daily Minimum Temperatures (T min) —
August 2023
Figure 2.43, b Comparison of ERA5 and Station Daily Minimum Temperatures (Tmin) —
August 2023
Figure 2.44, a Comparison of ERA5 and Station Daily Maximum Temperatures (T max) — July 202444
Figure 2.44, b Comparison of ERA5 and Station Daily Maximum Temperatures (T max) —
July 202445
Figure 2.45, a Comparison of ERA5 and Station Daily Minimum Temperatures (T min) —
July 202445
Figure 2.45, b Comparison of ERA5 and Station Daily Minimum Temperatures (T min) —
July 202446
Figure 2.46, a Comparison of ERA5 and Station Daily Maximum Temperatures (T max) —
August 2024
Figure 2.46, b Comparison of ERA5 and Station Daily Maximum Temperatures (T max) —
August 202447
Figure 2.47, a Comparison of ERA5 and Station Daily Minimum Temperatures (T min) —
August 202447
Figure 2.47, b Comparison of ERA5 and Station Daily Minimum Temperatures (T min) —
August 2024
Figure 2.48, a Comparison of ERA5 and Station Daily Maximum Temperatures (T max) —
September 2024
September 2024
Figure 2.49, a Comparison of ERA5 and Station Daily Minimum Temperatures (T min) —
September 2024
Figure 2.49, b Comparison of ERA5 and Station Daily Minimum Temperatures (T min) —
September 202450
Figure 2.50 Monthly mean bias ERA5 vs Local Station53
Figure 2.51 LBC of ERA5 Temperatures for May 202553
Figure 2.52 LBC of ERA5 Temperatures for June 2025
Figure 2.53 LBC of ERA5 Temperatures for July 2025
Figure 2.54 QM of ERA5 Temperatures for May 2025
Figure 2.55 QM of ERA5 Temperatures for June 2025
56
Figure 2.56 QM of ERA5 Temperatures for June 2025
56
Figure 2.57 Langarica water temperature trend, May 2025
Figure 2.58 Langarice boxplot for May 202558
Figure 2.59 Langarica water temperature trend, June 2025

Figure 2.60 Langarice boxplot for June 202559
Figure 2.61 Langarica water temperature trend, July 202561
Figure 2.62 Langarice boxplot for July 202562
Figure 2.63 Vjosa, Permet water temperature trend, May 2025
Figure 2.64 Permet boxplot for May 202563
Figure 2.66 Permet boxplot for June 202563
Figure 2.67 Vjosa, Permet water temperature trend, July 2025
65
Figure 2.68 Permet boxplot for July 202565
Figure 2.69 Langarica Water Temperature
Figure 2.70 Vjosa Water Temperature66
Figure 3.1 Gobigobio67
Figure 3.2 C. vardarense67
Figure 3.3 Salmfarioides67
Figure 3.4 G. scadarensis
Figure 3.5 T mean and species threshold of Barbus barbus
Figure 3.6 T mean and species threshold of Barbus meridionali69
Figure 3.7 T mean and species threshold of Barbus meridionalis70
Figure 3.8 T mean and species threshold of Gobigobio70
Figure 3.9 T mean and species threshold of Gobiscadarensis72
Figure 3.10 T mean and species threshold of Salmfarioides
Figure 3.12 T mean and species threshold of Barbus meridionalis73
Figure 3.11 T mean and species threshold of Barbus barbus
Figure 3.13 T mean and species threshold of Chindrostoma vardarense
74
Figure 3.14 T mean and species threshold of Gobigobio
Figure 3.15 T mean and species threshold of Gobiscadarensis
Figure 3.17 Threshold Exceedance Heatmap77
Figure 3.18 EED Lengarica river
Figure 3.20 T mean and species DVT in Langarica
Figure 3.21 T mean and species DVT in Vjosa80
Figure 3.21 Heatmap DVT80
Figure 3.23 EDD 21 in Vjosa and Langarica

List of tables

Table 2.1 Monthly Tmin Mann Kendall Test	32
Table 2. 2 Monthly Tmax Mann Kendall Test	32
Table 2. 3 Monthly Tmean Mann Kendall Test	
Table 2. 4 Heat-wave events	
Table 2. 5 Seasonal summary of EDD	63